The Physics of Compact Stars, SS 09

Andreas Schmitt

Contents

I. INTRODUCTION AND OUTLINE

A. Motivation

The purpose and motivation of this lecture can be summarized in the following two questions,

- What is the ground state (and its properties) of ultra-dense matter?
- What is the matter composition of a compact star?

To say it right away, the complete answer to neither of these two questions is currently known. This shows that we will be very close to present research in this lecture.

The two questions are, of course, strongly coupled to each other. Depending on your point of view, you can consider the first as the main question and the second as a "corollary" of the answer to the first or vice versa. If you are more interested in fundamental questions in particle physics you take the former point of view: you are interested in the question what happens to matter if you squeeze it more and more. This is interesting because at some level of sufficient "squeezing" you expect to reach the point where the fundamental degrees of freedom and their interactions become important. That is, at some point you will lose the structure of ordinary atoms and reach a form of matter where the constituents of an atom, namely neutrons, protons, and electrons, are the right degrees of freedom. If you squeeze further, you might reach a level where the constituents of neutrons and protons, namely quarks and gluons, become relevant degrees of freedom. Thus, by looking at ultra-dense matter, we might learn a lot about the fundamental theories and interactions of elementary particles. When trying to understand this kind of dense matter, we would like to perform experiments and check whether our fundamental theories work or whether there are new phenomena (or even new theories?) that we have not included into our description. Unfortunately, there are currently no experiments on earth which can produce matter at such ultra-high densities we are talking about. However, this does not mean that this kind of matter does not exist in nature. On the contrary, we are pretty sure that we have observed objects that contain matter at ultra-high density, namely compact stars. Thus, we may use stars as our "laboratory".

If you are more phenomenologically-minded, or if you are an astrophysicist, you may of course simply say, I observe an object in nature, and thus I would like to understand what its matter composition and its properties are. This will inevitably lead you from the above second to the first question.

In any case, we see that both questions are closely related and we don't have to decide which of the two points of view we take. Nevertheless, this lecture will not really be an astrophysics lecture. For instance, we shall neglect many complications that arise from considering a realistic compact star. A star is a finite system, it is inhomogeneous, it underlies the laws of general relativity etc. In most parts we are, for simplicity, interested in infinite, homogeneous systems and ignore general relativistic effects. Only in discussing the consequences of our simplified calculations we shall, on a qualitative level, discuss the more realistic setting. So in some sense we shall focus more on the first question, but keep the second question in mind as our motivation.

So what kind of physics will we discuss? As became clear above, different kinds of systems may be encountered in dense matter, depending on how much the matter is squeezed. We will discuss some nuclear physics, however when we talk about nuclear matter we do not mean ordinary nuclei (although they can also appear in a compact star), but rather think of the star, in a simplified picture, as one giant nucleus. Exotic variants of nuclear matter, such as pion or kaon condensation or hyperonic matter will also be relevant. And last but not least, there is the possibility of deconfined quark matter inside a star.

In any case, the dominant interaction that determins the state of matter in the systems we are interested, is the strong interaction, i.e., we will learn a lot about Quantum Chromodynamics (QCD). In its "purest" form when we talk about quark matter, and in a form of an effective description when we talk about nuclear matter. However, we also need to talk about the weak interaction. Since, as the name indicates, it is much weaker as the strong interaction, it acts on much longer time scales. However, in compact star physics, we are mostly interested in very long time scales, such as thousands of years or even millions of years. Therefore, we shall see that the weak interaction plays an important role too. In particular, the weak interaction is responsible for the chemical equilibrium of the system, i.e., it fixes the various chemical potentials. Finally, we should mention that we shall use these theories at nonzero temperatures, although in some cases it is a good approximation to consider the zero-temperature limit.

All this might sound like quite a challenge if you are not familiar with QCD and/or thermal field theory. And indeed, we shall not be able in the given time to develop all theoretical tools in detail. However, all calculations are physically motivated, and by understanding the physics behind the results and computations, you should be able to get familiar with the theories and technicalities via "learning by doing".

Finally, before getting a bit more quantitative (but still introductory), let's mention some literature. Good textbooks about compact stars are Refs. [1–3]. A shorter introduction into compact stars and dense matter can be found in the

nice review articles [4–6]. A review about quark matter (more precisely, about color-superconducting quark matter) with a detailed section about compact star applications is Ref. [7]. For an introduction to thermal field theory, see the textbooks [8] and [9], or my own online lecture notes from the previous semester [10]. As mentioned above, we shall consider problems which are currently discussed in research. Therefore, several other references that will be given in the course of this lecture, are actual research papers. I will not try to be exhaustive in the reference list but rather only include selected references which are useful for a deeper understanding of what we discuss in this lecture.

B. What is a compact star?

Compact stars are the densest objects in nature. They have masses of the order of the mass of the sun, $M \sim 1.4\, M_\odot$, but radii of only about ten kilometers, $R \sim 10\,\mathrm{km}$. Thus the mass of the sun $M_\odot = 1.989 \cdot 10^{33}\,\mathrm{g}$ is concentrated in a sphere with a radius which is 10^5 times small than that of the sun, $R_S = 6.96 \cdot 10^5\,\mathrm{km}$. This leads to a density

$$\rho \simeq 7 \cdot 10^{14}\,\mathrm{g\,cm^{-3}}\,. \tag{1}$$

This is a few times large than the nuclear ground state density

$$\rho_0 = 2.8 \cdot 10^{14}\,\mathrm{g\,cm^{-3}}\,. \tag{2}$$

(This is the density present in heavy nuclei and corresponds to a baryon density of $n_B \simeq 0.15\,\mathrm{fm^{-3}}$.)

In the traditional picture of a compact star, the star is made out of neutron-rich nuclear matter. Hence the traditional name is actually "neutron star". This is still the preferred name among astrophysicists, even if they talk about quark matter inside a star (then they would probably talk about an "exotic neutron star"). Here we shall always use the term "compact star" to include the possibilities of more exotic matter (after all, a significant part of this lecture is about this "exotic" matter).[1]

Compact stars are born in a supernova. This is a complicated, nonequilibrium processes that people try to understand with heavy numerical simulations. We shall not be concerned with supernovae in this lecture but might keep in mind that some properties of the star may be a result of this violent explosion. An example is the high velocity with which some of them travel through space.

Compact stars are not only extreme with respect to their density. They also rotate very fast with rotation frequencies up to one millisecond,

$$\nu \lesssim 1\,\mathrm{ms^{-1}}\,. \tag{3}$$

To see that this is really fast, notice that a point on the equator has a velocity of $v = 2\pi R/1\mathrm{ms} = 0.21\,c$, i.e., it moves with 21% of the speed of light. Several observations related to the rotation frequency will be of relevance in this lecture. For instance the pure fact that this rotation is so fast requires some explanation. From the microscopic point of view, this is related to transport properties such as viscosity of the matter inside the star. Also *glitches*, sudden spin-ups of the star, must find an explanation in the properties of ultra-dense matter.

Compact stars also have huge magnetic fields,

$$B \sim 10^{12}\,\mathrm{G}\,. \tag{4}$$

Even (surface) magnetic fields of the order of $B \sim 10^{15}\,\mathrm{G}$ have been observed (the magnetic field in the core of the star possibly being even higher). Such highly magnetized stars are also termed *magnetars*.[2]

Compact stars are quite cold. That is, they are actually quite hot compared to temperatures on earth. Namely, their temperatures right after they are born in a supernova explosion, is of the order of $T \sim 10^{11}\,\mathrm{K}$. This corresponds, in units where the Boltzmann constant is unity, $k_B = 1$, to $T \sim 10\,\mathrm{MeV}$. In their lives, this temperature decreases down to temperatures in the keV range. The reason why we call this "cold" is that we have to compare this with the scale set by QCD. For instance, the deconfinement phase transition at vanishing quark chemical potential (more precisely, the crossover) happens at about $T_c \simeq 170\,\mathrm{MeV}$. Therefore, in many of our calculations, $T = 0$ is a good approximation.

---

[1] The term "compact star" is also used for a second class of stars, namely *white dwarves* which are less dense than the stars we are concerned with. Since we shall not talk about white dwarves in this lecture, we can reserve the term "compact star" for objects with characteristic mass, radius etc. as given in this subsection.

[2] Compare these magnetic fields for instance to the earth's magnetic field, $B \sim 0.6\,\mathrm{G}$, a common hand-held magnet, $B \sim 100\,\mathrm{G}$, or the strongest steady magnetic fields in the laboratory, $B \sim 4.5 \cdot 10^5\,\mathrm{G}$.

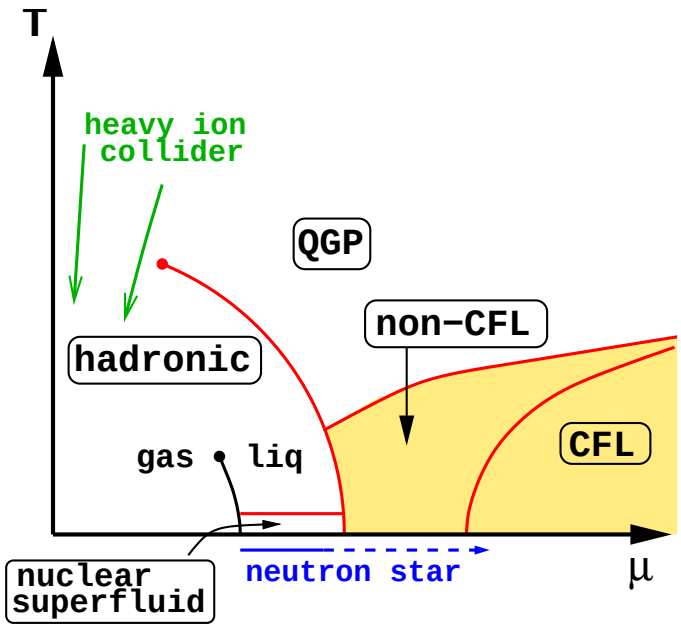

FIG. 1: Conjectured phase diagram of QCD in the plane of quark chemical potential μ and temperature T. While matter at low density and high temperature is probed in heavy-ion collisions, cold and dense matter can only be found in neutron stars (compact stars). We may find (superfluid) nuclear matter and/or deconfined quark matter inside a star. Deconfined quark matter (at high temperatures termed quark-gluon plasma (QGP)) will, at low temperatures, be in a color-superconducting state, here labelled by CFL (Color-Flavor Locking) and non-CFL (some color superconductor other than CFL).

C. What is ultra-dense matter?

Having stated some of the most important properties of compact stars (which gives a background behind the second question at the beginning of this introduction) we should now also specify what we mean by the first question. In particular, we should specify what we mean by "ultra-dense". We may rephrase the first question by asking "How does the QCD phase diagram look for large baryon chemical potentials and small temperatures?" We show a sketch of this phase diagram in Fig. 1. For now, we are not concerned with all the details of this diagram (some of them are given in the caption). We simply observe that compact stars, on the scales of this diagram, live somewhere in the region of small temperatures and intermediate densities. They may live in the region where quarks are confined, i.e., in the hadronic phase. This would imply that they are real *"neutron stars"*. They may also live in the deconfined region. This would imply they are *"quark stars"*, where quark matter may itself be in an "exotic state" indicated in the figure. For a third possibility, we have to take into account that a compact star actually has a density profile rather than a homogeneous density. In the interior, we expect the density to be larger than at the surface. Therefore, a third possibility is a *"hybrid star"* with a quark core and a nuclear mantle.

We do not know the exact location of the relevant phase transition lines in Fig. 1. Therefore, (and because we do not know the exact densities inside the star) the questions at the beginning of the introduction are not yet answered. We even have to be more modest. Not only are the locations of the phase transition lines unknown, even the phases themselves are not clear in the relevant density region. The reason is, simply speaking, that QCD is notoriously hard to solve in this region. The strong-coupling nature of the theory prevents us from using perturbative methods (we may, and shall in this lecture, use perturbative methods at much higher densities and extrapolate down to intermediate densities; however, this pushes the calculations out of their range of validity by many orders of magnitude). This emphasizes the significance of astrophysical observations: we do not simply like to *confirm* the results of our calculations by using astrophysical data, we *need* astrophysical input to *understand* the theory which we believe to be the underlying theory of strongly interacting matter, namely QCD.

II. MASS AND RADIUS OF THE STAR

In this section, we will discuss the simplest properties of a compact star, its mass and radius. We have already given typically values for these quantities above. Below we shall connect them with microscopic properties of nuclear and

quark matter. In this case, the defining property is the equation of state which, in particular, will provide an estimate for the maximum mass of the star. Let us begin with a simple estimate of mass and radius from general relativity. For the stability of the star we need $R > R_s$ where R is the radius of the star, and $R_s = 2MG$ the Schwarzschild radius, with the mass of the star M and the gravitational constant $G = 6.672 \cdot 10^{-11}\,\mathrm{m^3 kg^{-1} s^{-2}} = 6.707 \cdot 10^{-39}\,\mathrm{GeV^{-2}}$. (We shall mostly use units common in particle physics, $\hbar = c = k_B = 1$, although astrophysicists often use different units.) For $R < R_s$ the star becomes unstable with respect to the collapse into a black hole. Let us build a simple star made out of a number of nucleons A with mass $m \simeq 939\,\mathrm{MeV}$ and a distance $r_0 \simeq 0.5 \cdot 10^{-13}\,\mathrm{cm}$ (that's where the nucleon interaction becomes repulsive). We thus cover a volume $\sim r_0^3 A$ and thus have a radius

$$R \sim r_0 A^{1/3}\,, \tag{5}$$

(for our rough estimate we are not interested in factors of π) and a mass

$$M \simeq mA\,. \tag{6}$$

Now from the limit $R = 2MG$ we obtain

$$A \sim \Big(\frac{r_0}{2mG}\Big)^{3/2} \sim 2.6 \cdot 10^{57}\,. \tag{7}$$

This is the number of nucleons up to which we can fill our star before it gets unstable. We can plug this value back into the radius and mass of the star to obtain the limit values

$$R \simeq 7\,\mathrm{km}\,, \qquad M = 2.3\,M_\odot\,. \tag{8}$$

Adding more nucleons would make the star too heavy in relation to its radius.

Besides giving an estimate for the baryon number in the star, we see from this simple exercise that general relativistic effects will be important because the Schwarzschild radius will be a significant fraction of the radius of the star. In other words, using the above realistic values $M \simeq 1.4\,M_\odot$ and $R \simeq 10\,\mathrm{km}$ the gravitational energy E_grav is a sizable fraction of the mass of the star,

$$E_\mathrm{grav} = \frac{GM^2}{R} = 0.5\,M\,. \tag{9}$$

For the mass/radius relation we therefore need an equation that incorporates effects from general relativity. Let us first ignore these effects. We are looking for an equation that describes equilibrium between the gravitational force, seeking to compress the star, and the opposing force coming from the pressure of the matter inside the star. In the case of a compact star, this pressure is the degeneracy pressure of the matter inside the star, i.e., the pressure from the Pauli exclusion principle. The differential pressure dP at a given radius is related to the gravitational force dF via

$$dP = \frac{dF}{4\pi r^2}\,, \tag{10}$$

with

$$dF = -\frac{Gm(r)\,dm}{r^2}\,. \tag{11}$$

Here, $m(r)$ is the mass of the star up to a given radius r, in particular $m(R) = M$. The differential mass of the star at a given radius (i.e., the mass of a thin spherical layer) can be written in terms of the mass density $\rho(r)$ and thus in terms of the energy density $\epsilon(r) = \rho(r)$ (in units $c = 1$),

$$dm = \rho(r)\,dV = 4\pi r^2 \epsilon(r) dr\,. \tag{12}$$

This equation, together with Eq. (10) (into which we insert Eqs. (12) and (11)) yields the two coupled differential equations,

$$\frac{dm}{dr} = 4\pi r^2 \epsilon(r)\,, \tag{13a}$$

$$\frac{dP}{dr} = -\frac{G\epsilon(r)m(r)}{r^2}\,. \tag{13b}$$

The second equation, which is easy to understand from elementary Newtonian physics, now receives corrections from general relativity. It is beyond the scope of these lectures to derive these corrections. We will simply quote the resulting equation,

$$\frac{dP}{dr} = -\frac{G\epsilon(r)m(r)}{r^2}\left[1+\frac{P(r)}{\epsilon(r)}\right]\left[1+\frac{4\pi r^3 P(r)}{m(r)}\right]\left[1-\frac{2Gm(r)}{r}\right]^{-1} . \tag{14}$$

This equation is called Tolman-Oppenheimer-Volkov (TOV) equation and the derivation can be found in Ref. [11]. In order to solve it, one first needs the energy density for a given pressure. Only then do we have a closed system of equations. This input is given from the microscopic physics which yield an equation of state in the form $P(\epsilon)$. We have thus found a first example how the microscopic physics can potentially be "observed" from astrophysical data, namely the mass and radius of the star. We shall encounter several more of these examples. The equation of state will be discussed in the next subsection.

Once an equation of state is found, one needs two boundary conditions for the above TOV equation. The first is obviously $m(r=0)=0$, the second is a boundary value for the pressure in the center of the star, $P(r=0)=P_0$. Then, the solution of the equations will produce a mass and pressure profile $m(r)$, $P(r)$ with the pressure going to zero at some point $r=R$, giving the radius of the star. The mass of the star is then read off at this point, $M=m(R)$. Doing this for varying initial pressures P_0 yields a curve $M(R)$ in the mass-radius plane, parametrized by P_0. This curve of course depends on the chosen equation of state.

[End of 1st lecture, March 16, 2009]

A. Noninteracting nuclear matter

We start with a very simple system where we neglect all interactions. Therefore, the following arguments will follow from elementary statistical physics and thermodynamics. The thermodynamic potential for the grand-canonical ensemble is given by

$$\Omega = E - \mu N , \tag{15}$$

with the energy E, the chemical potential μ and the particle number N. The pressure is then

$$P = -\frac{\Omega}{V} = \mu n - \epsilon , \tag{16}$$

with the volume V, the number density $n \equiv N/V$, and the energy density $\epsilon = E/V$. Number density and energy density are

$$n = 2\int \frac{d^3\mathbf{k}}{(2\pi)^3} f_k , \tag{17a}$$

$$\epsilon = 2\int \frac{d^3\mathbf{k}}{(2\pi)^3} \epsilon_k f_k . \tag{17b}$$

Here we consider neutrons (n), protons (p), and electrons (e) which are all spin-$\frac{1}{2}$ fermions, hence the factor 2 for the two degenerate spin states. The Fermi distribution function is denoted by f_k and the one-particle energy is

$$\epsilon_k = \sqrt{k^2+m^2} . \tag{18}$$

For $T=0$ the Fermi distribution is a step function, $f_k = \Theta(k_F - k)$, and thus the k integrals will be cut off at the Fermi momentum k_F, i.e.,

$$n = \frac{1}{\pi^2}\int_0^{k_F} dk\, k^2 = \frac{k_F^3}{3\pi^2} , \tag{19a}$$

$$\epsilon = \frac{1}{\pi^2}\int_0^{k_F} dk\, k^2\sqrt{k^2+m^2} = \frac{1}{8\pi^2}\left[(2k_F^3+m^2k_F)\sqrt{k_F^2+m^2} - m^4 \ln\frac{k_F+\sqrt{k_F^2+m^2}}{m}\right] . \tag{19b}$$

Then, with $\mu = \sqrt{k_F^2+m^2}$ (see below), the pressure is

$$P = \frac{1}{\pi^2}\int_0^{k_F} dk\, k^2(\mu - \sqrt{k^2+m^2}) = \frac{1}{24\pi^2}\left[(2k_F^3-3m^2k_F)\sqrt{k_F^2+m^2} + 3m^4 \ln\frac{k_F+\sqrt{k_F^2+m^2}}{m}\right] . \tag{20}$$

For n, p, e matter, the total pressure is

$$P = \frac{1}{\pi^2} \sum_{i=n,p,e} \int_0^{k_{F,i}} dk\, k^2 (\mu_i - \sqrt{k^2 + m_i^2})\,. \tag{21}$$

The Fermi momenta can be thought of as variational parameters which have to be determined from maximizing the pressure, i.e., from the conditions

$$\frac{\partial P}{\partial k_{F,i}} = 0\,, \qquad i = n, p, e\,. \tag{22}$$

This implies

$$\mu_i = \sqrt{k_{F,i}^2 + m_i^2}\,. \tag{23}$$

We have additional constraints on the Fermi momenta from the following two conditions. First we have to require the star to be neutral[3], i.e., the densities of protons and electrons has to be equal,

$$n_e = n_p\,. \tag{27}$$

With Eq. (19a) this obviously means

$$k_{F,e} = k_{F,p}\,. \tag{28}$$

Second, we require chemical equilibrium with respect to the weak processes

$$n \;\rightarrow\; p + e + \bar{\nu}_e\,, \tag{29a}$$

$$p + e \;\rightarrow\; n + \nu_e\,. \tag{29b}$$

The first of these processes is "β-decay", the second is sometimes called "inverse β-decay" or "electron capture". We shall assume that the neutrino chemical potential vanishes, $\mu_{\nu_e} = 0$. This means we assume neutrinos simply leave the system. This assumption is justified for compact stars since the neutrino mean free path is of the order of the size of the star or larger (except for the very early stages in the life of the star). Consequently, we obtain the following constraint for the chemical potentials,

$$\mu_n = \mu_p + \mu_e\,. \tag{30}$$

Inserting Eq. (23) into this constraint yields

$$\sqrt{k_{F,n}^2 + m_n^2} = \sqrt{k_{F,p}^2 + m_p^2} + \sqrt{k_{F,e}^2 + m_e^2}\,. \tag{31}$$

---

[3] In fact, a compact star has to be electrically neutral to a very high accuracy, as one can see from the following simple estimate. Suppose the star has an overall charge of Z times the elementary charge, Ze, and we look at the Coulomb repulsion of a test particle (say a proton) with mass m and charge e (e having the same sign as the hypothetical overall charge of the star Ze). The Coulomb force, seeking to expel the test particle, has to be smaller than the gravitational force, seeking to keep the test particle within the star. This gives the condition

$$\frac{(Ze)e}{R^2} \leq \frac{GMm}{R^2}\,, \tag{24}$$

with the mass M and radius R of the star. Even if we are generous with the limit on the right-hand side by assigning the upper limit $M < Am$ to the mass of the star (if the star contains A nucleons, its total mass will be less than Am due to the gravitational binding energy), we will get a very restrictive limit on the overall charge. Namely, we find

$$\frac{(Ze)e}{R^2} < \frac{GAm^2}{R^2} \qquad \Rightarrow \qquad Z < G\frac{m^2}{e^2}\,A\,. \tag{25}$$

With the proton mass $m \sim 10^3$ MeV, the elementary charge $e^2 \sim 10^{-1}$ (remember $\alpha = e^2/(4\pi) \simeq 1/137$), and the gravitational constant from above, we find

$$Z < 10^{-37} A\,, \tag{26}$$

i.e., the average charge per nucleon has to be extremely small in order to ensure the stability of the star. Of course, since we have found such an extremely small number, it does not matter much for the argument whether we use a proton or an electron as a test particle. The essence of this argument is the weakness of gravitation compared to the electromagnetic interactions: a tiny electric charge per unit volume, distributed over the star, is sufficient to overcome the stability from gravity.

We can eliminate the electron Fermi momentum with the help of Eq. (28) and solve this equation to obtain the proton Fermi momentum as a function of the neutron Fermi momentum,

$$k_{F,p}^2 = \frac{(k_{F,n}^2 + m_n^2 - m_e^2)^2 - 2(k_{F,n}^2 + m_n^2 + m_e^2)m_p^2 + m_p^4}{4(k_{F,n}^2 + m_n^2)} \,. \tag{32}$$

To understand the physical meaning of this relation, first assume a vanishing proton contribution, $k_{F,p} = 0$. Then the equation gives

$$k_{F,n}^2 = (m_p + m_e)^2 - m_n^2 < 0 \,. \tag{33}$$

This square is negative because of $m_p \simeq 938.3\,\mathrm{MeV}$, $m_n \simeq 939.6\,\mathrm{MeV}$, $m_e \simeq 0.511\,\mathrm{MeV}$. Therefore, $k_{F,p} = 0$ is impossible and there will always be at least a small fraction of protons. On the other hand assume $k_{F,n} = 0$, which leads to

$$k_{F,p}^2 = \left(\frac{m_n^2 + m_e^2 - m_p^2}{2m_n}\right)^2 - m_e^2 \simeq 1.4\,\mathrm{MeV}^2 \,. \tag{34}$$

This is the threshold below which there are no neutrons and the charge neutral system in β-equilibrium contains only protons and electrons of equal number density. Above the threshold we may consider a given baryon density $n_B = n_n + n_p$ to express the neutron Fermi momentum as

$$k_{F,n} = (3\pi^2 n_B - k_{F,p}^3)^{1/3} \,. \tag{35}$$

Inserting this into Eq. (32) yields an equation for $k_{F,p}$ as a function of the baryon density. In the ultrarelativistic limit, neglecting all masses, Eq. (32) obviously yields $k_{F,p} = k_{F,n}/2$ and thus $n_p = n_n/8$ or

$$n_p = \frac{n_B}{9} \,. \tag{36}$$

One can check that this limit is approached from below, i.e., in a compact star containing nuclear matter we deal with neutron-rich matter, as mentioned in the introduction.

Let us therefore consider the simple case of pure neutron matter and also go to the nonrelativistic limit, $m_n > k_{F,n}$. In this case, the energy density (19b) and the pressure (20) become

$$\epsilon \;\simeq\; \frac{m_n k_{F,n}^3}{3\pi^2} \,, \tag{37a}$$

$$P \;\simeq\; \frac{k_{F,n}^5}{15 m_n \pi^2} \,. \tag{37b}$$

(To see this, note that the ln term cancels the term linear in k_F in the case of ϵ, and the linear and cubic terms in k_F in the case of P.) Consequently,

$$P(\epsilon) \simeq \left(\frac{3\pi^2}{m_n}\right)^{5/3} \frac{\epsilon^{5/3}}{15 m_n \pi^2} \,. \tag{38}$$

We have thus found a particularly simple equation of state, where the pressure is given by a power of the energy density.

Exercise 1: *Find the full equation of state numerically by plotting P versus ϵ. You should see the onset of neutrons and identify a region where the equation of state is well approximated by the power-law behavior of pure neutron matter in the nonrelativistic limit.*

We may use the power-law behavior in its general form,

$$P(\epsilon) = K\,\epsilon^\gamma \,, \tag{39}$$

to obtain the simplest version of the mass-radius equations. We use the Newtonian form, Eqs. (13), which, upon using Eq. (39),

$$\frac{dm}{dr} \;=\; \frac{4\pi}{K^{1/\gamma}}\, r^2 P^{1/\gamma}(r) \,, \tag{40}$$

$$\frac{dP}{dr} \;=\; -\frac{G}{K^{1/\gamma}} \frac{P^{1/\gamma}(r) m(r)}{r^2} \,. \tag{41}$$

Even in this simplest example, we need to solve the equations numerically.

Exercise 2:
(i) Solve these equations (for nonrelativistic pure neutron matter, i.e., $\gamma = 5/3$) numerically and plot $m(r)$, $P(r)$ for a given value of the pressure $P_0 = P(r = 0)$.
(ii) Use P_0 as a parameter to find the mass-radius relation $M(R)$. To this end, you need to do (i) for several values of P_0 and find for each P_0 the radius R at which $P(R) = 0$ and the corresponding mass $M(R)$.
(iii) You may incorporate general relativistic effects from the TOV equation (14) and/or the full (numerical) equation of state for noninteracting nuclear matter from Exercise 1.

The results of this exercise show that the maximum mass reached within this model is about $M < 0.7 M_\odot$ which is well below observed neutron star masses. (See Refs. [12–14] for a pedagogical introduction into the equation of state and mass-radius relation from solving the TOV equation.) This is a consequence of the assumption of noninteracting nucleons. Taking into account interactions will increase the maximum mass.

B. Noninteracting quark matter

Since we are interested in compact stars, we will ignore the heavy charm (c), bottom (b), and top (t) quarks throughout the lecture. Quark chemical potentials inside the star of at most 500 MeV are too small to create a population of these states. Therefore, we shall always consider at most three quark flavors, namely up (u), down (d), and strange (s). It is always a good approximation to neglect the masses of the u and d quarks (their *current masses* are $m_u \simeq m_d \simeq 5\,\mathrm{MeV} \ll \mu \simeq (300 - 500)\,\mathrm{MeV}$). The strange mass, however, may be important quantitatively, and, in some cases (depending on what we want to compute), even may be crucial for qualitative results. The current strange quark mass is $m_s \simeq 100\,\mathrm{MeV}$. In units of the elementary charge, the electric charges of the relevant quarks are

$$q_u = \frac{2}{3}\,, \qquad q_d = q_s = -\frac{1}{3}\,, \tag{42}$$

and the electron charge is, of course, $q_e = -1$.

If we consider free quarks, the energy density ϵ, the number density n, and the pressure P, are obtained as for nucleons in the previous subsection. We only have to remember that there are three colors for each quark flavor, $N_c = 3$, i.e., the degeneracy factor for a single quark flavor is $2N_c = 6$, the 2 counting the spin degrees of freedom. Consequently, for each quark flavor $f = u, d, s$ we have (cf. Eqs. (19a), (19b), (20)),

$$n_f = \frac{k_{F,f}^3}{\pi^2}\,, \tag{43a}$$

$$\epsilon_f = \frac{3}{\pi^2}\int_0^{k_{F,f}} dk\, k^2 \sqrt{k^2 + m_f^2}\,, \tag{43b}$$

$$P_f = \frac{3}{\pi^2}\int_0^{k_{F,f}} dk\, k^2 \left(\mu_f - \sqrt{k^2 + m_f^2}\right)\,. \tag{43c}$$

Again, we need to impose equilibrium conditions with respect to the weak interactions. In the case of 3-flavor quark matter, the relevant processes are

$$d \;\to\; u + e + \bar{\nu}_e\,, \qquad s \to u + e + \bar{\nu}_e\,, \qquad s + u \leftrightarrow d + u\,, \tag{44a}$$

$$u + e \;\to\; d + \nu_e\,, \qquad u + e \to s + \nu_e\,, \tag{44b}$$

yielding the conditions

$$\mu_d = \mu_e + \mu_u\,, \qquad \mu_s = \mu_e + \mu_u\,. \tag{45}$$

(This automatically implies $\mu_d = \mu_s$.) The charge neutrality condition can be written in a general way as

$$Q \equiv \sum_{f=u,d,s} q_f n_f - n_e = 0\,, \tag{46}$$

where n_e is the electron density.

1. Strange quark matter hypothesis

Before computing the equation of state, we discuss the so-called *bag model* and the *strange quark matter hypothesis*. The bag model is a very crude phenomenological way to incorporate confinement into the description of quark matter. The effect of confinement is needed in particular if we compare quark matter with nuclear matter (which is ultimately what we want to do in this section). Put another way, although we speak of noninteracting quarks, we need to account for a specific (and in general very complicated) aspect of the interaction, namely confinement. Apart from that, we indeed shall ignore interactions, i.e., we set the strong coupling constant to zero, $\alpha_s = 0$.

To understand how the bag constant accounts for confinement, we compare the pressure of a noninteracting gas of massless pions with the pressure of a noninteracting gas of quarks and gluons at finite temperature and zero chemical potential. First remember (for example from the lecture in the previous semester [10]), that the pressure of a single bosonic degree of freedom at $\mu = 0$ is

$$P_{\text{boson}} = -T \int \frac{d^3\mathbf{k}}{(2\pi)^3} \ln\left(1 - e^{k/T}\right) = \frac{\pi^2 T^4}{90}\,, \tag{47}$$

while a single fermionic degree of freedom gives

$$P_{\text{fermion}} = T \int \frac{d^3\mathbf{k}}{(2\pi)^3} \ln\left(1 + e^{k/T}\right) = \frac{7}{8}\frac{\pi^2 T^4}{90}\,. \tag{48}$$

Therefore, since there are three types of pions, their pressure is

$$P_\pi = 3\,\frac{\pi^2}{90}\,T^4\,. \tag{49}$$

This is a simple approximation for the pressure of the confined phase. In the deconfined phase, the degrees of freedom are gluons (8×2) and quarks ($4N_cN_f = 24$) thus (since $2 \times 8 + 7/8 \times 24 = 37$) we have

$$P_{q,g} = 37\,\frac{\pi^2}{90}\,T^4 - B\,, \tag{50}$$

where the bag constant B has been subtracted for the following reason. If B were zero, the deconfined phase would have the larger pressure and thus would be preferred for all temperatures. We know however, that at small temperatures (that's the world we live in), the confined phase is preferred. This is phenomenologically accounted for by the bag constant B which acts like an energy penalty for the deconfined phase (without this penalty, at least in this very simply model description, the deconfined phase would be "too favorable" compared to what we observe).

As a consequence, there is a phase transition at a certain temperature above which the deconfined phase is preferred, $P_{q,g} > P_\pi$. This is indeed what one expects from QCD. In the context of compact stars we are not talking about such large temperatures. In our case, the chemical potential is large and the temperature practically zero. Nevertheless we compare nuclear (confined) with quark (deconfined) matter and thus have to include the bag constant in the pressure and the free energy of quark matter,

$$P + B = \sum_f P_f\,, \tag{51a}$$

$$\epsilon = \sum_f \epsilon_f + B\,. \tag{51b}$$

In other words, the quarks are imagined to be confined in a "bag". Their pressure $\sum_f P_f$ is counterbalanced by the pressure of the bag B and an external pressure P. This phenomenological model of confinement is called the "MIT bag model" [15, 16].

[End of 2nd lecture, March 23, 2009]

Let us now for simplicity consider massless quarks. A nonzero strange mass will slightly change the results but is not important for now. Also let us first ignore electrons. They are not present in three-flavor massless quark matter at zero temperature. They are however required in two-flavor quark matter to achieve electric neutrality. But also in this case their population is small enough to render their effect negligible for the following argument.

With $m_f = 0$ we simply have

$$n_f = \frac{\mu_f^3}{\pi^2}\,, \qquad \epsilon_f = \frac{3\mu_f^4}{4\pi^2}\,, \qquad P_f = \frac{\mu_f^4}{4\pi^2}\,, \tag{52}$$

which in particular implies

$$P_f = \frac{\epsilon_f}{3}\,. \tag{53}$$

To explain the strange quark matter hypothesis, we consider the energy E per nucleon number A,

$$\frac{E}{A} = \frac{\epsilon}{n_B}\,, \tag{54}$$

where n_B is the baryon number density, given in terms of the quark number densities as

$$n_B = \frac{1}{3}\sum_f n_f\,, \tag{55}$$

because a baryon contains $N_c = 3$ quarks. At zero pressure, $P = 0$, Eqs. (51) and (53) imply $\epsilon = 4B$ and thus

$$\frac{E}{A} = \frac{4B}{n_B}\,. \tag{56}$$

We now apply this formula first to three-flavor quark matter ("strange quark matter"), then to two-flavor quark matter of only up and down quarks. For strange quark matter, the neutrality constraint (46) becomes

$$2n_u - n_d - n_s = 0\,. \tag{57}$$

Together with the conditions from chemical equilibrium (45) this implies

$$\mu_u = \mu_d = \mu_s \equiv \mu\,. \tag{58}$$

We see that strange quark matter is particularly symmetric. The reason is that the electric charges of an up, down, and strange quark happen to add up to zero. Now with $n_B = \mu^3/\pi^2$ and

$$B = \sum_f P_f = \frac{3\mu^4}{4\pi^2} \tag{59}$$

(still everything at $P = 0$) we have

$$\left.\frac{E}{A}\right|_{N_f=3} \;=\; (4\pi^2)^{1/4}\,3^{3/4}\,B^{1/4} \simeq 5.714\,B^{1/4} \simeq 829\,\mathrm{MeV}B_{145}^{1/4}\,. \tag{60}$$

We have expressed $B^{1/4}$ in units of 145 MeV for reasons that will become clear below, $B_{145}^{1/4} \equiv B^{1/4}/(145\,\mathrm{MeV})$.

For two-flavor quark matter (neglecting the contribution of electrons), the charge neutrality condition is

$$n_d = 2n_u\,. \tag{61}$$

Hence,

$$\mu_d = 2^{1/3}\mu_u\,. \tag{62}$$

Then, with $n_B = \mu_u^3/\pi^2$ and

$$B = \sum_f P_f = \frac{(1+2^{4/3})\mu_u^4}{4\pi^2}\,, \tag{63}$$

we find

$$\left.\frac{E}{A}\right|_{N_f=2} \;=\; (4\pi^2)^{1/4}\,(1+2^{4/3})^{3/4}\,B^{1/4} \simeq 6.441\,B^{1/4} \simeq 934\,\mathrm{MeV}B_{145}^{1/4}\,. \tag{64}$$

By comparing this to Eq. (60) we see that two-flavor quark matter has higher energy than three-flavor quark matter. This is a direct consequence of the Pauli principle: adding one particle species (and keeping the total number of

particles fixed) means opening a set of new available low-energy states that can be filled, thus lowering the total energy of the system.

We can now compare the results (60) and (64) with the energy per nucleon in nuclear matter. For pure neutron matter, it is simply given by the neutron mass,

$$\left.\frac{E}{A}\right|_{\text{neutrons}} = m_n = 939.6\,\text{MeV}\,. \tag{65}$$

For iron, ^{56}Fe, it is

$$\left.\frac{E}{A}\right|_{^{56}\text{Fe}} = \frac{56 m_N - 56 \cdot 8.8\,\text{MeV}}{56} = 930\,\text{MeV}\,, \tag{66}$$

with the nucleon mass $m_N = 938.9\,\text{MeV}$. Since we observe iron rather than deconfined quark matter, we know that

$$\left.\frac{E}{A}\right|_{^{56}\text{Fe}} < \left.\frac{E}{A}\right|_{N_f=2} \quad \Rightarrow \quad B^{1/4} > 144.4\,\text{MeV}\,. \tag{67}$$

We have thus found a lower limit for the bag constant from the stability of iron with respect to two-flavor quark matter. Now what if the bag constant were just a bit larger than this lower limit? What if it were small enough for three-flavor quark matter to have lower energy than iron? The condition for this would be

$$\left.\frac{E}{A}\right|_{N_f=3} < \left.\frac{E}{A}\right|_{^{56}\text{Fe}} \quad \Rightarrow \quad B^{1/4} < 162.8\,\text{MeV}\,. \tag{68}$$

This would imply that strange quark matter is absolutely stable, while nuclear matter is metastable. This possibility, which would be realized by a bag constant in the window $145\,\text{MeV} < B^{1/4} < 162\,\text{MeV}$, is called *strange quark matter hypothesis*, suggested by Bodmer [17] and Witten [18], see also [19].

Note that the existence of ordinary nuclei does *not* rule out the strange quark matter hypothesis. The conversion of an ordinary nucleus into strange quark matter requires the simultaneous conversion of many (roughly speaking A many) u and d quarks into s quarks. Since this has to happen via the weak interaction, it is practically impossible. In other words, there is a huge energy barrier between the metastable (if the hypothesis is true) state of nuclear matter and absolutely stable strange quark matter. This means that strange quark matter has to be created in another way ("going around" the barrier), by directly forming a quark-gluon plasma. This can for instance happen in a heavy-ion collision. Or, importantly for us, it may happen in the universe, giving rise to stars made entirely out of quark matter, so-called *strange stars*.

Small "nuggets" of strange quark matter are called *strangelets* (a strange star would then simply be a huge strangelet). If a strangelet is injected into an ordinary compact star (a neutron star), it would, assuming the strange quark matter hypothesis to be true, be able to "eat up" the nuclear matter, converting the neutron star into a strange star. Note the difference between this transition and the above described impossible transition from ordinary nuclear matter to strange quark matter: once there is a sufficiently large absolutely stable strangelet, *successive* conversion of up and down quarks into strange quarks increase the size of the strangelet; the energy barrier (originating from the *simultaneous* creation of a large number of strange quarks) now cannot cause the system to relax back into its original nuclear (metastable) state. This argument has important consequences. If there exist enough sizable strangelets in the universe to hit neutron stars, *every* neutron star would be converted into a strange star. In other words, the observation of a single ordinary neutron star would rule out the strange quark matter hypothesis. Therefore, it is important to understand whether there are enough strangelets around. Very recently, it has been discussed in the literature that there may not be enough strangelets [20], in contrast to what was assumed before.

2. Equation of state

Next we derive the equation of state for strange quark matter. We include the effect of the strange mass to lowest order and also include electrons. It is convenient to express the quark chemical potentials in terms of an average quark chemical potential $\mu = (\mu_u + \mu_d + \mu_s)/3$ and the electron chemical potential μ_e,

$$\mu_u = \mu - \frac{2}{3}\mu_e\,, \tag{69a}$$

$$\mu_d = \mu + \frac{1}{3}\mu_e\,, \tag{69b}$$

$$\mu_s = \mu + \frac{1}{3}\mu_e\,. \tag{69c}$$

Written in this form, the conditions from β-equilibrium (45) are automatically fulfilled. Taking into account the strange quark mass, the Fermi momenta are given by

$$k_{F,u} = \mu_u \,, \tag{70a}$$
$$k_{F,d} = \mu_d \,, \tag{70b}$$
$$k_{F,s} = \sqrt{\mu_s^2 - m_s^2} \,. \tag{70c}$$

The energy density and the pressure are

$$\sum_{i=u,d,s,e} \epsilon_i = \frac{3\mu_u^4}{4\pi^2} + \frac{3\mu_d^4}{4\pi^2} + \frac{3}{\pi^2}\int_0^{k_{F,s}} dk\, k^2 \sqrt{k^2+m_s^2} + \frac{\mu_e^4}{4\pi^2} \,, \tag{71a}$$

$$\sum_{i=u,d,s,e} P_i = \frac{\mu_u^4}{4\pi^2} + \frac{\mu_d^4}{4\pi^2} + \frac{3}{\pi^2}\int_0^{k_{F,s}} dk\, k^2 \left(\mu_s - \sqrt{k^2+m_s^2}\right) + \frac{\mu_e^4}{12\pi^2} \,. \tag{71b}$$

The neutrality condition can now be written as

$$0 = \frac{\partial P}{\partial \mu_e} = -\frac{2}{3} n_u + \frac{1}{3} n_d + \frac{1}{3} n_s + n_e \,. \tag{72}$$

(Note that μ_e is defined as the chemical potential for *negative* electric charge.) Solving this equation to lowest order in the strange mass, one finds

$$\mu_e \simeq \frac{m_s^2}{4\mu} \,. \tag{73}$$

Consequently, the quark Fermi momenta become

$$k_{F,u} \simeq \mu - \frac{m_s^2}{6\mu} \,, \tag{74a}$$
$$k_{F,d} \simeq \mu + \frac{m_s^2}{12\mu} \,, \tag{74b}$$
$$k_{F,s} \simeq \mu - \frac{5m_s^2}{12\mu} \,. \tag{74c}$$

We see that the Fermi momenta are split by an equal distance of $m_s^2/(4\mu)$, and $k_{F,s} < k_{F,u} < k_{F,d}$. Inserting the result for μ_e back into the energy density and the pressure yields

$$\sum_i \epsilon_i \simeq \frac{9\mu^4}{4\pi^2} - \frac{3\mu^2 m_s^2}{2\pi^2} \,, \tag{75a}$$
$$\sum_i P_i \simeq \frac{3\mu^4}{4\pi^2} - \frac{3\mu^2 m_s^2}{4\pi^2} \,. \tag{75b}$$

Consequently,

$$\sum_i \epsilon_i \simeq 3\sum_i P_i + \frac{3\mu^2 m_s^2}{2\pi^2} \,. \tag{76}$$

Inserting these results into Eqs. (51) yields the pressure

$$P \simeq \frac{3\mu^4}{4\pi^2} - \frac{3\mu^2 m_s^2}{4\pi^2} - B \,, \tag{77}$$

and, expressing P in terms of the energy density, we obtain

$$P \simeq \frac{\epsilon - 4B}{3} - \frac{\mu^2 m_s^2}{2\pi^2} \,. \tag{78}$$

This is the equation of state of strange quark matter in the bag model with strange mass corrections to lowest order.

C. Mass/radius relation including interactions

Let us now briefly discuss the results for the mass/radius relation of a compact star for given equations of state for nuclear and quark matter. So far we have only discussed the simplest cases of noninteracting matter. Interactions have a significant effect on both the equation of state and the mass/radius relation. We shall discuss these effects briefly here, and only in the subsequent chapters we will study the nature and details of these interactions. To appreciate the effect of interactions, notice that, while the maximum mass of a star for noninteracting nuclear matter is $\sim 0.7 M_\odot$ (see for instance Ref. [14]), including interactions increases the mass to values well above $2M_\odot$. In Fig. 2 several models for the nuclear equation of state are applied to obtain maximum masses up to $2.4\, M_\odot$. We shall discuss one of these phenomenological models for nuclear matter and its extensions in the next section, Sec. III A. For the case of quark matter, we can understand some of the corrections through interactions in an easy way. A generalization of the pressure (77) is

$$P = \frac{3\mu^4}{4\pi^2}(1-c) - \frac{3\mu^2}{4\pi^2}(m_s^2 - 4\Delta^2) - B\,. \tag{79}$$

One correction is included in the coefficient c. This originates from the (leading order) correction of the Fermi momentum,

$$p_F = \mu\left(1 - \frac{2\alpha_s}{3\pi}\right)\,, \tag{80}$$

resulting in a correction of the μ^4 term in the pressure with $c = 2\alpha_s/\pi$. Higher order calculations suggest $c \gtrsim 0.3$ at densities relevant for compact stars. However, the exact value of c is unknown, since we are interested in density regions where perturbative calculations are not valid. Therefore, c should be treated as a parameter with values of the order 0.3, as done for example in the left panel of Fig. 2.

The second correction in Eq. (79) is the quantity Δ. This is the energy gap of *color superconductivity*, about which we will have to say more in the course of this lecture. Here we only observe that it corrects the μ^2 term in the pressure. One might think that this correction is negligible compared to the μ^4 term and the bag constant. However, it turns out that for reasonable values of the bag constant these two terms largely cancel each other and the μ^2 term becomes important. However, the effect of superconductivity is still hard to determine. Firstly, it would require a precise knowledge of the strange mass. Secondly, it turns out that the maximum mass of the (hybrid) star is not very sensitive to the value of $m_s^2 - 4\Delta^2$ [21].

As a result of this discussion and the results in Fig. 2, two points are important for the further contents of this lecture. First, they should motivate us to understand more about the nature and the details of interactions in nuclear and quark matter, for instance their superfluidity/superconductivity. We will get to these points during this lecture. Second, we have learned that, given our ignorance of the precise quantitative effects of the strong interaction and the uncertainty in astrophysical observations, the mass and the radius of the star are not very good observables to distinguish between a neutron star, a hybrid star, and possibly a quark star. Therefore, we shall look for other observables. It will turn out that these more restrictive observables are linked to transport properties of nuclear and quark matter. This will be a second important topic in the following weeks.

[End of 3rd lecture, March 30, 2009]

III. INTERACTING NUCLEAR MATTER

There are several models, mostly phenomenologically inspired, to describe nuclear matter. Some of them have been used to obtain the curves in Fig. 2. In the following we will discuss one of them, namely the Walecka model. Then, we will discuss how this model is extended by including hyperons. Finally, we discuss kaon condensation in the framework of chiral perturbation theory.

A. The Walecka model

In the Walecka model, nucleon interactions are modeled by the exchange of mesons. We should keep in mind that nucleons are ultimately built of quarks and gluons which are the fundamental degrees of freedom of the strong interactions. Of course, it is a highly nontrivial task to describe even the mass of a nucleon from quarks and gluons, let alone nucleon interactions. A very important tool for such a case is an effective theory. This effective theory has

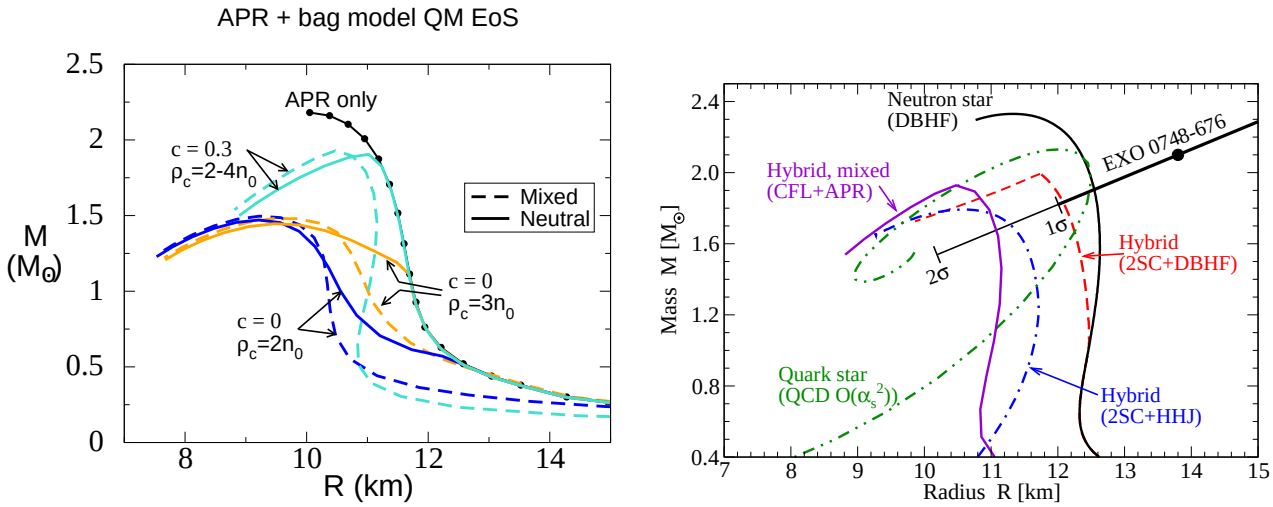

FIG. 2: Two mass radius plots from Refs. [21] (left panel) and [22] (right panel). The left panel serves to show the dependence of the mass/radius curve on the (unknown) parameters of the quark matter equation of state in a hybrid star. We see that reasonable choices of the parameters lead to almost indistinguishable curves compared to nuclear matter (with the "APR" equation of state). In this plot, the transition density ρ_c between quark matter and nuclear matter has been used as a parameter, rather than the bag constant. From our discussion it is clear that one can be translated into the other. The coefficient c describes QCD corrections to the quark Fermi momentum and thus to the μ^4 term in the pressure. The right panel shows the comparison of different nuclear equations of state combined with different quark phases and also includes the mass/radius relation of a pure quark star. For more details and explanations of the various abbreviations, see the respective references.

non-fundamental degrees of freedom, in our case nucleons and mesons instead of quarks and gluons. An effective theory can in principle be obtained by taking the low-energy limit of the underlying fundamental theory, in this case QCD. However, this procedure may turn out to be very difficult. Therefore, one tries to "guess" an effective theory, for instance guided by symmetry principles. One obtains a theory with some unknown parameters which have to be fit, for instance to experimental results. Once the parameters are fitted, one may extrapolate the theory beyond the regime where the fit has been done. In our case, this will be the high-density region for which we have no experiments in the laboratory. There is of course no guarantee that this extrapolation works. Models for interacting nuclear matter at high densities have to be understood in this spirit. Of course, an upper density limit for the validity is the deconfinement phase transition to quarks and gluons. This limit density is not precisely known but may just be the density we find in compact stars.

The Walecka model contains nucleons which interact via the exchange of the scalar σ meson and the ω meson which is a vector meson. The Lagrangian is

$$\mathcal{L} = \mathcal{L}_N + \mathcal{L}_{\sigma,\omega} + \mathcal{L}_I \,, \tag{81}$$

with the free nucleon Lagrangian

$$\mathcal{L}_N = \bar{\psi}\left(i\gamma^\mu\partial_\mu - m_N + \mu\gamma_0\right)\psi \,, \tag{82}$$

where $\bar{\psi} \equiv \psi^\dagger\gamma_0$, and $\psi = \begin{pmatrix}\psi_n \\ \psi_p\end{pmatrix}$, the free mesonic Lagrangian

$$\mathcal{L}_{\sigma,\omega} = \frac{1}{2}\left(\partial_\mu\sigma\partial^\mu\sigma - m_\sigma^2\sigma^2\right) - \frac{1}{4}\omega_{\mu\nu}\omega^{\mu\nu} + \frac{1}{2}m_\omega^2\omega_\mu\omega^\mu \,, \tag{83}$$

where $\omega_{\mu\nu} \equiv \partial_\mu\omega_\nu - \partial_\nu\omega_\mu$, and the interaction Lagrangian with Yukawa interactions between the nucleons and the mesons,

$$\mathcal{L}_I = g_\sigma\bar{\psi}\sigma\psi + g_\omega\bar{\psi}\gamma^\mu\omega_\mu\psi \,. \tag{84}$$

We shall consider isospin-symmetric matter, i.e., the masses and chemical potentials of protons and neutrons are identical. In general, μ is a matrix $\mu = \mathrm{diag}(\mu_n, \mu_p) = \mathrm{diag}(\mu_B + \mu_I, \mu_B - \mu_I)$. Thus, in other words, we assume the isospin chemical potential to vanish. Also the interactions between the nucleons are symmetric, i.e., the nn, pp, and

np interactions are identical. An isospin-asymmetry in the interactions can be included by adding ρ-meson exchange. We will briefly discuss this in Sec. III B. Also kaon condensation induces an asymmetry, discussed in Sec. III C.

The parameters of the model are the masses and the coupling constants. The masses are

$$m_N = 939\,\mathrm{MeV}\,, \qquad m_\omega = 783\,\mathrm{MeV}\,, \qquad m_\sigma = (500-600)\,\mathrm{MeV}\,. \tag{85}$$

The σ meson is in fact a broad resonance and thus we can only approximately assign a mass to this meson. Below we shall use $m_\sigma = 550\,\mathrm{MeV}$. The additional parameters are the coupling constants g_σ, g_ω. We shall discuss below how they will be fixed.

In order to compute the equation of state, we need to consider the partition function

$$Z = \int \mathcal{D}\bar\psi\mathcal{D}\psi\mathcal{D}\sigma\mathcal{D}\omega\, \exp\int_X \mathcal{L}\,, \tag{86}$$

where we abbreviated

$$\int_X \equiv \int_0^\beta d\tau \int d^3x\,, \tag{87}$$

with the inverse temperature $\beta = 1/T$. We shall allow for vacuum expectation values of the mesons. To this end, we write the meson fields as a sum of the condensate and fluctuations,

$$\sigma \;\to\; \bar\sigma + \sigma\,, \tag{88a}$$
$$\omega \;\to\; \bar\omega_0\delta_{0\mu} + \omega\,. \tag{88b}$$

Now the simplest approximation is to neglect the fluctuations. This corresponds to the mean-field approximation. In this approximation the interaction between the nucleons and the mesons is simplified to a mesonic background, or mesonic mean field, which is seen by the nucleons. In this approximation, we can simply drop all derivative terms of the mesons. We then see that the meson mean fields act as corrections to the nucleon mass and chemical potential. We thus obtain the Lagrangian

$$\mathcal{L} = \bar\psi\left(i\gamma^\mu\partial_\mu - m_N^* + \mu^*\gamma_0\right)\psi - \frac{1}{2}m_\sigma^2\bar\sigma^2 + \frac{1}{2}m_\omega^2\bar\omega_0^2\,, \tag{89}$$

with

$$m_N^* \;\equiv\; m_N - g_\sigma\bar\sigma\,, \tag{90a}$$
$$\mu^* \;\equiv\; \mu - g_\omega\bar\omega_0\,. \tag{90b}$$

It is important to keep in mind that the real chemical potential, associated with nucleon number is μ, not μ^*. This becomes important for the correct thermodynamic relations, see footnote before Eqs. (107). In this sense, μ^* has to be viewed simply as an abbreviation.

The partition function now becomes

$$Z = e^{\frac{V}{T}\left(-\frac{1}{2}m_\sigma^2\bar\sigma^2+\frac{1}{2}m_\omega^2\bar\omega_0^2\right)}\int \mathcal{D}\bar\psi\mathcal{D}\psi\exp\int_X \bar\psi\left(i\gamma^\mu\partial_\mu - m_N^* + \mu^*\gamma_0\right)\psi\,. \tag{91}$$

The evaluation of the free fermionic part (with modified mass and chemical potential) is now straightforward and was done in detail in the previous semester. So if the following (up to Eq. (99)) is too quick for you, consult Sec. VI in Ref. [10]. One first introduces the Fourier transforms via

$$\psi(X) = \frac{1}{\sqrt{V}}\sum_K e^{-iK\cdot X}\psi(K)\,, \qquad \bar\psi(X) = \frac{1}{\sqrt{V}}\sum_K e^{iK\cdot X}\bar\psi(K)\,, \qquad \int_X e^{iK\cdot X} = \frac{V}{T}\delta_{K,0}\,. \tag{92}$$

Remember that our conventions are $K = (-i\omega_n, \mathbf{k})$, $X = (-i\tau, \mathbf{x})$, and $K\cdot X = k_0x_0 - \mathbf{k}\cdot\mathbf{x} = -(\omega_n\tau + \mathbf{k}\cdot\mathbf{x})$, with the fermionic Matsubara frequencies $\omega_n = (2n+1)\pi T$. Thus, after performing the X integral in the exponent one obtains

$$Z = e^{\frac{V}{T}\left(-\frac{1}{2}m_\sigma^2\bar\sigma^2+\frac{1}{2}m_\omega^2\bar\omega_0^2\right)}\int \mathcal{D}\psi^\dagger\mathcal{D}\psi\exp\left[-\sum_K \psi^\dagger(K)\frac{G^{-1}(K)}{T}\psi(K)\right]\,, \tag{93}$$

with the inverse nucleon propagator

$$G^{-1}(K) = -\gamma^\mu K_\mu - \gamma_0 \mu^* + m_N^* \,. \tag{94}$$

Now using the standard formula for the functional integral over Grassmann variables one obtains

$$Z = e^{\frac{V}{T}\left(-\frac{1}{2}m_\sigma^2\bar{\sigma}^2 + \frac{1}{2}m_\omega^2\bar{\omega}_0^2\right)} \det \frac{G^{-1}(K)}{T} \,, \tag{95}$$

where the determinant is taken over momentum space, Dirac space, and the (here trivial) neutron-proton space. Consequently,

$$\begin{aligned}
\ln Z &= \frac{V}{T}\left(-\frac{1}{2}m_\sigma^2\bar{\sigma}^2 + \frac{1}{2}m_\omega^2\bar{\omega}_0^2\right) + \ln\det\frac{G^{-1}(K)}{T} \\
&= \frac{V}{T}\left(-\frac{1}{2}m_\sigma^2\bar{\sigma}^2 + \frac{1}{2}m_\omega^2\bar{\omega}_0^2\right) + 2\sum_K \left(\ln\frac{\omega_n^2 + (\epsilon_k - \mu^*)^2}{T^2} + \ln\frac{\omega_n^2 + (\epsilon_k + \mu^*)^2}{T^2}\right) \\
&= \frac{V}{T}\left(-\frac{1}{2}m_\sigma^2\bar{\sigma}^2 + \frac{1}{2}m_\omega^2\bar{\omega}_0^2\right) + 4V\int\frac{d^3\mathbf{k}}{(2\pi)^3}\left[\frac{\epsilon_k}{T} + \ln\left(1 + e^{-(\epsilon_k - \mu^*)/T}\right) + \ln\left(1 + e^{-(\epsilon_k + \mu^*)/T}\right)\right] \,,
\end{aligned} \tag{96}$$

where, in the last step, we have performed the Matsubara sum and taken the thermodynamic limit, and where we have defined the single-nucleon energy

$$\epsilon_k = \sqrt{k^2 + (m_N^*)^2} \,. \tag{97}$$

The pressure then becomes

$$P = \frac{T}{V}\ln Z = -\frac{1}{2}m_\sigma^2\bar{\sigma}^2 + \frac{1}{2}m_\omega^2\bar{\omega}_0^2 + P_N \,, \tag{98}$$

with the nucleon pressure (after subtracting the vacuum part)

$$P_N \equiv 4T\int\frac{d^3\mathbf{k}}{(2\pi)^3}\left[\ln\left(1 + e^{-(\epsilon_k - \mu^*)/T}\right) + \ln\left(1 + e^{-(\epsilon_k + \mu^*)/T}\right)\right] \,. \tag{99}$$

The meson condensates have to be determined by maximizing the pressure. We obtain

$$0 = \frac{\partial P}{\partial\bar{\sigma}} = -m_\sigma^2\bar{\sigma} - g_\sigma\frac{\partial P_N}{\partial m_N^*} \,, \tag{100a}$$

$$0 = \frac{\partial P}{\partial\bar{\omega}_0} = m_\omega^2\bar{\omega}_0 - g_\omega\frac{\partial P_N}{\partial\mu^*} \,. \tag{100b}$$

In terms of the baryon and scalar densities

$$n_B = \langle\psi^\dagger\psi\rangle = \frac{\partial P_N}{\partial\mu} = \frac{\partial P_N}{\partial\mu^*} = 4\sum_{e=\pm} e\int\frac{d^3\mathbf{k}}{(2\pi)^3}\frac{1}{e^{(\epsilon_k - e\mu^*)/T} + 1} \,, \tag{101a}$$

$$n_s = \langle\bar{\psi}\psi\rangle = -\frac{\partial P_N}{\partial m_N^*} = 4\sum_{e=\pm}\int\frac{d^3\mathbf{k}}{(2\pi)^3}\frac{m_N^*}{\epsilon_k}\frac{1}{e^{(\epsilon_k - e\mu^*)/T} + 1} \tag{101b}$$

we can write the equations for the condensates as

$$\bar{\sigma} = \frac{g_\sigma}{m_\sigma^2}\, n_s \,, \tag{102a}$$

$$\bar{\omega}_0 = \frac{g_\omega}{m_\omega^2}\, n_B \,. \tag{102b}$$

It is useful to rewrite the first of these equations as an equation for the corrected mass m_N^* rather than for the condensate $\bar{\sigma}$,

$$m_N^* = m_N - \frac{g_\sigma^2}{m_\sigma^2}\, n_s \,. \tag{103}$$

Let us now take the zero temperature limit, $T \ll m_N, \mu$. This is a good approximation since we are interested in cold and dense matter inside a compact star, i.e., temperatures of interest are at most of the order of 10 MeV, while the baryon chemical potentials are above 1 GeV. The Fermi distribution function then becomes a step function. In particular, all antiparticle contributions vanish. Moreover, for the pressure, we use

$$\lim_{T\to 0} T \ln\left(1 + e^{-E/T}\right) = -E\Theta(-E)\,. \tag{104}$$

We obtain[4]

$$P = \frac{1}{2}\frac{g_\omega^2}{m_\omega^2}\, n_B^2 - \frac{1}{2}\frac{g_\sigma^2}{m_\sigma^2}\, n_s^2 + \frac{1}{4\pi^2}\left[\left(\frac{2}{3}k_F^3 - (m_N^*)^2 k_F\right)\epsilon_F^* + (m_N^*)^4 \ln\frac{k_F + \epsilon_F^*}{m_N^*}\right], \tag{107a}$$

$$\epsilon = \frac{1}{2}\frac{g_\omega^2}{m_\omega^2}\, n_B^2 + \frac{1}{2}\frac{g_\sigma^2}{m_\sigma^2}\, n_s^2 + \frac{1}{4\pi^2}\left[\left(2k_F^3 + (m_N^*)^2 k_F\right)\epsilon_F^* - (m_N^*)^4 \ln\frac{k_F + \epsilon_F^*}{m_N^*}\right], \tag{107b}$$

where we have defined the Fermi energy

$$\epsilon_F^* = \mu^* = \sqrt{k_F^2 + (m_N^*)^2}\,, \tag{108}$$

and where the zero-temperature densities are

$$n_B = \frac{2k_F^3}{3\pi^2}\,, \tag{109a}$$

$$n_s = \frac{m_N^*}{\pi}\left[k_F\epsilon_F^* - (m_N^*)^2 \ln\frac{k_F + \epsilon_F^*}{m_N^*}\right]. \tag{109b}$$

Eqs. (107) define the equation of state which has to be determined numerically. We may discuss the limits of small ($k_F \to 0$) and large ($k_F \to \infty$) density analytically. For small density we find

$$n_s \simeq \frac{2k_F^3}{3\pi^2} = n_B\,. \tag{110}$$

Therefore, from Eq. (103) we conclude

$$m_N^* = m_N\,. \tag{111}$$

The pressure and the energy density become

$$P \simeq \frac{2k_F^5}{15 m_N \pi^2}\,, \qquad \epsilon \simeq \frac{2 m_N k_F^3}{3\pi^2}\,, \tag{112}$$

resulting in an equation of state of the form $P \propto \epsilon^{5/3}$.

For large k_F we have

$$n_s \simeq \frac{m_N^* k_F^2}{\pi^2}\,, \tag{113}$$

---

[4] Note that one has to be a bit careful with the thermodynamic relations in deriving the energy density (107b): remember that the "real" chemical potential associated with baryon number n_B is μ, not μ^*. This means that the pressure can be written as $P = -\epsilon + \mu n_B$. The first term of the pressure (term in square brackets on the right-hand side of Eq. (107a)) comes from a term of the structure $-\epsilon_0 + \mu^* n_B$. With $\mu^* = \mu - g_\omega \bar\omega_0$ and the expression for $\bar\omega_0$ in Eq. (102b) we can write this as

$$\begin{aligned} P &= -\epsilon_0 + \mu^* n_B + \frac{1}{2}\frac{g_\omega^2}{m_\omega^2}\, n_B^2 - \frac{1}{2}\frac{g_\sigma^2}{m_\sigma^2}\, n_s^2 \\ &= -\left(\epsilon_0 + \frac{1}{2}\frac{g_\omega^2}{m_\omega^2}\, n_B^2 + \frac{1}{2}\frac{g_\sigma^2}{m_\sigma^2}\, n_s^2\right) + \mu n_B\,. \end{aligned} \tag{105}$$

From this we can read off the energy density

$$\epsilon = \epsilon_0 + \frac{1}{2}\frac{g_\omega^2}{m_\omega^2}\, n_B^2 + \frac{1}{2}\frac{g_\sigma^2}{m_\sigma^2}\, n_s^2\,, \tag{106}$$

which yields Eq. (107b).

and thus

$$m_N^* \simeq \frac{m_N}{1+\frac{g_\sigma^2 k_F^2}{m_\sigma^2 \pi^2}}\,. \tag{114}$$

We see that the effective nucleon mass goes to zero for large densities. For general values of the Fermi momentum, the effective mass has to be computed numerically, see left panel of Fig. 3.

At large densities, the nucleonic pressure as well as the pressure from the scalar meson go like k_F^4. Therefore, the total pressure is dominated by the vector meson contribution which goes like k_F^6,

$$P \simeq \epsilon \simeq \frac{1}{2}\frac{g_\omega^2}{m_\omega^2}\, n_B^2\,. \tag{115}$$

We see that the speed of sound approaches the speed of light at large densities,

$$c_s \equiv \frac{\partial P}{\partial \epsilon} \simeq 1\,. \tag{116}$$

So far, our model cannot be used quantitatively since we have not yet fixed the numerical values of the coupling constants. One uses the full zero-temperature expressions to do so. To this end we require the model to reproduce the binding energy per nucleon and the corresponding saturation density

$$\frac{\epsilon}{n_B} - m_N = 16.3\,\mathrm{MeV}\,, \qquad n_0 = 0.153\,\mathrm{fm}^{-3}\,. \tag{117}$$

One obtains $g_\omega^2/(4\pi) = 14.717$ and $g_\sigma^2/(4\pi) = 9.537$.

Exercise 3: *Solve Eq. (103) at zero temperature numerically for different values of the baryon density. Use the solution to compute the binding energy per nucleon and check that the values (117) are obtained upon using the given values of the coupling constants. In other words, reproduce the results from Fig. 3. (If you are a bit more ambitious you can also do it the other way around: set up and solve the two equations that are needed to determine the coupling constants from the conditions (117.))*

From the shape of the binding energy curve we see that the Walecka model has the feature of self-bound matter, i.e., there is a finite *saturation density* at which the binding energy is minimal (it is then a trivial fact that the values (117) can be fitted with the two free parameters of the model). What is the physical meaning of the self-boundedness? One consequence is that there is a liquid-gas phase transition, shown in Fig. 1. Consider for instance nuclear matter below the saturation density at zero temperature. The fact that there is a minimum of the binding energy at finite density n_0 implies that it is favorable for the nucleons to form liquid droplets of density n_0 rather than to be distributed homogeneously. If we increase the temperature, the density in the droplets will decrease due to the increased kinetic energy of the nucleons. At the same time, the density of the surrounding space (which has zero density at $T = 0$) will increase because single nucleons may evaporate from the droplets. Consequently, there is a mixed phase of droplets (liquid phase) and a gas in which the droplets are immersed. The densities of the two phases approach each other with rising temperature until there is no distinction between the two phases. In the phase diagram of Fig. 1 one is then above the critical point. Note that in this phase diagram the chemical potential is fixed. Therefore, there is no mixed gas-liquid phase present (this phase is shrunk to the line which ends at the critical point.

1. Including scalar interactions

The Walecka model in the previous section accomodates the self-boundedness of nuclear matter, i.e., it has a saturation density. However, the value of this density and the binding energy at this value have to be accomodated by fitting the parameters of the model. Then one can extrapolate the model to higher (and lower) densities, as required for the physics of compact stars. Of course, this extrapolation is not controlled, i.e., a priori we do not know whether reality is well described by the model. Therefore, the Walecka model (and all similar models of this kind) have to be improved in an interplay with experimental observations, for example astrophysical data.

The simple version of the Walecka model discussed so far even has a more severe problem. Even at the saturation density it fails in its prediction for the *compressibility*. The compressibility is defined as

$$K \equiv k_F^2 \frac{d^2(\epsilon/n_B)}{dk_F^2}\,, \tag{118}$$

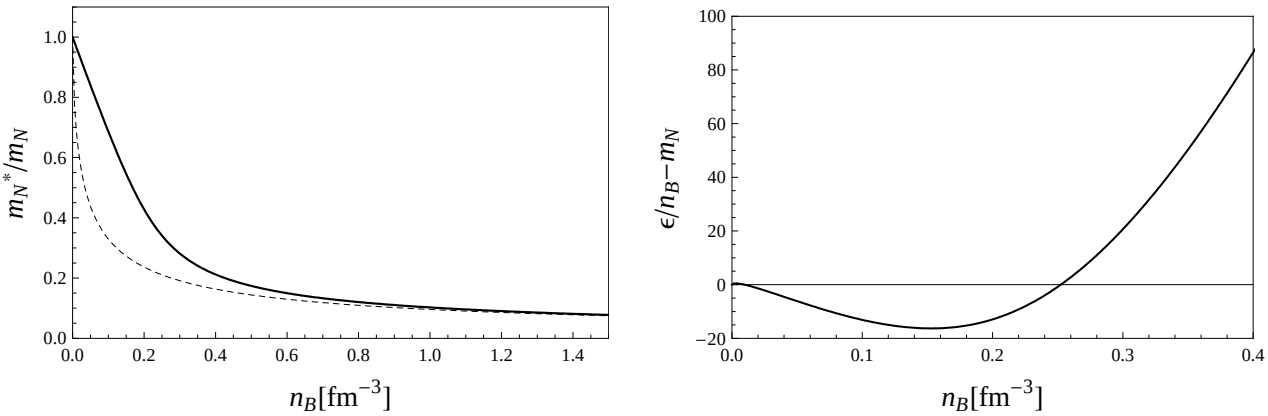

FIG. 3: Left panel: effective nucleon mass in the Walecka model (solid line). The dashed line is the high-density approximation from Eq. (114). Right panel: binding energy per nucleon as a function of density. The two parameters of the Walecka model, namely the coupling constants g_σ and g_ω are fixed such that the binding energy per nucleon is 16.3 MeV at the saturation density $n_0 = 0.153\,\mathrm{fm}^{-3}$.

which can also be written as

$$K = k_F^2 \frac{d^2(\epsilon/n_B)}{dn_B^2} \left(\frac{dn_B}{dk_F}\right)^2 = 9n_B^2 \frac{d^2(\epsilon/n_B)}{dn_B^2}\,, \tag{119}$$

where Eq. (109a) has been used.

It is straightforward to compute K in the given model at the saturation density. One obtains $K = 563\,\mathrm{MeV}$ which is about twice as much as the experimental value. Also the nucleon mass itself can be determined experimentally and compared to the prediction of the model. In total, there are thus four values which the model should reproduce. To improve the model, we add cubic and quartic scalar self-interactions of the form

$$\mathcal{L}_{I,\sigma} = -\frac{b}{3} m_N (g_\sigma \sigma)^3 - \frac{c}{4}(g_\sigma \sigma)^4 \tag{120}$$

to the Lagrangian (81). This introduces two new constants b and c which can be used, together with the two couplings g_σ, g_ω to fit four experimental values. Namely, the two from Eq. (117) plus the compressibility and the *Landau mass*

$$K \simeq 250\,\mathrm{MeV}\,, \qquad m_L = 0.83 m_N\,. \tag{121}$$

The Landau mass is defined as

$$m_L = \frac{k_F}{v_F}\,, \tag{122}$$

where

$$v_F = \frac{\partial \epsilon_k}{\partial k} \tag{123}$$

is the Fermi velocity.

In the mean field approximation, it is easy to include the effect of the scalar self-interactions. The pressure becomes

$$P = -\frac{1}{2} m_\sigma^2 \bar{\sigma}^2 - \frac{b}{3} m_N (g_\sigma \bar{\sigma})^3 - \frac{c}{4}(g_\sigma \bar{\sigma})^4 + \frac{1}{2} m_\omega^2 \bar{\omega}_0^2 + P_N\,, \tag{124}$$

with P_N defined in Eq. (99). The implicit equation for the effective nucleon mass (103) now receives contributions from the additional terms and becomes

$$m_N^* = m_N - \frac{g_\sigma^2}{m_\sigma^2} n_s + \frac{g_\sigma^2}{m_\sigma^2}\left[b m_N (m_N - m_N^*)^2 + c(m_N - m_N^*)^3\right]\,. \tag{125}$$

To fit the four above mentioned values, one has to choose $g_\sigma^2/(4\pi) = 6.003$, $g_\omega^2/(4\pi) = 5.948$, $b = 7.950 \cdot 10^{-3}$, and $c = 6.952 \cdot 10^{-4}$. The numerical result for the binding energy is shown in Fig. 4.

Exercise 4: *Reproduce the result of this figure numerically.*

We see that the behavior at large densities has changed significantly compared to the case without scalar interactions. [End of 4th lecture, April 20, 2009]

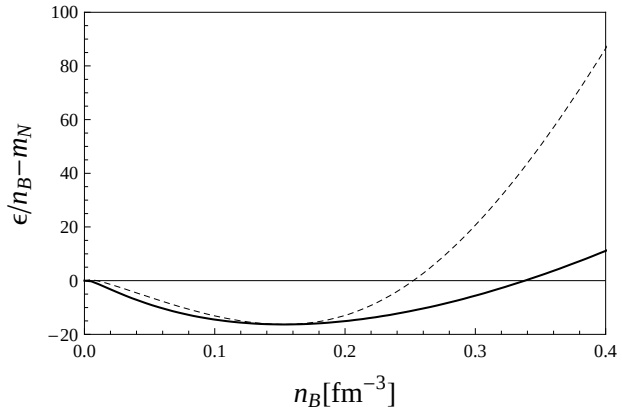

FIG. 4: Binding energy per nucleon as a function of density in the Walecka model, including cubic and quartic scalar self-interactions. The four parameters of the model are fixed to the saturation density, the binding energy per nucleon at the saturation density, the compressibility, and the Landau mass. For comparison, the dashed line shows the result from Fig. 3, i.e., without scalar interactions.

	p	n	Λ	Σ^+	Σ^0	Σ^-	Ξ^0	Ξ^-
m (MeV)	939		1115	1190			1315	
I_3	1/2	−1/2	0	1	0	−1	1/2	−1/2
Q	1	0	0	1	0	−1	0	−1
S	0		−1				−2	
J	1/2							
quark content	uud	udd	uds	uus	uds	dds	uss	dss

TABLE I: Mass, isospin, electric charge, strangeness, spin, and quark content for the spin-1/2 baryon octet.

B. Hyperons

In the interior of a compact star, densities can be as high as several times nuclear saturation density. Therefore, baryons with strangeness, *hyperons*, may occur (as well as muons). The lightest of these states are given by the baryon octet, see Table I.

It is rather straightforward to incorporate hyperons in the kind of model discussed above. Of course, the evaluation becomes a bit more laborious, and the model has many more parameters. Let us therefore briefly discuss the model with the hyperon octet without going into too much detail.

The interaction between the baryons is now extended by interactions mediated by the ϕ and ρ vector mesons. (The ϕ meson has quark content $\bar{s}s$; the ρ meson has the same quark content as a pion, i.e., it can be considered as an excited state of the pion.) The Lagrangian is

$$\begin{aligned}
\mathcal{L} \;=\; & \sum_j \bar{\psi}_j \left(i\gamma^\mu \partial_\mu - m_j + \mu_j \gamma_0 + g_{\sigma j}\sigma - g_{\omega j}\gamma^\mu \omega_\mu - g_{\phi j}\gamma^\mu \phi_\mu - g_{\rho j}\gamma^\mu \rho_\mu^a \tau_a \right) \psi_j \\
& + \frac{1}{2}\left(\partial^\mu \sigma \partial_\mu \sigma - m_\sigma^2 \sigma^2 \right) - \frac{b}{3} m_N (g_\sigma \sigma)^3 - \frac{c}{4}(g_\sigma \sigma)^4 \\
& - \frac{1}{4}\omega^{\mu\nu}\omega_{\mu\nu} + \frac{1}{2} m_\omega^2 \omega^\mu \omega_\mu \\
& - \frac{1}{4}\phi^{\mu\nu}\phi_{\mu\nu} + \frac{1}{2} m_\phi^2 \phi^\mu \phi_\mu \\
& - \frac{1}{4}\rho_a^{\mu\nu}\rho_{\mu\nu}^a + \frac{1}{2} m_\rho^2 \rho_a^\mu \rho_\mu^a \,. \qquad (126)
\end{aligned}$$

Here, j runs over all eight baryons and τ_a are the isospin generators. In a compact star, we have to require chemical

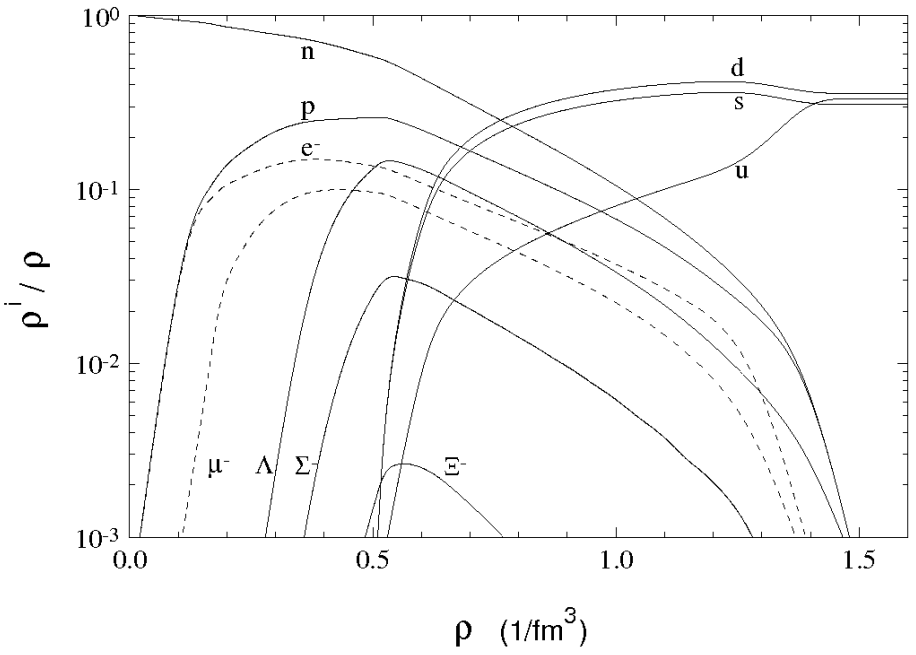

FIG. 5: Density fractions of baryons and leptons (and quarks, for a bag constant $B = 250\,\mathrm{MeV/fm^{-3}}$) as a function of total density. For more details see Ref. [5] and references therein. There is a region of coexistence of deconfined quark matter and baryonic matter, see Sec. IV for a discussion of these mixed phases.

equilibrium with respect to the weak interactions. In the case of hyperons, the conditions are

$$\mu_p = \mu_n - \mu_e\,, \qquad \mu_\Lambda = \mu_n \tag{127a}$$
$$\mu_{\Sigma^+} = \mu_n - \mu_e\,, \qquad \mu_{\Sigma^0} = \mu_n \tag{127b}$$
$$\mu_{\Sigma^-} = \mu_n + \mu_e\,, \qquad \mu_{\Xi^0} = \mu_n \tag{127c}$$
$$\mu_{\Xi^-} = \mu_n + \mu_e\,, \tag{127d}$$

and, including muons, $\mu_e = \mu_\mu$. The conditions (127) all come from weak processes which we have already discussed, see Eqs. (44). For example the process $n \to \Sigma^+ + e + \bar{\nu}_e$ can be understood from the elementary processes as

$$\left.\begin{array}{l} u + e \to s + \nu_e \\ d \to u + e + \bar{\nu}_e \\ d \to u + e + \bar{\nu}_e \end{array}\right\} \qquad udd \to uus + e + \bar{\nu}_e\,. \tag{128}$$

Electric neutrality is given by the constraint

$$n_p + n_{\Sigma^+} = n_e + n_\mu + n_{\Sigma^-} + n_{\Xi^-}\,. \tag{129}$$

We show the result of baryon and lepton density fractions in a model similar to the one discussed here in Fig. 5. As a result of this rough discussion we have learned that hyperons can be included in a rather straightforward extension of the simple Walecka model and that hyperons do appear for sufficiently large densities. The physical reasons are that (*i*) they *can* appear because the baryon chemical potential is large enough to provide energies larger than their mass, (*ii*) they *do* appear because (*a*) the systems seeks to acquire neutrality and does so with electrons at low densities; if hyperons are available, electrons in high-energy states can be replaced by hyperons in low-energy states and (*b*) the system seeks to become isospin symmetric; at low densities it is highly isospin asymmetric, and hyperons with nonzero isospin number provide a means to symmetrize the system.

C. Kaon condensation

Another possible variant of nuclear matter, besides the occurrence of hyperons, is meson condensation. Originally, pion condensation was suggested [23]. Only many years later, it was realized that kaon condensation is possible in

compact stars [24]. This is somewhat surprising since kaons are much heavier than pions and thus pion condensation seems more likely. However, in the medium, the effective kaon mass becomes sufficiently light in order to trigger a kaon condensate.

To explain kaon condensation, we introduce several concepts. We first have to say what a kaon is and will do so with the help of chiral symmetry and spontaneous breaking thereof. Then, we will discuss chiral perturbation theory. This is one possible method to study kaon condensation and has been used in the original work [24]. For another approach, using models similar to the above discussed Walecka model, see for instance Ref. [25] and references therein. The evaluation of the chiral model has to be done numerically, so we will more or less only be concerned with setting up and understanding the basic equations. As a modest goal, we will try to understand the onset of kaon condensation, i.e., we will show how to compute the critical baryon density at which there is a second-order phase transition to the kaon-condensed phase.

1. Chiral symmetry of QCD

Kaon condensation can be discussed in a low-energy effective theory, here chiral perturbation theory. This theory should describe the fundamental theory, QCD, in the low-energy limit. In order to construct the theory, we need to understand the underlying symmetries. The fermionic part of the QCD Lagrangian is

$$\mathcal{L}_{\rm QCD} = i\bar{\psi}\gamma^\mu D_\mu \psi - \bar{\psi} M \psi + \mathcal{L}_{\rm gluons}\,, \tag{130}$$

with $\bar{\psi} = \psi^\dagger \gamma_0$, with the mass matrix

$$M = \begin{pmatrix} m_u & 0 & 0 \\ 0 & m_d & 0 \\ 0 & 0 & m_s \end{pmatrix}, \tag{131}$$

and the covariant derivative $D_\mu = \partial_\mu - igT_a A^a_\mu$, where T_a ($a = 1, \ldots 8$) are the generators of the color gauge group $SU(3)_c$ and A^a_μ the corresponding gauge fields. Here we are only interested in the transformations of the fermion fields and the resulting symmetries of the Lagrangian. Therefore, we ignore the purely gluonic contribution to the Lagrangian. Also later, when we shall use QCD for explicit calculations, the gluonic part is negligible because we always work at very small temperatures compared to the quark (or baryon) chemical potential.

We now introduce the chirality projectors

$$P_R = \frac{1+\gamma_5}{2}\,, \qquad P_L = \frac{1-\gamma_5}{2}\,. \tag{132}$$

They obey the identities

$$P^2_{R/L} = P_{R/L}\,, \qquad P^\dagger_{R/L} = P_{R/L}\,, \qquad P_R P_L = 0\,, \qquad P_R + P_L = 1\,, \tag{133}$$

i.e., they are a complete set of orthogonal projectors. (To see these identities one needs $\gamma_5^2 = 1$ and $\gamma_5^\dagger = \gamma_5$.) For a physical picture, remember that, for massless quarks, chirality eigenstates are also eigenstates of helicity. Therefore, in this case, one can picture chirality as helicity (= projection of the momentum of the fermion onto its spin). We define left- and right-handed quark spinors by

$$\psi_{R/L} \equiv P_{R/L}\psi\,, \tag{134}$$

such that $\psi = P_R\psi + P_L\psi = \psi_R + \psi_L$. Then, using

$$\{\gamma_5, \gamma_\mu\} = 0\,, \tag{135}$$

we can write the Lagrangian as

$$\mathcal{L}_{\rm QCD} = i\bar{\psi}_R\gamma^\mu D_\mu \psi_R + i\bar{\psi}_L\gamma^\mu D_\mu \psi_L - \bar{\psi}_R M \psi_L - \bar{\psi}_L M \psi_R\,. \tag{136}$$

Let us first discuss the massless case, $M = 0$. In this case, separate rotations of left- and right-handed spinors leave the Lagrangian invariant,

$$\psi_R \to e^{i\phi^a_R t_a}\psi_R\,, \qquad \psi_L \to e^{i\phi^a_L t_a}\psi_L\,. \tag{137}$$

Since we talk about the 3-flavor case, t_a are the nine generators of the flavor group $U(3)$, i.e., $t_0 = \mathbf{1}$ and $t_a = T_a$ ($a = 1, \dots 8$) the Gell-Mann matrices. Consequently, the Lagrangian is invariant under $U(3)_L \times U(3)_R$. The corresponding Noether currents are

$$J^a_{\mu,R/L} = \bar\psi_{R/L} \gamma_\mu t^a \psi_{R/L} \,. \tag{138}$$

As usual, this can be seen by formally making the flavor transformation local and writing down the equation of motion for the field $\phi^a_{R/L}(x)$, see for instance the lecture notes of the previous semester, Sec. V of Ref. [10]. We can also rewrite these currents as vector and axial-vector currents

$$V^a_\mu \equiv J^a_{\mu,R} + J^a_{\mu,L} = \bar\psi \gamma_\mu t^a \psi \,, \tag{139a}$$

$$A^a_\mu \equiv J^a_{\mu,R} - J^a_{\mu,L} = \bar\psi \gamma_\mu t^a \gamma_5 \psi \,. \tag{139b}$$

To see this, note that $P_R \gamma_5 = P_R$ and $P_L \gamma_5 = -P_L$. In fact, in QCD the singlet (= t_0-component of the) axial-vector current is not conserved (which is referred to as the *anomaly*),

$$\partial^\mu A^0_\mu = \frac{N_f}{8\pi^2} \mathrm{Tr}[G_{\mu\nu} \tilde G^{\mu\nu}] \,, \tag{140}$$

where $G_{\mu\nu}$ is the gluon field strength and $\tilde G^{\mu\nu} = \epsilon^{\mu\nu\sigma\rho} G_{\sigma\rho}$ the dual field strength. We are left with the symmetry group $SU(3)_R \times SU(3)_L \times U(1)_V$. The vector symmetry $U(1)_V$ corresponds to baryon number conservation, and the flavor symmetry group $SU(3)_R \times SU(3)_L$ is referred to as *chiral symmetry*. As we can see from Eq. (136), nonzero masses break the chiral symmetry *explicitly* (they still preserve the vector part of the chiral symmetry).

Spontaneous breaking of the chiral symmetry is realized by a chiral condensate of the form $\langle \bar\psi_L \psi_R \rangle$. We shall not discuss the details of this mechanism. It is analogous to spontaneous symmetry breaking in simple models such as ϕ^4 theory (see for instance Sec. IX in the lecture notes of the previous semester [10]), or in a superconductor, or in the Higgs mechanism. Just as the mass terms, the chiral condensate is only invariant under simultaneous right- and left-handed rotations, i.e., the symmetry breaking pattern is

$$G \equiv SU(3)_R \times SU(3)_L \to H \equiv SU(3)_{R+L} \,. \tag{141}$$

As a comparison, remember that in ϕ^4 theory, $G = U(1)$, $H = \mathbf{1}$. Spontaneous breaking of a global symmetry goes along with massless Goldstone bosons. Here, there are eight generators of the coset space G/H, i.e., there are eight Goldstone modes. They are described by the $SU(3)$ matrix

$$U = e^{i \phi_a T_a / f_\pi} \,, \tag{142}$$

with the pion decay constant $f_\pi \simeq 93\,\mathrm{MeV}$. The mesons of the Goldstone octet are parametrized as

$$\phi_a T_a = \begin{pmatrix} \frac{\pi^0}{\sqrt{2}} + \frac{\eta}{\sqrt{6}} & \pi^+ & K^+ \\ \pi^- & -\frac{\pi^0}{\sqrt{2}} + \frac{\eta}{\sqrt{6}} & K^0 \\ K^- & \bar K^0 & -\sqrt{\frac{2}{3}}\eta \end{pmatrix} . \tag{143}$$

Since the rows (columns) of this matrix carry left-handed flavor (right-handed anti-flavor) labels, it is easy to read off the quark content of the various mesons, e.g., $K^+ \sim \bar s u$, $\pi^+ \sim \bar d u$ etc. According to its chiral structure, the chiral matrix transforms under a transformation $g = (g_L, g_R) \in G$ as

$$U \to g_L U g_R^\dagger \,. \tag{144}$$

2. Chiral Lagrangian

In the (unrealistic) case of vanishing quark masses, the chiral symmetry is an exact symmetry and the Goldstone bosons are exactly massless. Quark masses break the chiral symmetry explicitly. However, if the masses are small (small compared to the characteristic scale of chiral symmetry breaking $\sim 1\,\mathrm{GeV}$) we can still consider the chiral symmetry as approximate, and the Goldstone bosons (now more precisely *pseudo*-Goldstone bosons) have a small

mass. In particular, we might still hope to describe the system at low energies by an effective theory which is built on the underlying chiral symmetry. We require the mass matrix M to transform just as the chiral field U, i.e.,

$$M \to g_L M g_R^\dagger \,. \tag{145}$$

We require the chiral Lagrangian to be invariant under G. Then, the kinetic term and the mass term are

$$\mathcal{L}_U = \frac{f_\pi^2}{4}\mathrm{Tr}[\partial_\mu U \partial^\mu U^\dagger] + c\mathrm{Tr}[M^\dagger(U-1) + M(U^\dagger - 1)] \,, \tag{146}$$

where the trace is taken over flavor space. The two constants f_π and c which have to be fitted to experimental values, similarly as we have discussed for the constants of the Walecka model. Note that the vacuum (all Goldstone fields ϕ_a vanish) corresponds to $U = 1$. Hence the -1 in the last two terms ensures that the vacuum Lagrangian vanishes. In principle, higher order terms in U can be added. Note however, that the Goldstone fields themselves appear in the exponent, i.e., they are already present to all orders.

[End of 5th lecture, April 27, 2009]

In the context of compact stars, we do not only want to describe isolated mesons. We also need to include baryons and their interactions. We summarize the baryon octet in the matrix

$$B = \begin{pmatrix} \frac{\Sigma^0}{\sqrt{2}} + \frac{\Lambda}{\sqrt{6}} & \Sigma^+ & p \\ \Sigma^- & -\frac{\Sigma^0}{\sqrt{2}} + \frac{\Lambda}{\sqrt{6}} & n \\ \Xi^- & \Xi^0 & -\sqrt{\frac{2}{3}}\Lambda \end{pmatrix} , \tag{147}$$

which includes the proton, the neutron and the hyperons from Table I. then, the free baryon Lagrangian is

$$\mathcal{L}_B = \mathrm{Tr}[\bar{B}(i\gamma^\mu\partial_\mu - m_B)B] \,, \tag{148}$$

where $m_B \simeq 1.2\,\mathrm{GeV}$ is the $SU(3)_L \times SU(3)_R$ symmetric baryon mass. To write down the interaction between baryons and the mesons it is convenient to decompose the chiral field into left- and right-handed fields,

$$U = \xi_L \xi_R^\dagger \,, \tag{149}$$

where, without loss of generality, we may choose

$$\xi \equiv \xi_L = \xi_R^\dagger \,, \tag{150}$$

such that

$$U = \xi^2 \,. \tag{151}$$

We now add the meson-baryon interaction terms

$$\begin{aligned} \mathcal{L}_I &= i\mathrm{Tr}[\bar{B}\gamma_\mu[V^\mu, B]] + D\,\mathrm{Tr}[\bar{B}\gamma_\mu\gamma_5\{A^\mu, B\}] + F\,\mathrm{Tr}[\bar{B}\gamma_i\gamma_5[A_i, B]] \\ &\quad + a_1\mathrm{Tr}[B^\dagger(\xi M\xi + \xi^\dagger M^\dagger \xi^\dagger)B] + a_2\mathrm{Tr}[B^\dagger B(\xi M\xi + \xi^\dagger M^\dagger\xi^\dagger)] + a_3\mathrm{Tr}[B^\dagger B]\mathrm{Tr}[M\xi^2 + M^\dagger(\xi^\dagger)^2] \,, \end{aligned} \tag{152}$$

with the additional constants D, F, a_1, a_2, a_3, and the vector and axial-vector currents

$$V_\mu = \frac{1}{2}(\xi^\dagger\partial_\mu\xi + \xi\partial_\mu\xi^\dagger) \,, \tag{153a}$$

$$A_\mu = \frac{i}{2}(\xi^\dagger\partial_\mu\xi - \xi\partial_\mu\xi^\dagger) \,. \tag{153b}$$

The Lagrangian is an expansion in M/Λ and ∂/Λ, where Λ is the scale of chiral symmetry breaking, $\Lambda \sim 1\,\mathrm{GeV}$. Higher order terms in these parameters are omitted. We shall also drop the terms coming from $\boldsymbol{\gamma}\cdot\mathbf{V}$ and $\gamma_0\gamma_5 A_0$ which is consistent with this expansion. In summary, we have the Lagrangian

$$\mathcal{L} = \mathcal{L}_U + \mathcal{L}_B + \mathcal{L}_I \,. \tag{154}$$

Later we shall also add electron and muon contributions, but they are simple and we ignore them for now.

3. Kaon-nucleon matter

We now drop all mesons other than the charged kaons and all baryons other than the proton and the neutron. Let us temporarily abbreviate the exponent of the chiral matrix by

$$U = e^{iQ} = \cos Q + i \sin Q\,, \qquad Q \equiv \frac{\phi_4 T_4 + \phi_5 T_5}{f_\pi} = \frac{1}{2f_\pi} \begin{pmatrix} 0 & 0 & \phi_4 - i\phi_5 \\ 0 & 0 & 0 \\ \phi_4 + i\phi_5 & 0 & 0 \end{pmatrix}. \tag{155}$$

We find $Q^2 = \phi^2/(2f_\pi)^2\,\mathrm{diag}(1,0,1)$, with

$$\phi^2 \equiv \phi_4^2 + \phi_5^2\,. \tag{156}$$

Consequently, we can write $Q^2 = P^2$ with $P \equiv \phi/(2f_\pi)\mathrm{diag}(1,0,1)$. From this identity we conclude

$$\cos Q = 1 - \frac{Q^2}{2!} + \frac{Q^4}{4!} - \ldots = 1 - \frac{P^2}{2!} + \frac{P^4}{4!} - \ldots = \begin{pmatrix} \cos[\phi/(2f_\pi)] & 0 & 0 \\ 0 & 1 & 0 \\ 0 & 0 & \cos[\phi/(2f_\pi)] \end{pmatrix}. \tag{157}$$

And

$$\sin Q = Q - \frac{Q^3}{3!} + \frac{Q^5}{5!} - \ldots = QP'(P - \frac{P^3}{3!} + \frac{P^5}{5!} - \ldots) = QP' \begin{pmatrix} \sin[\phi/(2f_\pi)] & 0 & 0 \\ 0 & 0 & 0 \\ 0 & 0 & \sin[\phi/(2f_\pi)] \end{pmatrix}, \tag{158}$$

where $P' \equiv 2f_\pi/\phi\,\mathrm{diag}(1,0,1)$. Performing the remaining matrix multiplications yields

$$\sin Q = \begin{pmatrix} 0 & 0 & (\phi_4 - i\phi_5)/\phi\,\sin[\phi/(2f_\pi)] \\ 0 & 0 & 0 \\ (\phi_4 + i\phi_5)/\phi\,\sin[\phi/(2f_\pi)] & 0 & 0 \end{pmatrix}. \tag{159}$$

Consequently,

$$U = \begin{pmatrix} \cos[\phi/(2f_\pi)] & 0 & i(\phi_4 - i\phi_5)/\phi\,\sin[\phi/(2f_\pi)] \\ 0 & 1 & 0 \\ i(\phi_4 + i\phi_5)/\phi\,\sin[\phi/(2f_\pi)] & 0 & \cos[\phi/(2f_\pi)] \end{pmatrix}. \tag{160}$$

Now we replace the fields $\phi_{4,5}$ by vacuum expectation values, accounting for kaon condensation. We shall neglect the fluctuations around this background, and introduce a time dependence of these condensates in the following form

$$\langle K^- \rangle = \frac{\langle\phi_4\rangle + i\langle\phi_5\rangle}{2} = \theta\, f_\pi e^{-i\mu t}\,, \tag{161a}$$

$$\langle K^+ \rangle = \frac{\langle\phi_4\rangle - i\langle\phi_5\rangle}{2} = \theta\, f_\pi e^{i\mu t}\,, \tag{161b}$$

where μ plays the role of a kaon chemical potential (as we shall see more explicitly below). In this parametrization we have $\phi \to 2\theta f_\pi$ and thus

$$U = \begin{pmatrix} \cos\theta & 0 & ie^{i\mu t}\sin\theta \\ 0 & 1 & 0 \\ ie^{-i\mu t}\sin\theta & 0 & \cos\theta \end{pmatrix}. \tag{162}$$

We are now prepared to evaluate the various terms in the Lagrangian. We shall neglect the masses of the up and down quarks such that $M \simeq \mathrm{diag}(0,0,m_s)$. We also define the kaon mass

$$m_K^2 = \frac{2cm_s}{f_\pi^2} \tag{163}$$

(note that the constant c has mass dimension 3). This yields

$$\mathcal{L}_U = \frac{f_\pi^2 \mu^2}{2} \sin^2\theta + m_K^2 f_\pi^2 (\cos\theta - 1)\,. \tag{164}$$

Expanding this expression for small condensates θ yields

$$\mathcal{L}_U \simeq \frac{\mu^2 - m_K^2}{2}\, f_\pi^2 \theta^2\,. \tag{165}$$

This is the familiar expression for the (negative) free energy of a non-interacting Bose condensate with chemical potential μ and mass m_K.

The free baryon Lagrangian trivially becomes

$$\mathcal{L}_B = \bar{p}(i\gamma^\mu \partial_\mu - m_N)p + \bar{n}(i\gamma^\mu \partial_\mu - m_N)n\,. \tag{166}$$

For the other terms we need

$$\xi = \begin{pmatrix} \cos\theta/2 & 0 & ie^{i\mu t}\sin\theta/2 \\ 0 & 1 & 0 \\ ie^{-i\mu t}\sin\theta/2 & 0 & \cos\theta/2 \end{pmatrix}. \tag{167}$$

From this we compute the currents $A_i = 0$ (since there is no spatial dependence in the condensate) and

$$V_0 = i\mu \sin^2\theta/2 \begin{pmatrix} -1 & 0 & 0 \\ 0 & 0 & 0 \\ 0 & 0 & 1 \end{pmatrix}. \tag{168}$$

Hence the various nonzero terms needed for $\mathcal{L}_I$ become

$$\begin{aligned}
i\mathrm{Tr}[\bar{B}\gamma_0[V_0, B]] &= \mu\,(2p^\dagger p + n^\dagger n)\sin^2\theta/2\,, && \text{(169a)}\\
a_1\mathrm{Tr}[B^\dagger(\xi M\xi + \xi^\dagger M^\dagger \xi^\dagger)B] &= -2a_1 m_s\, p^\dagger p \sin^2\theta/2\,, && \text{(169b)}\\
a_2\mathrm{Tr}[B^\dagger B(\xi M\xi + \xi^\dagger M^\dagger \xi^\dagger)] &= 2a_2 m_s (p^\dagger p + n^\dagger n)\cos^2\theta/2\,, && \text{(169c)}\\
a_3\mathrm{Tr}[B^\dagger B]\mathrm{Tr}[M\xi^2 + M^\dagger(\xi^\dagger)^2] &= 2a_3 m_s (p^\dagger p + n^\dagger n)(1 - 2\sin^2\theta/2)\,. && \text{(169d)}
\end{aligned}$$

It is left as a simple exercise to verify these results. Consequently, the Lagrangian becomes

$$\mathcal{L} = \frac{f_\pi^2\mu^2}{2}\sin^2\theta + m_K^2 f_\pi^2(\cos\theta - 1) + \bar{p}[i\gamma^\mu\partial_\mu - m_N + \gamma_0(\mu_p^* + m_N)]p + \bar{n}[i\gamma^\mu\partial_\mu - m_N + \gamma_0(\mu_n^* + m_N)]n\,, \tag{170}$$

with the effective chemical potentials

$$\begin{aligned}
\mu_p^* &= 2(a_2 + a_3)m_s - m_N + 2[\mu - (a_1 + a_2 + 2a_3)m_s]\sin^2\theta/2\,, && \text{(171a)}\\
\mu_n^* &= 2(a_2 + a_3)m_s - m_N + 2[\mu/2 - (a_2 + 2a_3)m_s]\sin^2\theta/2\,. && \text{(171b)}
\end{aligned}$$

(We have included the nucleon mass m_N into the definition for later convenience; it will drop out later in the nonrelativistic approximation.) These quantities μ_p^*, μ_n^* appear as chemical potentials in the Lagrangian. It should be remembered, however, that these are not the real chemical potentials associated with nucleon number. The latter ones are denoted μ_p and μ_n and have not yet been included. We can now, analogously to Sec. III A, compute the energy density from $\mathcal{L}$,

$$\begin{aligned}
\epsilon_{n,p,K} &= -\frac{f_\pi^2\mu^2}{2}\sin^2\theta + m_K^2 f_\pi^2(1 - \cos\theta) + 2\sum_{i=p,n}\int \frac{d^3\mathbf{k}}{(2\pi)^3}\left[\sqrt{k^2 + m_N^2} - (\mu_i^* + m_N)\right]\Theta(k_{F,i} - k) \\
&\simeq -\frac{f_\pi^2\mu^2}{2}\sin^2\theta + m_K^2 f_\pi^2(1 - \cos\theta) + \frac{3}{5}\left[\rho_p\frac{(3\pi^2\rho_p)^{2/3}}{2m_N} + \rho_n\frac{(3\pi^2\rho_n)^{2/3}}{2m_N}\right] - \rho_p\mu_p^* - \rho_n\mu_n^*\,, \qquad \text{(172)}
\end{aligned}$$

where we denoted the nucleon densities by $\rho_i = k_{F,i}^3/(3\pi^2)$, and where we employed the nonrelativistic approximation $\sqrt{k^2 + m_N^2} \simeq m_N + k^2/(2m_N)$.

Next, we have to find the relations between the various chemical potentials through the conditions of chemical equilibrium. We already know the leptonic processes with nucleons,

$$n \to p + \ell + \bar{\nu}_\ell \,, \qquad p + \ell \to n + \nu_\ell \,. \tag{173}$$

Here, $\ell = e, \mu$ can either be an electron or a muon. We also have the purely leptonic processes,

$$e \to \mu + \bar{\nu}_\mu + \nu_e \,, \qquad \mu \to e + \bar{\nu}_e + \nu_\mu \,, \tag{174}$$

and the processes involving kaons,

$$n \leftrightarrow p + K^- \,, \qquad e \leftrightarrow K^- + \nu_e \,. \tag{175}$$

These processes lead to the independent conditions

$$\mu_e = \mu = \mu_\mu \,, \qquad \mu_n = \mu_p + \mu_e \,. \tag{176}$$

(Remember that μ denotes the kaon chemical potential.) We shall be interested in the case of fixed baryon density, i.e., we shall determine the proton fraction dynamically. Therefore, we need to add a term $\mu\rho_p$ to the energy density (note that μ counts negative charge, hence we need to add, not subtract, this term). Also we add the electron and muon contributions to obtain

$$\begin{aligned} \epsilon &= \epsilon_{n,p,K} + \mu\rho_p + \epsilon_e - \mu\rho_e + \Theta(\mu^2 - m_\mu^2)(\epsilon_\mu - \mu\rho_\mu) \\ &= -\frac{f_\pi^2 \mu^2}{2} \sin^2\theta + m_K^2 f_\pi^2 (1 - \cos\theta) + E - \rho_p \mu_p^* - \rho_n \mu_n^* + \mu\rho_p \\ &\quad - \frac{\mu^4}{12\pi^2} + \Theta(\mu^2 - m_\mu^2) \left(\epsilon_\mu - \mu \frac{k_{F,\mu}^3}{3\pi^2} \right) \,, \end{aligned} \tag{177}$$

where we abbreviated

$$E \equiv \frac{3}{5} \left[\rho_p \frac{(3\pi^2\rho_p)^{2/3}}{2m_N} + \rho_n \frac{(3\pi^2\rho_n)^{2/3}}{2m_N} \right] \,. \tag{178}$$

The muon energy density ϵ_μ is given by an expression analogous to Eq. (107b). However, its specific form is irrelevant for the following. By introducing the step function we take into account that muons only appear if μ is larger than their mass $m_\mu = 106\,\mathrm{MeV}$. We introduce the proton fraction x and nuclear saturation density ρ_0 via

$$\rho_p = x\rho \,, \qquad \rho_n = (1-x)\rho \,, \qquad \rho = \rho_0 u \,. \tag{179}$$

Then, we minimize the energy with respect to x and θ and require charge neutrality, i.e., we need to solve the three equations

$$\frac{\partial \epsilon}{\partial x} = \frac{\partial \epsilon}{\partial \theta} = \frac{\partial \epsilon}{\partial \mu} = 0 \,. \tag{180}$$

They read

$$\mu = -\frac{1}{u\rho_0 \cos^2\theta/2} \frac{\partial E}{\partial x} - 2a_1 m_s \tan^2\theta/2 \,, \tag{181a}$$

$$0 = f_\pi^2 \mu \sin^2\theta + (1+x)\rho_0 u \sin^2\theta/2 - x\rho_0 u + \frac{\mu^3}{3\pi^2} + \Theta(\mu^2 - m_\mu^2) \frac{(\mu^2 - m_\mu^2)^{3/2}}{3\pi^2} \,, \tag{181b}$$

$$0 = \left\{ \cos\theta - \frac{m_K^2}{\mu^2} + \frac{\rho_0 u}{\mu^2 f_\pi^2} \left[\frac{\mu}{2}(1+x) - (a_1 x + a_2 + 2a_3) m_s \right] \right\} \sin\theta \,. \tag{181c}$$

We see that the third equation is trivially fulfilled for a vanishing kaon condensate, $\theta = 0$. To determine the solutions for a nonvanishing kaon condensate, one divides the third equation by $\sin\theta$. This also means that we can determine the critical density where kaon condensation sets in by setting $\theta = 0$ in the first two equations and dropping the third (which then is trivially fulfilled).

Exercise 5: *Solve these equations numerically to determine the critical baryon density for the onset of kaon condensation. Compute then the neutron, proton, electron, muon, and kaon densities as a function of the baryon density and compare the result with Fig. 6. (You should consult Ref. [26] where E is replaced by an expansion around the isospin symmetric case $x = 1/2$, see Eq. (2.34) in this reference.)*

[End of 6th lecture, May 4, 2009]

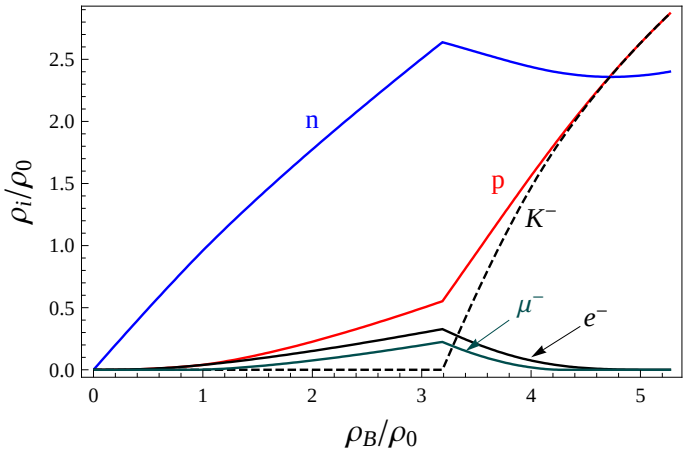

FIG. 6: Density contributions of neutrons (blue), protons (red), electrons (black solid), muons (green), and the kaon condensate (black dashed) from Eqs. (181) with E modified as described in Ref. [26] (and the choice of the function $F(u) = u$ in this modification). The parameters are (also taken from Ref. [26]) $a_1 m_s = -67\,\mathrm{MeV}$, $a_2 m_s = 134\,\mathrm{MeV}$, $a_3 m_s = -222\,\mathrm{MeV}$, $m_\mu = 106\,\mathrm{MeV}$, $f_\pi = 93\,\mathrm{MeV}$, $m_K = 494\,\mathrm{MeV}$. We see that the onset of kaon condensation is around $\rho_B \simeq 3.2\rho_0$.

IV. FROM HADRONIC TO QUARK PHASES: POSSIBILITY OF A MIXED PHASE

We have already mentioned the possibility of a hybrid star, i.e., a star with a quark matter core surrounded by nuclear matter. How does the interface between these two phases look? Is it a sharp interface or is there a shell in the star where the hadronic and quark phases coexist? If the former is true, there will be a jump in the density profile of the star, while the latter allows for a continuous change in density.

Mixed phases are a very general phenomenon. In our context, not only the mixed hadronic/quark matter phase is of relevance, but also for instance phases in the inner crust of the star. There one may expect a neutron superfluid coexisting with a lattice of ions, i.e., a mixed phase of neutron matter and nuclei. In this lecture, we shall not discuss the properties of the crust of a compact star, although this is an interesting topic and important for the phenomenology of the star. See for instance chapter 3 in Ref. [3] for a detailed discussion of the structure of the crust. Other examples of mixed phases, independent of our context, are liquid-gas mixtures or simply a solid, which is a mixture of an electron gas and nuclear matter (sitting in the lattice of ions).

In Fig. 7 the possibility of a mixed phase is illustrated. We see that the condition of charge neutrality plays an important role here. It is important that in a neutron star, charge neutrality is required globally, not locally. In other words, certain regions in the star may very well have a nonzero electric charge as long as other regions have opposite charge to ensure an overall vanishing charge.

It is plausible that such a mixed phase will have a crystalline structure. For instance, one phase may form spheres which are immersed in the other phase. Other possibilities are rods or slabs. In any case, if a mixed phase is possible because of a general argument such as given in Fig. 7, this does not mean that it is indeed realized. One has to take into account Coulomb forces (which seek to break charged regions into smaller regions) and surface forces (which seek to minimize the surface and thus work in the opposite direction). We shall not discuss these forces quantitatively but rather give some general arguments about mixed phases.

We start from the simple picture that at small quark density (or quark chemical potential μ) the hadronic phase is preferred and that there is a first-order phase transition to the quark matter phase at some critical density (or chemical potential). The question is whether there is a mixed phase between these two pure phases. The pressures of the two phases $P_h(\mu, \mu_e)$ and $P_q(\mu, \mu_e)$ depend on the quark chemical potential and the charge chemical potential μ_e (we work at zero temperature). Phase coexistence is possible when the pressures of the two phases is equal,

$$P_h(\mu, \mu_e) = P_q(\mu, \mu_e)\,. \tag{182}$$

Now suppose the neutrality condition were *local* (which it isn't in our context). Then the charge must vanish in each phase separately,

$$Q_h(\mu, \mu_e) = Q_q(\mu, \mu_e) = 0\,. \tag{183}$$

These two conditions yield μ_e for each phase separately as a function of μ, $\mu_e^h(\mu)$ and $\mu_e^q(\mu)$. Consequently, the

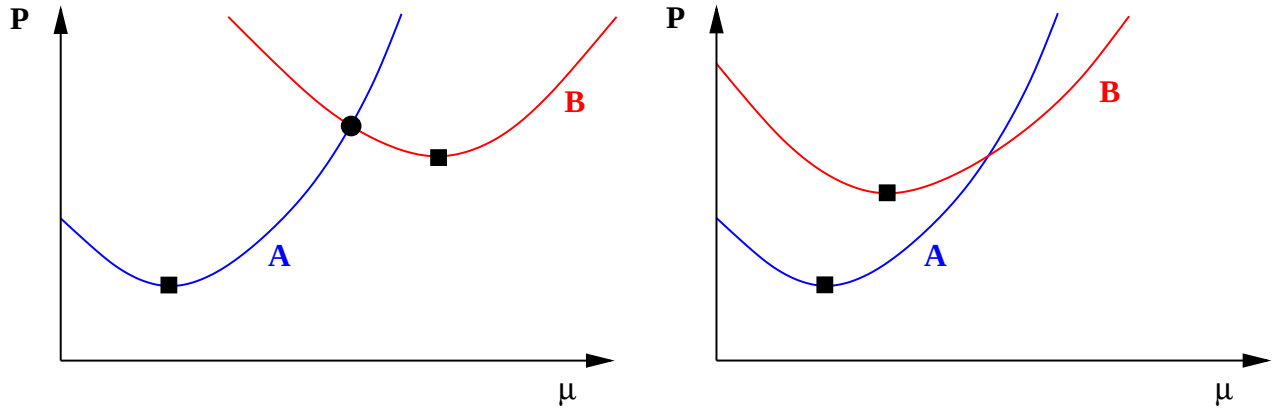

FIG. 7: Illustration for the possibility of a mixed phase. The pressure P of two phases A and B is given by the respective curves as a function of a chemical potential μ. Note that $\partial P/\partial\mu$ has to increase with increasing μ (increasing μ cannot lead to a decrease of the corresponding charge; this would lead to an instability). Suppose μ is the electric charge chemical potential and we require charge neutrality. Then the squares mark the points at which a given phase is charge neutral. The circle in the left panel marks a point where the two phases have equal pressure and opposite charge. Since this point has higher pressure than either of the squares, this is the ground state (neglecting surface tension and Coulomb energy). In this state, phase A and B coexist and occupy different volume fractions, determined by the different slopes of the curves. In the right panel, there is no point where both phases have equal pressure and opposite charges. Therefore, the square on the curve B is the ground state.

condition of equal pressure,

$$P_h(\mu, \mu_e^h(\mu)) = P_q(\mu, \mu_e^q(\mu))\,, \tag{184}$$

yields a unique μ. Only at this μ do the phases coexist. This amounts to a sharp interface at a given value for the pressure, where on both sides of the interface the pure hadronic and the pure quark phases exist with different densities, i.e., there is a density jump in the profile of the star.

Now we only impose *global* neutrality. This means that in any mixed phase only the total charge has to vanish. We denote

$$\chi = \frac{V_q}{V_h + V_q} \in [0, 1]\,, \tag{185}$$

where V_q and V_h are volume fractions of the quark and hadron phases, respectively. Then, neutrality reads

$$(1-\chi)Q_h(\mu, \mu_e) + \chi Q_q(\mu, \mu_e) = 0\,. \tag{186}$$

This yields a function $\mu_e(\chi, \mu)$ which is then inserted into the condition of equal pressure,

$$P_h(\mu, \mu_e(\chi, \mu)) = P_q(\mu, \mu_e(\chi, \mu))\,. \tag{187}$$

The result is a chemical potential as a function of χ, $\mu(\chi)$. Thus there is a finite interval on the μ-axis where a mixed phase is possible. We see that the looser condition of global charge neutrality allows for a shell with a mixed phase in a hybrid star.

These formal arguments become more understandable in a geometric picture, see Fig. 8.

We shall not go into the details of an explicit calculation of the mixed phase. Even neglecting surface tension and Coulomb energy, these calculations are numerical and not appropriate for this lecture. Therefore, we simply discuss a result of such a calculation, see Fig. 9 (see also Fig. 5 where we have already seen a mixed phase). One recovers the (projection of the) topology of Fig. 8 in Fig. 9.

V. SUPERCONDUCTIVITY AND SUPERFLUIDITY IN A COMPACT STAR

In our discussion of interacting nuclear matter we have so far ignored a very important physical effect. We have not included the possibility of superfluidity and/or superconductivity. We have briefly discussed one effect of superconductivity for quark matter, see Sec. II C. In the following, we shall discuss these effects in more detail. But first we

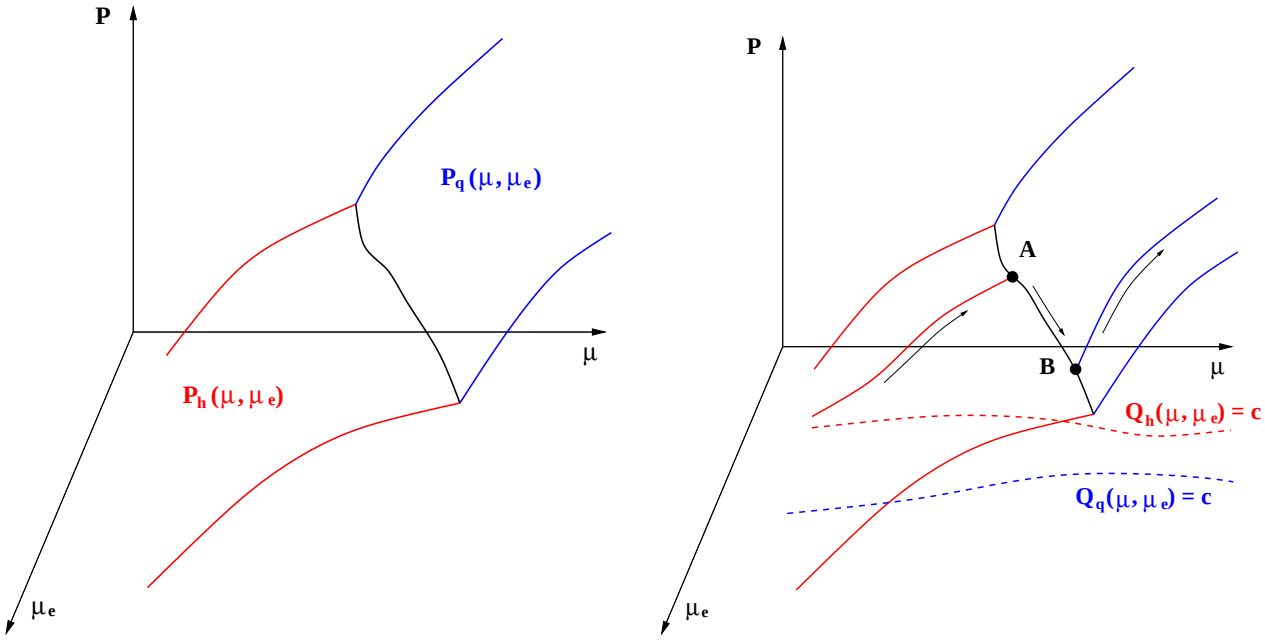

FIG. 8: Schematic picture of a hadron-quark mixed phase in a finite interval of μ. Left panel: the pressures of the two phases define two surfaces parametrized by μ and μ_e. The intersection of the two surfaces forms a line (black curve). Only the part of the surfaces that lies above the surface of the other phase is indicated (since the ground state corresponds to the maximal pressure). Right panel: the neutrality condition for each of the phases defines a curve in the μ-μ_e plane, and thus a curve on the respective surfaces (for illustrative purposes let the charge be nonzero – denoted by c – since for zero charge there would have to be a valley of the pressure). Coexistence of the phases is possible only along the black curve. A mixed phase may exist from A (where $\chi = 0$) to B (where $\chi = 1$). In this segment none of the phases is neutral separately, but they may combine to a globally neutral phase. Note that the extra direction μ_e is crucial to have a finite segment along the μ axis where a mixed phase is possible.

have to understand what superconductivity is. Once we have introduced the basic concept we shall see that it comes in many variants in a compact star. And we will see that it is very important for the understanding of transport properties of ultra-dense matter. And the transport properties, in turn, are related to the phenomenology of the star, as we shall discuss in later chapters.

So let us first discuss the basic concept and the basic properties of a superconductor. We shall do so with physical arguments and shall only later elaborate on the technical details. Consider a system of fermions at zero temperature with chemical potential μ and thermodynamical potential

$$\Omega = E - \mu N \,. \tag{188}$$

Now first suppose the fermions are non-interacting. Then, adding a fermion with energy μ, i.e., at the Fermi surface, leaves the free energy Ω obviously unchanged: the energy E is increased by μ, but the second term subtracts the same amount since we add $N = 1$ fermion. Now let us switch on an arbitrarily small attractive interaction between the fermions. Then, by adding two fermions at the Fermi surface, we can actually lower the free energy because the attractive interaction will lead to an energy gain from the binding energy. Therefore, the Fermi surface we have started with is unstable. A new ground state is formed in which pairs of fermions are created at the Fermi surface. Since two fermions formally can be viewed as a boson[5], these fermion pairs will form a Bose condensate. This formation of a condensate of fermion pairs due to an arbitrarily small interaction is called *Cooper's Theorem* and the fermion pairs are called *Cooper pairs*.

[5] In fact, the fermions are correlated in momentum space, not in real space. Consequently, in the weak-coupling limit, the fermion pairs are not spatially separated bosons. The typical size of a pair is rather larger than the mean distance between fermions. Therefore, one apparently has to be careful to describe the pairs as bosons. However, recent experiments with cold fermionic atoms show that there is no phase transition between the weak-coupling limit (where the pairs are wide spread) and the strong-coupling limit (where the pairs are actual difermions, i.e., bosons). This is the so called BCS-BEC crossover. It says in particular, that it is not too bad to think of the fermion pairs as bosons even in the weak-coupling limit.

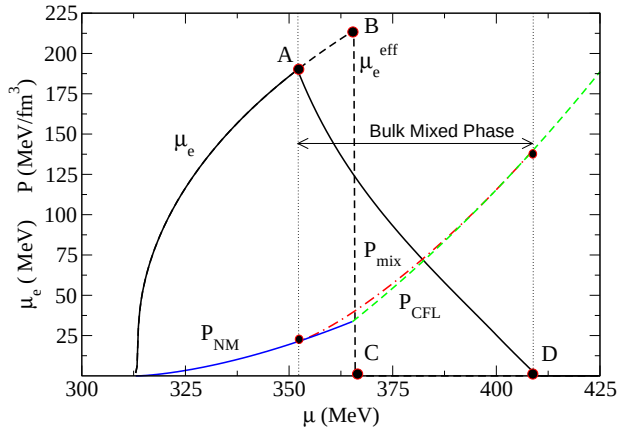

FIG. 9: Figure from Ref. [27] showing the transition from nuclear matter (NM) to a mixed phase (mix) to a quark matter phase (CFL) (we shall explain what CFL is in a later section). In the mixed phase, μ_e is lowered in order to make the nuclear phase positively charged and the CFL phase negatively charged. Taking into account Coulomb energy and surface energy shows that the μ interval for the mixed phase shrinks with increasing surface tension σ until it completely disappears for $\sigma \gtrsim 40\,\mathrm{MeV/fm^2}$. The exact value of σ is not known but it is likely to be larger than that limit value such that a mixed phase appears unlikely. The limit value does not depend much on whether the mixed phase has spheres, rods, or slabs.

This mechanism is completely general, i.e., it holds for arbitrary fermions with a Fermi surface as long as their interaction is attractive. It holds for electrons in a usual superconductor, i.e., a metal or alloy, it holds for ^{3}He atoms in superfluid helium etc. In our context, it is of relevance that it holds for protons, neutrons, and quarks. Anticipating that the Cooper mechanism leads to *superfluidity* for neutral fermions and to *superconductivity* for charged fermions, we thus expect (*i*) neutron superfluidity, (*ii*) proton superconductivity, and (*iii*) quark superconductivity to be possible in a compact star. Especially the latter statement about quarks will have to be made more precise below.

Let us first stay on a very general level and discuss the basic consequences of Cooper pairing. A Cooper pair is held together by a "binding energy" (although it is not a bound state), i.e., one needs a finite amount of energy to break a pair. Consequently, the one-particle dispersion relations acquire an *energy gap* Δ. For massless fermions this means

$$\epsilon_k = \sqrt{(k-\mu)^2 + \Delta^2}\,. \tag{189}$$

(Note that here, in contrast to the quantity denoted by ϵ_k in the previous chapters, we have included the chemical potential in ϵ_k.) The excitation described by this relation is also called *quasiparticle* since it effectively contains the interaction of the original particles. The energy gap in the dispersion relation is responsible for most of the phenomenological properties of a superconductor. For instance, it gives rise to the frictionless charge transport in an electronic superconductor, since (sufficiently low energy) scattering of electrons off phonons cannot excite a single-electron state. Or, in the context of superfluidity, the energy gap explains the frictionless flow in the same way. It is thus the main task to compute the magnitude of Δ. We shall discuss this calculation in the context of quarks.

A. Specific heat for isotropic and anisotropic superconductors

As a example of the effect of Δ let us compute the specific heat of a superconductor[6]. The specific heat is easy to compute and shows characteristic features of a superconductor. We keep our discussion general and start from the free energy of a superconductor made of massless fermions with two degenerate (spin-) degrees of freedom,

$$\Omega = 2T \int \frac{d^3\mathbf{k}}{(2\pi)^3} \ln\left(1 + e^{-\epsilon_k/T}\right)\,, \tag{190}$$

[6] More precisely, here we compute the fermionic contribution to the specific heat. For instance in a superfluid, there is a light Goldstone mode which dominates the specific heat at small temperatures. In this section we ignore such modes for the purpose of illustrating the effect of the energy gap.

where the quasiparticle energy ϵ_k is given by Eq. (189). The entropy (density) is given by the derivative with respect to the temperature (with respect to the *explicit* T-dependence only!)

$$s = \frac{\partial \Omega}{\partial T} = -2 \int \frac{d^3\mathbf{k}}{(2\pi)^3} \left[(1-f_k) \ln(1-f_k) + f_k \ln f_k \right] . \tag{191}$$

with the Fermi distribution

$$f_k = \frac{1}{e^{\epsilon_k/T}+1} . \tag{192}$$

To derive Eq. (191) one uses the identities

$$\frac{\epsilon_k}{T} = \ln(1-f_k) - \ln f_k , \qquad \ln\left(1+e^{-\epsilon_k/T}\right) = -\ln(1-f_k) . \tag{193}$$

From the entropy we then compute the specific heat (at constant volume)

$$c_V \equiv T \frac{\partial s}{\partial T} = 2 \int \frac{d^3\mathbf{k}}{(2\pi)^3} \epsilon_k \frac{\partial f_k}{\partial T} . \tag{194}$$

[End of 7th lecture, May 11, 2009]

For the temperature dependence of the gap we assume the following form,

$$\Delta(T) = \Theta(T_c - T) \Delta_0 \sqrt{1 - \frac{T^2}{T_c^2}} , \tag{195}$$

such that the zero-temperature gap is Δ_0, the gap approaches zero at the critical temperature T_c and vanishes for all temperatures larger than T_c. Then, for $T < T_c$ we have

$$\frac{\partial \Delta}{\partial T} = -\frac{\Delta_0^2}{T_c^2} \frac{T}{\Delta} \quad \Rightarrow \quad \frac{\partial \epsilon_k}{\partial T} = -\frac{T}{\epsilon_k} \frac{\Delta_0^2}{T_c^2} \quad \Rightarrow \quad \frac{\partial f_k}{\partial T} = \frac{1}{\epsilon_k} \frac{e^{\epsilon_k/T}}{\left(e^{\epsilon_k/T}+1\right)^2} \left(\frac{\epsilon_k^2}{T^2} + \frac{\Delta_0^2}{T_c^2} \right) , \tag{196}$$

and consequently

$$c_V = 2 \int \frac{d^3\mathbf{k}}{(2\pi)^3} \frac{e^{\epsilon_k/T}}{\left(e^{\epsilon_k/T}+1\right)^2} \left(\frac{\epsilon_k^2}{T^2} + \frac{\Delta_0^2}{T_c^2} \right) . \tag{197}$$

We shall only be interested in temperatures much smaller than the chemical potential, $T \ll \mu$. Then, the main contribution comes from the Fermi surface, we can approximate $dk\, k^2 \to \mu^2 dk$. Also we shall allow for anisotropic gaps; we introduce the new variable $x = (k-\mu)/T$, and we define

$$\varphi \equiv \frac{\Delta}{T} . \tag{198}$$

Then, we have

$$c_V \simeq \frac{\mu^2 T}{\pi^2} \int_0^\infty dx \int_0^\pi d\theta \, \sin\theta \left(x^2 + \varphi^2 + \frac{\Delta_0^2}{T_c^2} \right) \frac{e^{\sqrt{x^2+\varphi^2}}}{\left(e^{\sqrt{x^2+\varphi^2}}+1\right)^2} , \tag{199}$$

where we have approximated the lower boundary by $\mu/T \simeq \infty$ and have used that the integrand is even in x (which gives rise to the new integration boundaries $[0,\infty]$ and a factor 2). From this general expression we easily get the limit of a vanishing gap, $\varphi = \Delta_0 = 0$, i.e., the result for the non-superconducting state,

$$c_V^0 \simeq \frac{\mu^2 T}{\pi^2} \int_0^\infty dx \, \frac{x^2}{1+\cosh x} = \frac{\mu^2 T}{3} . \tag{200}$$

Before evaluating the superconducting specific heat at small temperature, let us discuss the behavior at the critical temperature. Approaching T_c from above, c_V is simply given by Eq. (197) with $\Delta_0 = 0$, Δ in ϵ_k set to zero, and

$T = T_c$. In the superconducting phase, approaching T_c from below, is equivalent to just setting Δ to zero in ϵ_k. Consequently, at T_c there is a jump in the specific heat which is given by

$$\begin{aligned} \Delta c_V &= 2\frac{\Delta_0^2}{T_c^2}\int \frac{d^3\mathbf{k}}{(2\pi)^3}\frac{e^{\epsilon_k/T}}{\left(e^{\epsilon_k/T}+1\right)^2} \\ &\simeq \frac{\Delta_0^2\mu^2}{\pi^2 T_c}\int_0^\infty dx\,\frac{1}{1+\cosh x} = \frac{\Delta_0^2\mu^2}{\pi^2 T_c}\,, \end{aligned} \tag{201}$$

where we have assumed the gap to be isotropic. This jump is a typical signature for a second-order phase transition, since the specific heat is the second derivative of the thermodynamic potential.

Next we evaluate Eq. (199) for small temperatures, i.e., in the limit $\varphi \to \infty$. First we consider an isotropic gap. We can approximate

$$\frac{e^{\sqrt{x^2+\varphi^2}}}{\left(e^{\sqrt{x^2+\varphi^2}}+1\right)^2} \simeq e^{-\sqrt{x^2+\varphi^2}} \simeq e^{-\varphi-\frac{x^2}{2\varphi}}\,. \tag{202}$$

Consequently,

$$\begin{aligned} c_V &\simeq \frac{2\mu^2 T}{\pi^2}e^{-\varphi}\left[\int_0^\infty dx\,x^2 e^{-\frac{x^2}{2\varphi}} + \left(\varphi^2+\frac{\Delta_0^2}{T_c^2}\right)\int_0^\infty dx\,e^{-\frac{x^2}{2\varphi}}\right] \\ &\simeq \frac{\sqrt{2}\mu^2 T}{\pi^{3/2}}\varphi^{5/2}e^{-\varphi}\,, \end{aligned} \tag{203}$$

where we used

$$\int_0^\infty dx\,x^2 e^{-\frac{x^2}{2\varphi}} = \varphi^{3/2}\sqrt{\frac{\pi}{2}}\,, \qquad \int_0^\infty dx\,e^{-\frac{x^2}{2\varphi}} = \varphi^{1/2}\sqrt{\frac{\pi}{2}}\,. \tag{204}$$

The main result is that the specific heat is exponentially suppressed by the factor $e^{-\varphi}$ for temperatures much smaller than the gap.

Next let us assume an anisotropic gap of the form

$$\Delta \to \Delta \sin\theta\,. \tag{205}$$

Anisotropic gaps can be expected for neutron superfluidity and possibly for quark superconductivity. This form implies that the spectrum depends on the angle θ in momentum space. For θ being the angle between momentum and the z-axis, this form implies point-like nodes of the gap function at the north and south pole of the Fermi sphere. For small temperatures, these nodes will give the dominant contribution to the specific heat. Therefore, in the low-temperature approximation, we only integrate over angles in the vicinity of the nodes. We restrict the angular integration by requiring the quasiparticle energy (with respect to the Fermi surface) to be at most of the order of the scale set by the temperature,

$$\Delta_0 \sin\theta \lesssim \pi T \tag{206}$$

which, for small angles θ and small temperatures implies $\theta \lesssim \pi/\varphi$. Therefore, the specific heat becomes (note the factor 2 since we obtain the same result for north and south pole)

$$\begin{aligned} c_V &\simeq \frac{\mu^2 T}{\pi^2}\int_0^\infty dx\,\frac{1}{1+\cosh x}\int_0^{\pi/\varphi} d\theta\,\theta(x^2+\varphi^2\theta^2) \\ &\simeq \frac{5\pi^2}{4}\frac{\mu^2 T}{3}\frac{1}{\varphi^2} \end{aligned} \tag{207}$$

We see that instead of an exponential suppression, we now get a power-law suppression $\propto (T/\Delta)^2$ of the specific heat compared to the non-superconducting result.

Exercise 6: *Compute the low-temperature behavior of the specific heat for a gap function with line nodes, i.e., instead of Eq. (205), take $\Delta \to \Delta|\cos\theta|$ and apply analogous approximations as for the case of point nodes.*

The low-temperature results for the specific heat are relevant for the physics of compact stars because the superconducting gap of either nucleonic superconductivity/superfluidity or quark superconductivity may well be much larger than the temperature of the star. In particular, the specific heat is important in the context of the cooling of the star, for example through neutrino emissivity ϵ_ν. With ϵ_ν being the energy loss per unit time and volume through neutrino emission (for example through the processes (29) in nuclear matter or the neutrino processes in Eq. (44) in quark matter), the relation between ϵ_ν, c_V, and the change in temperature is

$$\epsilon_\nu(T) = -c_V(T)\frac{dT}{dt}\,. \tag{208}$$

(The minus sign is needed since a positive ϵ_ν is an energy loss, i.e., the temperature will decrease, $dT/dt < 0$.) Integrating this relation from a time t_0 (with temperature $T(t_0) = T_0$) yields

$$t - t_0 = -\int_{T_0}^{T} dT' \, \frac{c_V(T')}{\epsilon_\nu(T')}\,. \tag{209}$$

This shows that the ratio of the specific heat and the neutrino emissivity enters the cooling behavior of the star. Typically, for a given phase, the neutrino emissivity will exhibit a similar behavior as the specific heat. For instance, in a superconductor, the emissivity as well as the specific heat are exponentially suppressed and the subleading behavior becomes important. In a real compact star, however, there is most likely not just a single phase and different phases might dominate the behavior of the emissivity and the specific heat. We shall see that the neutrino emissivity itself is much more difficult to compute than the specific heat. We will do this calculation in Sec. VI and then discuss the simplest cooling scenarios. Here we just point out the relevance of the specific heat and thus the relevance of superconductivity for the cooling behavior.

The suppression of the specific heat in a superconductor (exponential or, if the gap as nodes, by power-law) provides a good example to get some intuition for the properties of superconductors. Note that the specific heat is a measure of how many degrees of freedom are available to store heat. A large number of degrees of freedom means a lot of "storage room" and thus a large specific heat. A small specific heat, such as for a superconductor at sufficiently small temperature, thus means there are very few states available. This is a direct consequence of the energy gap which obviously leads to a region in the energy spectrum with no allowed states. Only by increasing the temperature does the exponential suppression disappear because temperature provides the energy to populate states above the gap which in turn are then available to store thermal energy.

B. Color-flavor locked quark matter

In our discussion of superconductivity and superfluidity in compact stars we shall focus on a density region where we can perform rigorous calculations from first principles. This is the region of asymptotically large densities, where we deal with weakly coupled, deconfined quark matter[7]. The quarks are weakly coupled due to *asymptotic freedom*, which says that the coupling of QCD becomes weak for large exchanged momenta. For our purpose, the QCD coupling can be considered as a function of the quark chemical potential and becomes arbitrarily small for large chemical potentials. In other words, quarks at infinite chemical potential are free. Because of this important property of QCD we may use perturbative methods at high densities. The high-density region of the QCD phase diagram shown in Fig. 1 is therefore maybe the best understood regime of QCD. The other regimes in that phase diagram are more complicated: we have seen that for nuclear matter one usually relies on phenomenological models; the high-temperature, small-density region, where the QCD coupling also becomes small, has subtle nonperturbative effects because of infrared degrees of freedom; first-principle QCD calculations via computer simulations (*"lattice QCD"*) are much more complicated than perturbative physics at high densities and are so far restricted to vanishing chemical potential. All this seems a good motivation to study ultra-dense quark matter. However, we should mention that these studies are valid at densities much larger than expected in compact stars. In a compact star, the quark chemical potential is at most of the order of $\mu \lesssim 500\,\mathrm{MeV}$. The perturbative calculation of the energy gap Δ, to be discussed in Sec. V C, can be estimated to be reasonable at chemical potentials $\mu \gtrsim 10^8\,\mathrm{MeV}$ (!) Then, extrapolation of our perturbative results down to compact star densities may seem bold. However, the (rough) quantitative agreement of these extrapolations with different approaches, using phenomenological models, gives us some confidence that the

[7] We shall not go into details of neutron superfluidity and proton superconductivity. For a detailed review of these matters, see Ref. [28]. Shorter discussions can be found in the textbooks and reviews listed in the references, see for instance Sec. 3.2 in Ref. [6].

ultra-high density calculation may be of relevance for astrophysical calculations. Furthermore, we shall also apply general arguments, based on symmetries, which we can expect to hold even for strong coupling. In summary, the following discussion, strictly speaking only valid for extreme densities, is of theoretical interest and may also give us insight into compact star physics.

In this lecture, we have already discussed the approch to compact star densities "from the other side". In the Walecka model of Sec. III A, we have constructed the model such that we have reproduced properties of nuclear matter at densities accessible in the laboratory. These densities are *lower* than the ones in compact stars. We had to extrapolate up to higher densities to obtain predictions of astrophysical relevance. Therefore, we learn that matter inside compact stars is quite hard to tackle; we have to approach it from different sides, and we do not have rigorous control over our approaches. This reflects the discussion begun in the introduction: it shows that the question "What is the matter composition inside a compact star?" is, due to our lack of understanding of dense, strongly-interacting matter, not only an *application* of QCD but also relevant to *understand* QCD.

But now back to superconductivity. From the above general argument (*Cooper's Theorem*) we know that an attractive interaction, however small it may be, leads to the formation of a quark Cooper pair condensate. At asymptotically high densities, this attractive interaction is provided by single-gluon exchange. We can formulate quark pairing in terms of representaions of the color gauge group $SU(3)_c$,

$$SU(3)_c: \qquad [\mathbf{3}]_c \otimes [\mathbf{3}]_c = [\bar{\mathbf{3}}]_c^A \oplus [\mathbf{6}]_c^S \,. \tag{210}$$

On the left-hand side we have two quarks in the fundamental representation, i.e., two complex three-vectors since the number of colors is three, $N_c = 3$. They interact in an antisymmetric (A) anti-triplet channel and a symmetric (S) sextet channel which are attractive and repulsive, respectively. The attractive channel thus provides a triplet of diquarks which has (anti-)color charge. The attractiveness of this channel can also be understood from thinking of a baryon as a bound state of a diquark and a quark. The diquark lives in the above $[\bar{\mathbf{3}}]_c^A$; if it is made of, say, a red and a green quark it has color anti-blue. The baryon is then color-neutralized by combining this diquark with a blue quark.

An obvious property of a quark Cooper pair is that it is color-charged. Therefore, it breaks the color symmetry $SU(3)_c$ spontaneously. In analogy to electronic superconductors, which break the electromagnetic $U(1)_{\rm em}$, quark Cooper pairing is thus termed *color superconductivity*. For a recent review of color superconductivity, see Ref. [7]. The order parameter of color superconductivity is the expectation value of the quark-quark two-point function $\langle\psi\psi\rangle$. The color structure of this object has to be antisymmetric because of the attractiveness of the color $[\bar{\mathbf{3}}]_c^A$. The flavor structure is governed by the chiral symmetry group $SU(3)_R \times SU(3)_L$[8], discussed in Sec. III C 1. For now, we may consider these symmetries to be exact, since at the high densities we are working we may neglect all three quark masses. Each of these global $SU(3)$'s leads to the same representations as the color group,

$$SU(3)_f: \qquad [\mathbf{3}]_f \otimes [\mathbf{3}]_f = [\bar{\mathbf{3}}]_f^A \oplus [\mathbf{6}]_f^S \,, \tag{211}$$

with $f = L, R$. Since the overall wave function of the Cooper pair has to be antisymmetric and since pairing in the antisymmetric spin-zero channel is preferred, we need to pair in the flavor $[\bar{\mathbf{3}}]_f^A$ channel. In other words, the color-flavor structure of the Cooper pair is

$$\langle\psi\psi\rangle \in [\bar{\mathbf{3}}]_c^A \otimes [\bar{\mathbf{3}}]_f^A \,. \tag{212}$$

More specifically,

$$\langle\psi_i^\alpha C\gamma_5\psi_j^\beta\rangle \propto \epsilon^{\alpha\beta A}\epsilon_{ijB}\phi_B^A \,. \tag{213}$$

Here, we have added the Dirac structure with the charge-conjugation matrix $C \equiv i\gamma^2\gamma^0$, leading to even-parity, spin-singlet pairing. The 3×3 matrix ϕ now determines the specific color-flavor structure within the given antisymmetric representations. This shows that there are in principle many different possible color-superconducting phases. They are distinguished by different pairing patterns, i.e., by which quark pairs with which other quark. In particular, one may construct phases in which some of the quarks are paired while some others are not.

At high densities, the favored phase is the *color-flavor locked (CFL)* phase [29]. We can characterize it by the following properties,

---

[8] As already mentioned in the introduction, we consider three-flavor quark matter. Since we discuss asymtotically large densities, one might say that more quark flavors should be taken into account. However, we are ultimately interested in extrapolating our results down to compact star densities where we only have u, d, and s quarks.

(*i*) the CFL order parameter is given by

$$\phi_A^B = \delta_A^B \quad \Rightarrow \quad \langle \psi_i^\alpha C\gamma_5 \psi_j^\beta \rangle \propto \epsilon^{\alpha\beta A}\epsilon_{ijA}\,. \tag{214}$$

(*ii*) in the CFL phase, all quarks are paired with pairing pattern $rd-gu$, $bu-rs$, $bd-gs$, $ru-gd-bs$, and there are 8 quasiparticles with gap Δ and 1 quasiparticle with gap 2Δ.

(*iii*) the CFL phase has the following symmetry breaking pattern,

$$SU(3)_c \times SU(3)_R \times SU(3)_L \times U(1)_B \to SU(3)_{c+L+R} \times \mathbb{Z}_2\,. \tag{215}$$

[End of 8th lecture, May 18, 2009]

These three properties are in fact equivalent. Before discussing their physical implications, many of which can be read off from properties (*ii*) and (*iii*), let us show how (*ii*) follows from (*i*). To get a clear picture of the matrix structure of the order parameter, let us denote the bases of the color and flavor antitriplet through $(J^A)^{\alpha\beta} = -i\epsilon^{\alpha\beta A}$, $(I_B)_{ij} = -i\epsilon_{ijB}$. Then, we can write Eq. (214) as

$$\langle \psi C\gamma_5\psi\rangle_{\rm CFL} \propto \mathbf{J}\cdot\mathbf{I} = \begin{pmatrix} 0 & -iI_3 & iI_2 \\ iI_3 & 0 & -iI_1 \\ -iI_2 & iI_1 & 0 \end{pmatrix} = \begin{pmatrix} 0&0&0&0&-1&0&0&0&-1\\ 0&0&0&1&0&0&0&0&0\\ 0&0&0&0&0&0&1&0&0\\ 0&1&0&0&0&0&0&0&0\\ -1&0&0&0&0&0&0&0&-1\\ 0&0&0&0&0&0&0&1&0\\ 0&0&1&0&0&0&0&0&0\\ 0&0&0&0&0&1&0&0&0\\ -1&0&0&0&-1&0&0&0&0 \end{pmatrix}. \tag{216}$$

This 9×9 matrix is obviously symmetric, as required (the color-flavor structure is symmetric, giving overall antisymmetry through the antisymmetric Dirac structure). Its rows and columns are labeled with the nine quarks, ru, rd, rs, gu, gd, gs, bu, bd, bs. A nonzero entry indicates that the corresponding quarks pair. We see that the matrix has a block structure with three 2×2 blocks and one 3×3 block. This leads to the pairing pattern given in point (*ii*). Note that this is a basis dependent statement. In particular, since the color symmetry is a gauge symmetry, $\langle\psi C\gamma_5\psi\rangle$ is a gauge variant object. The physically relevant statement, however, is the second part of point (*ii*) about the physical excitations. This statement is gauge invariant. The gap structure is given by the eigenvalues of the square of the above 9×9 matrix,

$$\epsilon_{k,r} = \sqrt{(k-\mu)^2 + \lambda_r\Delta^2}\,, \tag{217}$$

where λ_r are the eigenvalues of

$$L \equiv (\mathbf{J}\cdot\mathbf{I})^2\,. \tag{218}$$

We shall see in the next subsection why (217) is true. Here we simply compute the eigenvalues λ_r. They are given by the solutions of

$$\det(\lambda - L) = 0\,. \tag{219}$$

This can be rewritten as

$$0 = \exp\left[\mathrm{Tr}\ln(\lambda - L)\right] = \exp\left[\mathrm{Tr}\left(\ln\lambda - \sum_{n=1}^{\infty}\frac{L^n}{n\lambda^n}\right)\right]. \tag{220}$$

We now have to compute L^n. First note that

$$(\mathbf{J}\cdot\mathbf{I})_{ij}^{\alpha\beta} = -\epsilon^{\alpha\beta A}\epsilon_{ijA} = -\delta_i^\alpha\delta_j^\beta + \delta_j^\alpha\delta_i^\beta \quad \Rightarrow \quad L_{ij}^{\alpha\beta} = \delta^{\alpha\beta}\delta_{ij} + \delta_i^\alpha\delta_j^\beta\,. \tag{221}$$

From this one computes

$$L^2 = 5L - 4\,. \tag{222}$$

This shows that all powers of L only have the structures L and $\mathbf{1}$. Thus we make the ansatz

$$L^n = a_n L + b_n\,. \tag{223}$$

Multiplying both sides of this equation by L yields

$$a_{n+1} = 5a_n + b_n\,, \qquad b_{n+1} = -4a_n\,. \tag{224}$$

These recursion relations can be solved with the ansatz $a_n = p^n$. This yields the equation $p^2 = 5p - 4$ which is solved by $p_1 = 4$ and $p_2 = 1$. Consequently, the general solution is the linear combination

$$a_n = \alpha p_1^n + \beta p_2^n = 4^n\alpha + \beta\,. \tag{225}$$

From above we know $a_1 = 1$ and $a_2 = 5$ which yields $\alpha = -\beta = -1/3$. Hence

$$L^n = \frac{4^n - 1}{3}\,L - \frac{4^n - 4}{3}\,. \tag{226}$$

Inserting this into Eq. (220) yields

$$0 = \exp\left\{\mathrm{Tr}\left[\frac{L-1}{3}\ln(\lambda - 4) - \frac{L-4}{3}\ln(\lambda - 1)\right]\right\}\,. \tag{227}$$

Now we use $\mathrm{Tr}\,\mathbf{1} = 9$ and, from Eq. (221), $\mathrm{Tr}\,L = 12$. Thus we have

$$0 = \exp\left[\ln(\lambda - 4) + 8\ln(\lambda - 1)\right] = (\lambda - 4)(\lambda - 1)^8\,. \tag{228}$$

Consequently, the eigenvalues of L are 1 (8-fold) and 4 (1-fold). Physically speaking (recalling Eq. (217)) this means that in the CFL phase 8 quasiparticle excitations have a gap Δ and 1 quasiparticle excitation has a gap 2Δ. This is the second part of the above point (*ii*). Of course, this discussion says nothing about the magnitude of Δ, which has to be computed from the QCD gap equation, see subsequent section.

We leave it as an exercise to show that (*iii*) follows from (*i*):

Exercise 7: *Show that from the structure of the CFL order parameter given in Eq. (214) it follows that the CFL symmetry breaking pattern is as given in Eq. (215). Hints: it is sufficient to treat the chiral group $SU(3)_L \times SU(3)_R$ as one single flavor group $SU(3)_f$. A color-flavor transformation $(U, V) \in SU(3)_c \times SU(3)_f$ with $U = \exp(i\phi_a^c T_a)$, $V = \exp(i\phi_a^f T_a)$ acts on the order parameter as $(U, V)(\mathbf{J}\cdot\mathbf{I}) = (UJ^AU^T)\,(VI_AV^T)$. One then has to show that only $SU(3)_{c+f}$ transformations leave the order parameter invariant.*

Points (*ii*) and (*iii*) already reveal many important physical properties of the CFL state. Since these points are solely based on the symmetries of the CFL state, they are independent of the details of the interaction. Therefore, they can be expected to hold also at lower densities where perturbative QCD is not applicable. First, one may ask why CFL is the ground state and not any other order parameter given by a different matrix ϕ_A^B. The simple answer is that the CFL order parameter is the only one in which all quarks participate in pairing, as we have seen. All other possible order parameters leave several excitations ungapped. Therefore, the CFL phase leads to the largest condensation energy and thus is the ground state at high densities (at lower densities the situation is more complicated). A more formal argument is that the CFL phase is the color superconductor with the largest residual symmetry group. It is thus a particularly symmetric state which also indicates that it is preferred over other color superconductors.

From (*iii*) we read off the following properties of CFL,

- CFL breaks chiral symmetry. We see that the CFL symmetry breaking pattern (215) is, regarding chiral symmetry, the same as in Eq. (141). However, the mechanisms are different. The latter is caused by a chiral condensate of the form $\langle\bar\psi_R\psi_L\rangle$, while the CFL condensate has the form $\langle\psi_R\psi_R\rangle$ (and the same with $R \to L$). At first sight, the CFL condensate thus preserves the full chiral symmetry. However, the symmetry breaking occurs through the "locking" with color, i.e., in order to leave the order parameter invariant, a color rotation has to be "undone" by equal rotations in the left- and right-handed sectors. Although caused by different mechanisms, the two scenarios lead to similar physics. As for the "usual" chiral symmetry breaking, the CFL phase also has an octet of Goldstone modes. Since all fermions acquire an energy gap, these Goldstone modes become very important for the phenomenology of the CFL phase. Moreover, at lower densities, where the strange quark mass cannot be neglected, kaon condensation, not unlike the one discussed in Sec. III C, is expected in the CFL phase (then termed CFL-K^0).

- The color gauge group is completely broken. While spontaneous breaking of a global group leads to Goldstone bosons, spontaneous breaking of a gauge group leads to masses for the gauge bosons. Here, all gluons acquire a Meissner mass, just as the photon acquires a Meissner mass in an electronic superconductor. In fact, one linear combination of a gluon and the photon remains massless in the CFL phase. In other words, there is an unbroken $U(1)_{\tilde{Q}} \subseteq SU(3)_{c+L+R}$, generated by $\tilde{Q}$ which is a linear combination of the original charge generator Q and the eighth gluon generator T_8 (if you have done Exercise 7 you can easily show this and determine the exact form of the linear combination). This phenomenon is also called *rotated electromagnetism*. Since the admixture of the gluon to the new gauge boson is small, one may say that the CFL phase is a color superconductor but no electromagnetic superconductor. This is of relevance for compact stars since it implies that the CFL phase does not expel magnetic fields.
- The CFL phase is a superfluid since it breaks the baryon number conservation group $U(1)_B$. This is important since this is an exact symmetry, even at lower densities. Therefore, there is always one exactly massless Goldstone mode in the CFL phase.

C. Color-superconducting gap from QCD

In the theoretical treatment of superconductivity one introduces charge-conjugate fermions, which can be thought of as hole degrees of freedom. This formally doubles the degrees of freedom. The fermion spinors are then spinors in the so-called *Nambu-Gorkov* space and the fermion propagator is then a 2×2 matrix in this space. The Cooper pair condensate is taken into account in the off-diagonal elements of this propagator, i.e., it couples fermions with holes. The inverse tree-level propagator in Nambu-Gorkov space is

$$S_0^{-1} = \begin{pmatrix} [G_0^+]^{-1} & 0 \\ 0 & [G_0^-]^{-1} \end{pmatrix}, \tag{229}$$

with the inverse tree-level fermion and charge-conjugate fermion propagators

$$[G_0^\pm]^{-1} = \gamma^\mu K_\mu \pm \mu\gamma_0 = \sum_{e=\pm} [k_0 \pm (\mu - ek)]\gamma_0 \Lambda_k^{\pm e}, \tag{230}$$

where

$$\Lambda_k^{\pm e} \equiv \frac{1}{2}\left(1 + e\gamma_0 \boldsymbol{\gamma}\cdot\hat{\mathbf{k}}\right) \tag{231}$$

are projectors onto positive and negative energy states. From Eq. (230) we immediately get the tree-level propagator

$$G_0^\pm = \sum_{e=\pm} \frac{\Lambda_k^{\pm e}\gamma_0}{k_0 \pm (\mu - ek)}. \tag{232}$$

The full inverse propagator S^{-1} is obtained from a Dyson-Schwinger equation

$$S^{-1} = S_0^{-1} + \Sigma, \tag{233}$$

with the self-energy

$$\Sigma \simeq \begin{pmatrix} 0 & \Phi^- \\ \Phi^+ & 0 \end{pmatrix}. \tag{234}$$

In principle, Σ also has nonvanishing diagonal elements which we may neglect here. The off-diagonal elements contain the gap function,

$$\Phi^+(K) = \Delta(K)\mathcal{M}\gamma_5, \qquad \Phi^-(K) = -\Delta(K)\mathcal{M}^\dagger\gamma_5, \tag{235}$$

where $\mathcal{M}$ specifies the color-flavor structure of the color-superconducting phase, in the CFL phase $\mathcal{M} = \mathbf{J}\cdot\mathbf{I}$. From the Dyson-Schwinger equation (233) we obtain the inverse propagator, which we invert to obtain the propagator,

$$S = \begin{pmatrix} G^+ & F^- \\ F^+ & G^- \end{pmatrix}, \tag{236}$$

with

$$G^{\pm} = \left([G_0^{\pm}]^{-1} - \Phi^{\mp} G_0^{\mp} \Phi^{\pm}\right)^{-1} , \tag{237a}$$

$$F^{\pm} = -G_0^{\mp} \Phi^{\pm} G^{\pm} . \tag{237b}$$

The off-diagonal elements $F^{\pm}$ are termed *anomalous propagators*. They are typical for all superconductors, not only in the present context, see for example Ref. [30]. From their structure (237b) we see that they describe the propagation of a charged-conjugate fermion that is converted into a fermion through the condensate (or vice versa). One can thus think of the condensate as a reservoir of fermions and holes, and the quasiparticles are not just single fermions but superpositions of states with fermion number $\ldots, -5, -3, -1, 1, 3, 5, \ldots$.

With Eqs. (230), (232), and (235) we may compute the diagonal elements of the propagator (for simplicity we assume $\mathcal{M}^{\dagger} = \mathcal{M}$ which is true in the CFL phase, but may not be true in other phases),

$$G^{\pm} = \left\{ \sum_{e=\pm} \left[k_0 \pm (\mu - ek) - \frac{\Delta^2 L}{k_0 \mp (\mu - ek)} \right] \Lambda_k^{\mp e} \gamma_0 \right\}^{-1} , \tag{238}$$

with $L = \mathcal{M}^2$, as defined for the CFL phase in Eq. (218). Now we write L in its spectral representation,

$$L = \sum_r \lambda_r \mathcal{P}_r , \tag{239}$$

with λ_r being the eigenvalues of L, $\lambda_1 = 1$, $\lambda_2 = 4$, and $\mathcal{P}_r$ the projectors onto the corresponding eigenstates,

$$\mathcal{P}_1 = -\frac{L-4}{3} , \qquad \mathcal{P}_2 = \frac{L-1}{3} . \tag{240}$$

This yields

$$\begin{aligned} G^{\pm} &= \left\{ \sum_{e,r} \left[k_0 \pm (\mu - ek) - \frac{\lambda_r \Delta^2}{k_0 \mp (\mu - ek)} \right] \mathcal{P}_r \Lambda_k^{\mp e} \gamma_0 \right\}^{-1} \\ &= \sum_{e,r} \left[k_0 \pm (\mu - ek) - \frac{\lambda_r \Delta^2}{k_0 \mp (\mu - ek)} \right]^{-1} \mathcal{P}_r \gamma_0 \Lambda_k^{\mp e} \\ &= [G_0^{\mp}]^{-1} \sum_{e,r} \frac{\mathcal{P}_r \Lambda_k^{\mp e}}{k_0^2 - (\epsilon_{k,r}^e)^2} , \end{aligned} \tag{241}$$

with

$$\epsilon_{k,r}^e = \sqrt{(ek - \mu)^2 + \lambda_r \Delta^2} . \tag{242}$$

The poles of the propagator are $k_0 = \pm \epsilon_{k,r}^e$, i.e., $\epsilon_{k,r}^e$ are the dispersion relations of the quasiparticles. We have thus confirmed Eq. (217), in particular we now understand how the eigenvalues of L arise in the excitation energies.

[End of 9th lecture, May 25, 2009]

Using the result (241) for $G^{\pm}$ and Eq. (237b), one easily obtains the anomalous propagators,

$$F^{\pm} = \pm \Delta \mathcal{M} \gamma_5 \sum_{e,r} \frac{\mathcal{P}_r \Lambda_k^{\mp e}}{k_0^2 - (\epsilon_{k,r}^e)^2} . \tag{243}$$

The gap equation is a self-consistent equation for the off-diagonal elements of the self-energy Σ. We shall not discuss the detailed derivation of the gap equation (see Sec. IV.A in Ref. [7] for this derivation). It reads

$$\Phi^{+}(K) = g^2 \frac{T}{V} \sum_Q \gamma^{\mu} T_a^T F^{+}(Q) \gamma^{\nu} T_b D_{\mu\nu}^{ab}(K - Q) , \tag{244}$$

where g is the QCD coupling constant, which will be our expansion parameter, and where $D_{\mu\nu}^{ab}$ is the gluon propagator. See Fig. 10 for the diagrammatic representation of the gap equation.

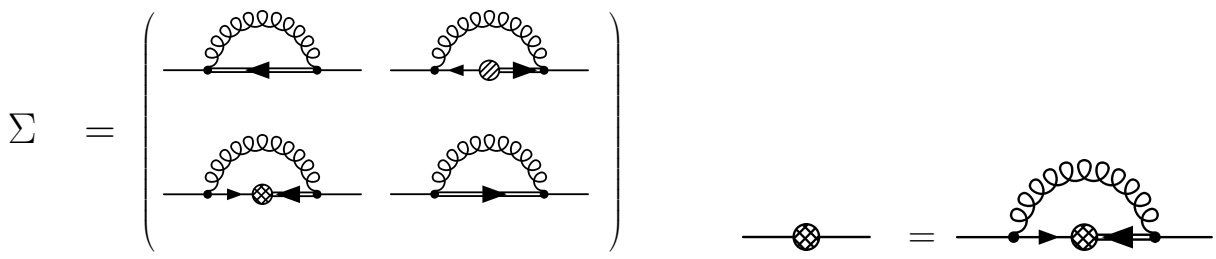

FIG. 10: Diagrammatic representation of the self-energy in Nambu-Gorkov space and the resulting gap equation. Curly lines are gluon propagators, double lines correspond to G^+ (left-pointing arrow) and G^- (right-pointing arrow), single lines to G_0^+ (left-pointing arrow) and G_0^- (right-pointing arrow), and the circles are the gap matrices Φ^+ (cross-hatched) and Φ^- (hatched). The vertices have the form $g\gamma^\mu T_a$ with the QCD coupling g. The gap equation arises as follows. On the one hand, the self-energy is given by cutting a fermion line in the two-loop "sunset" diagram. Due to the Nambu-Gorkov structure, this yields the matrix of four diagrams shown on the left-hand side. On the other hand, the self-energy is given by Eq. (234). Equating these two matrices leads to the gap equation in the off-diagonal elements. The gap equation is shown diagrammatically on the right-hand side and algebraically in Eq. (244). It is a self-consistency equation for Φ^+ (equivalently, one may solve the equation for Φ^-), and thus for the gap function $\Delta(K)$.

We multiply both sides of the gap equation with $\gamma_5\mathcal{M}\Lambda_k^+$ from the right, take the trace on both sides, neglect the antiparticle contribution $e = -$ (and denote $\epsilon_{k,r} \equiv \epsilon_{k,r}^+$), use the fact that the gluon propagator can be taken to be diagonal in color space, $D_{\mu\nu}^{ab} = \delta^{ab} D_{\mu\nu}$, to obtain

$$\begin{aligned}\Delta(K) &= \frac{g^2}{24}\frac{T}{V}\sum_Q\sum_r \frac{\Delta(Q)}{q_0^2-\epsilon_{q,r}^2}\mathrm{Tr}[\gamma^\mu\gamma_5\Lambda_q^-\gamma^\nu\gamma_5\Lambda_k^+]\,\mathrm{Tr}[T_a^T\mathcal{M}\mathcal{P}_r T_a\mathcal{M}]D_{\mu\nu}(K-Q)\\ &= -\frac{g^2}{3}\frac{T}{V}\sum_Q\left[\frac{2}{3}\frac{\Delta(Q)}{q_0^2-\epsilon_{q,1}^2}+\frac{1}{3}\frac{\Delta(Q)}{q_0^2-\epsilon_{q,2}^2}\right]\mathrm{Tr}[\gamma^\mu\gamma_5\Lambda_q^-\gamma^\nu\gamma_5\Lambda_k^+]\,D_{\mu\nu}(K-Q)\,, \end{aligned} \tag{245}$$

where we have used the results for the color-flavor traces

$$\mathrm{Tr}[T_a^T\mathcal{M}\mathcal{P}_1 T_a\mathcal{M}] = 2\mathrm{Tr}[T_a^T\mathcal{M}\mathcal{P}_2 T_a\mathcal{M}] = -\frac{16}{3}\,. \tag{246}$$

It is left as an exercise to verify these traces. With the gluon propagator in Coulomb gauge,

$$D_{00}(P) = D_\ell(P)\,, \qquad D_{0i}(P) = 0\,, \qquad D_{ij} = (\delta_{ij}-\hat{p}_i\hat{p}_j)D_t(P)\,, \tag{247}$$

where we abbreviated $P \equiv K - Q$, we have

$$\Delta(K) = \frac{g^2}{3}\frac{T}{V}\sum_Q\left[\frac{2}{3}\frac{\Delta(Q)}{q_0^2-\epsilon_{q,1}^2}+\frac{1}{3}\frac{\Delta(Q)}{q_0^2-\epsilon_{q,2}^2}\right]\Big[(1+\hat{\mathbf{q}}\cdot\hat{\mathbf{k}})D_\ell(P) - 2(1-\hat{\mathbf{p}}\cdot\hat{\mathbf{q}}\,\hat{\mathbf{p}}\cdot\hat{\mathbf{k}})D_t(P)\Big]\,. \tag{248}$$

Again, it is left as an exercise to verify this result by performing the trace in Dirac space. For the sake of brevity, let us now skip a few steps. One inserts the specific form of the longitudinal and transverse gluon propagators, performs the Matsubara sum and the angular integral. Details of all these steps can be found for instance in Ref. [31]. Let us also ignore the two-gap structure of the CFL phase. Then,

$$\Delta_k \simeq \frac{g^2}{24\pi^2}\int_{\mu-\delta}^{\mu+\delta} dq\,\frac{\Delta_q}{\epsilon_q}\tanh\frac{\epsilon_q}{2T}\left(\ln\frac{4\mu^2}{3m_g^2}+\ln\frac{4\mu^2}{M^2}+\frac{1}{3}\ln\frac{M^2}{|\epsilon_q^2-\epsilon_k^2|}\right)\,, \tag{249}$$

Here, the three terms in parentheses arise from static electric gluons, non-static magnetic gluons, and soft, Landau-damped magnetic gluons, respectively. The last of these terms is responsible for the leading behavior of the gap which will turn out to be different from the usual BCS behavior in electronic superconductors. The reason is the existence of a long-range interaction mediated by the magnetic gluons. We have defined $m_g^2 \equiv N_f g^2\mu^2/(6\pi^2)$ and $M^2 \equiv (3\pi/4)m_g^2$, and we have restricted the momentum integral to a small vicinity of the Fermi surface, $\delta \ll \mu$. The three logarithms can be combined to obtain

$$\Delta_k = \bar{g}^2\int_0^\delta d(q-\mu)\frac{\Delta_q}{\epsilon_q}\frac{1}{2}\ln\frac{b^2\mu^2}{|\epsilon_q^2-\epsilon_k^2|}\,, \tag{250}$$

with

$$\bar{g} \equiv \frac{g}{3\sqrt{2}\pi}\,, \qquad b \equiv 256\pi^4 \left(\frac{2}{N_f g^2}\right)^{5/2}\,, \tag{251}$$

and where we have taken the zero-temperature limit. The logarithm can be approximated by

$$\frac{1}{2}\ln\frac{b^2\mu^2}{|\epsilon_q^2-\epsilon_k^2|} \simeq \Theta(k-q)\ln\frac{b\mu}{\epsilon_k} + \Theta(q-k)\ln\frac{b\mu}{\epsilon_q}\,. \tag{252}$$

Moreover, we define the new integration variable

$$y \equiv \bar{g}\ln\frac{2b\mu}{q-\mu+\epsilon_q}\,, \tag{253}$$

and abbreviate

$$x \equiv \bar{g}\ln\frac{2b\mu}{k-\mu+\epsilon_k}\,, \qquad x^* \equiv \bar{g}\ln\frac{2b\mu}{\Delta}\,, \qquad x_0 \equiv \bar{g}\ln\frac{b\mu}{\delta}\,, \tag{254}$$

where Δ is the value of the gap at the Fermi surface, $\Delta \equiv \Delta_{q=\mu}$. We have

$$dy = -\frac{\bar{g}}{\epsilon_q}d(q-\mu)\,, \qquad \epsilon_q = b\mu e^{-y/\bar{g}}\left[1+\frac{\Delta_q^2}{(q-\mu+\epsilon_q)^2}\right]\,. \tag{255}$$

With the latter relation we approximate $\ln(b\mu/\epsilon_q) \simeq y/\bar{g}$, $\ln(b\mu/\epsilon_k) \simeq x/\bar{g}$ to obtain

$$\Delta(x) = x\int_x^{x^*} dy\,\Delta(y) + \int_{x_0}^{x} dy\,y\,\Delta(y)\,. \tag{256}$$

We can rewrite this integral equation as a differential equation,

$$\frac{d\Delta}{dx} = \int_x^{x^*} dy\Delta(y)\,, \qquad \frac{d^2\Delta}{dx^2} = -\Delta(x)\,. \tag{257}$$

This equation is solved by

$$\Delta(x) = \Delta\cos(x^*-x)\,, \tag{258}$$

such that the value of the gap at the Fermi surface (which corresponds to $x = x^*$) is Δ and such that the first derivative of the gap at the Fermi surface vanishes, since the gap peaks at the Fermi surface. To compute the value of the gap at the Fermi surface, we insert the solution (258) back into the gap equation (256) and consider the point $x = x^*$,

$$\begin{aligned}\Delta &= \Delta\int_{x_0}^{x^*} dy\,y\,\cos(x^*-y) = \Delta\left[\cos(x^*-y) - y\sin(x^*-y)\right]_{y=x_0}^{y=x^*} \\ &= \Delta\left[1-\cos(x^*-x_0)+x_0\sin(x^*-x_0)\right]\,.\end{aligned} \tag{259}$$

Since x_0 is of order $\bar{g}$, we may approximate $\cos(x^*-x_0) = \cos x^*\cos x_0 + \sin x^*\sin x_0 \simeq \cos x^* + x_0\sin x^*$, $\sin(x^*-x_0) = \sin x^*\cos x_0 - \cos x^*\sin x_0 \simeq \sin x^* - x_0\cos x^*$, and thus

$$\Delta \simeq \Delta(1-\cos x^*)\,. \tag{260}$$

Hence $\cos x^* \simeq 0$ and thus

$$\Delta = 2b\mu\exp\left(-\frac{3\pi^2}{\sqrt{2}g}\right)\,. \tag{261}$$

This important result shows that the color-superconducting gap is parametrically enhanced compared to the BCS gap. In the BCS gap equation the interaction between the fermions is point-like, and the gap equation has the form

$$\Delta \propto g^2\int_0^{\delta} d(q-\mu)\frac{\Delta}{\epsilon_q}\,. \tag{262}$$

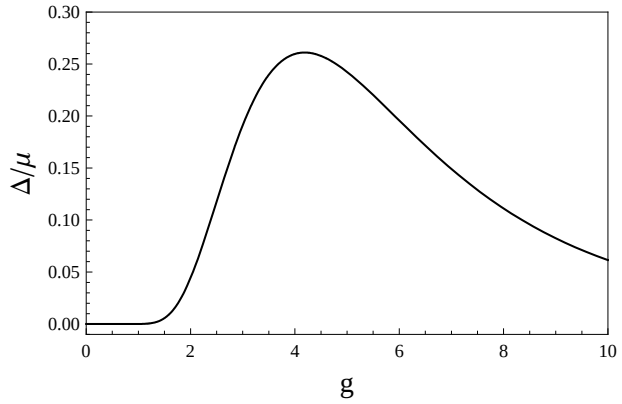

FIG. 11: Color-superconducting gap Δ over quark chemical potential μ as a function of the QCD coupling g. The curve shows the result from Eq. (261) with $N_f = 2$, predicting a weak-coupling behavior $\Delta/\mu \propto \exp(-\text{const}/g)$. The values of Δ/μ for large coupling is a simple (and in principle unreliable) extrapolation of the weak-coupling result.

Here the gap does not depend on momentum and one obtains $\Delta \propto \exp(-\text{const}/g^2)$, i.e., the coupling appears quadratic in the denominator of the exponential. This is in contrast to the color-superconducting gap (261) where the coupling appears linear in the denominator of the exponential. As mentioned above, this is due to the long-range interaction from magnetic gluons, showing up in the third term in parantheses on the right-hand side of Eq. (249). For more details and a more general solution for the QCD gap equation see Sec. IV in Ref. [7].

The solution of the QCD gap equation is a weak-coupling result and thus only valid at very large chemical potentials where the QCD coupling is sufficiently small. It is nevertheless interesting to extrapolate this result to larger couplings. Of course one should keep in mind that this extrapolation has no theoretical justification. We show the gap as a function of the coupling in Fig. 11. We see the exponentially small gap at small coupling and observe a maximum of the gap at a coupling of about $g \simeq 4.2$. For compact stars we make the following rough estimate. According to the two-loop β-function (which should of course not be taken seriously at these low densities), the coupling at $\mu = 400\,\text{MeV}$ is $g \simeq 3.5$. From Fig. 11 we then read off $\Delta \simeq 80\,\text{MeV}$. However in our derivation of the result we have ignored a subleading effect which yields an additional prefactor $\simeq 0.2$. Therefore, we estimate the color-superconducting gap for compact star densities to be of the order of $\Delta \simeq 10\,\text{MeV}$.

This result suggests that the critical temperature of color superconductivity is of the same order $T_c \simeq 10\,\text{MeV}$ (in BCS theory, $T_c = 0.57\,\Delta$). Remember that compact stars have temperatures well below that value (only in the very early stages of the life of the star, temperatures around 10 MeV are reached). This suggests that color superconductors are viable candidates for the matter inside the star. More precisely, if there is deconfined quark matter inside the star, it is very likely that it is in a color-superconducting state.

We conclude this chapter about color superconductivity by noticing that, besides the strong-coupling nature, other interesting questions arise at lower densities. We have seen in Sec. II B 2, that in unpaired quark matter the Fermi momenta of up, down, and strange quarks split apart. This is due to the nonzero strange quark mass and the conditions of neutrality and weak equilibrium. In our discussion of superconductivity we have always assumed that the fermions that form Cooper pair have identical Fermi momenta. This is true in the region of asymptotically large densities where the strange quark mass can be neglected. It is not true, however, at lower densities. The different Fermi momenta rather put a "stress" on the pairing. It is a quantitative question whether the pairing gap is large enough to overcome this stress. Roughly speaking, if the gap is larger than the mismatch in Fermi momenta, the usual pairing is still possible. It is therfore possible that the CFL phase persists down to densities where the transition to hadronic matter takes place. If the gap is too small, however, or the mismatch too large, Cooper pairing in the conventional way is not possible anymore. There are several versions of unconventional pairing which may take over and constitute one or several phases between the CFL phase at high densities and hadronic matter. Some of them break rotational and translational invariance, and thus may exhibit crystalline structures. More details can be found in Ref. [7], see also Ref. [32] for recent lecture notes in the form of a talk given at a graduate school. Here we simply emphasize that not only the strong-coupling nature but also the less symmetric situation (due to the finite strange quark mass) complicates our understanding of quark matter at compact star densities. This supports the arguments started above that we need to compute properties of candidate phases and check them for their compatibility with astrophyiscal observations. In the following section we shall turn to one of these properties, namely the neutrino emissivity.

[End of 10th lecture, June 8, 2009]

VI. NEUTRINO EMISSIVITY AND COOLING OF THE STAR

We have discussed at the end of Sec. II that mass and radius of a compact star are not very good observables to distinguish between nuclear matter and quark matter or between unpaired quark matter and color-superconducting quark matter. We now turn to an observable which is much more sensitive to the microscopic properties of dense matter, namely the temperature of the star. More precisely, its cooling curve, i.e., the temperature as a function of the age of the star. Approximately one minute after the star is born, the temperature has cooled below 1 MeV and the star becomes transparent for neutrinos. Consequently, neutrinos (and antineutrinos) which are produced in the star can leave the system and carry away energy. Neutrino emission is thus the dominant cooling mechanism of a compact star in about the first million years of its life. After that, photon emission takes over. We shall not be interested in this late regime here.

A very detailed review about neutrino emissivity in nuclear matter is Ref. [33]. If you are interested in a shorter review, also discussing quark matter, I recommend Ref. [34]. Before turning to the microscopic calculation of the neutrino emissivity ϵ_ν, let us discuss its importance for the cooling curves. First of all, as already discussed briefly in Sec. V A it is not only the emissivity which is important for the cooling. Once you know how much energy per time and volume is carried away, you need to know how this affects the temperature of the star. Hence you also need to know the specific heat. The specific heat c_V is a thermodynamical quantity and thus much easier to compute than the neutrino emissivity. We have done so in Sec. V A and have seen that superconductivity has a huge effect on c_V, namely, due to the energy gap, c_V is exponentially suppressed at sufficiently small temperatures. We shall see that superconductivity has a similar effect on the neutrino emissivity. Besides ϵ_ν and c_V, also the heat conductivity is important for the cooling behavior. Most forms of dense matter are very good heat conductors, such that the star becomes isothermal. As a consequence, in a realistic star which may have layers of different phases of dense matter, cooling tends to be dominated by the phase with the highest emissivity and the phase with the highest specific heat.

A. Urca processes in nuclear matter

In Fig. 12 we show some data and schematic comparison with calculations for the cooling curves. We see that there are different classes of processes which have lead to significanlty different cooling scenarios. The most efficient process is the so-called *direct Urca process* which leads to a very fast cooling.[9] In nuclear matter, the direct Urca processes are

$$n \to p + e + \bar{\nu}_e \,, \qquad p + e \to n + \nu_e \,. \tag{263}$$

We have discussed these processes in the context of β-equilibrium, where they serve to establish the relation $\mu_p + \mu_e = \mu_n$, where we have already assumed that the neutrinos escape from the star by setting $\mu_\nu = 0$. If the equilibrium relation is not fulfilled, one of the processes will happen at a faster rate than the other until chemical equilibrium is achieved. Here we are interested in the question how both processes contribute to the neutrino emissivity. Since it does not matter for the energy balance whether neutrinos or anti-neutrinos are emitted, both processes contribute – in chemical equilibrium – equally to the emissivity. For the neutron, proton, and electron, the dominant contribution in momentum space to the processes comes from the momenta close to the Fermi momentum. The neutrino momentum is of the order of the temperature T which can be neglected compared to the Fermi momenta. Therefore, momentum conservation for both processes in Eq. (263) reads

$$\mathbf{k}_{F,n} = \mathbf{k}_{F,p} + \mathbf{k}_{F,e} \,. \tag{264}$$

In other words, the Fermi momenta $\mathbf{k}_{F,n}$, $\mathbf{k}_{F,p}$, and $\mathbf{k}_{F,e}$ must form a triangle. For this triangle to exist, the triangle inquality has to be fulfilled,

$$k_{F,n} < k_{F,p} + k_{F,e} \,. \tag{265}$$

We know that in a neutral system we have $k_{F,p} = k_{F,e}$, and thus the triangle inequality becomes

$$k_{F,n} < 2k_{F,p} \,. \tag{266}$$

[9] This process is as efficient in carrying away energy as the *Casino de Urca* in Rio de Janeiro is in carrying away the money from the gamblers. Hence the name.

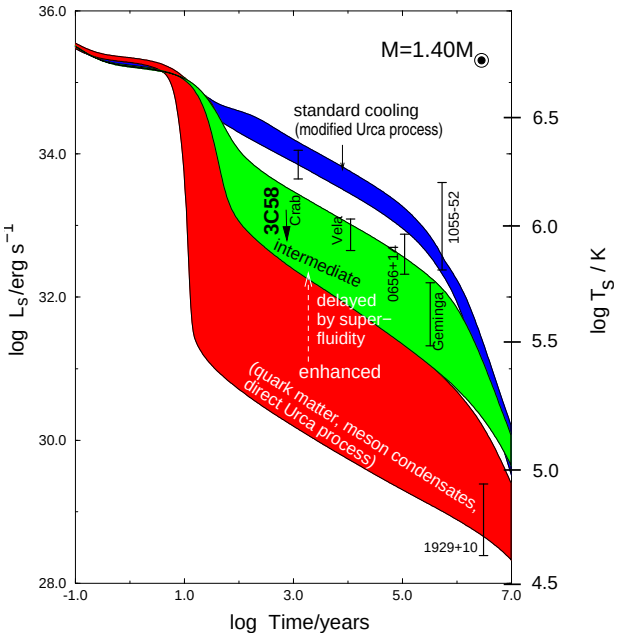

FIG. 12: Temperature/age measurements of compact stars and schematic comparison of the data with cooling curves from microscopic calculations. Figure taken from Ref. [5].

Consequently,

$$n_n < 8n_p \quad \Rightarrow \quad \frac{n_p}{n_B} > \frac{1}{9}\,, \tag{267}$$

i.e., the proton fraction has to be larger than 11%. We have seen in Sec. II A that this is not the case for noninteracting nuclear matter. Interactions will change this, especially for very large densities. At lower densities, this means that the direct Urca process does not work in nuclear matter.

This brings us to a second class of processes which are less efficient than the direct Urca process. Momentum conservation can be fulfilled by adding a spectator neutron or proton. This is the so-called *modified Urca process*,

$$N + n \to N + p + e + \bar{\nu}_e\,, \qquad N + p + e \to N + n + \nu_e\,, \qquad N = n, p\,. \tag{268}$$

As can be seen from Fig. 12, this process results in a much slower cooling. The cooling is thus very sensitive to the proton fraction of nuclear matter, especially around the threshold of 11%. In other words, this sensitivity provides a good check on the equation of state. Phenomenological models with equations of state which predict the proton fraction to be below this threshold can be excluded since the star would cool too fast.

There are several other neutrino emissivity processes in nuclear matter which we shall not discuss here. Some of these processes happen only with superconducting proton and superfluid neutrons, and are due to constant formation of Cooper pairs.

B. Direct Urca process in quark matter

The direct Urca processes in quark matter are

$$d \;\to\; u + e + \bar{\nu}_e\,, \qquad u + e \to d + \nu_e\,, \tag{269a}$$

$$s \;\to\; u + e + \bar{\nu}_e\,, \qquad u + e \to s + \nu_e\,. \tag{269b}$$

We have seen that the color-flavor locked phase is the ground state at very high densities. In this phase all quarks are gapped. This suggests that the direct Urca process is highly suppressed. Recall that the gap is of the order of 10 MeV, and the temperature of the star is well below that. Therefore, the exponential suppression $\exp(-\Delta/T)$ forbids any sizable effect of the Urca process. Other processes coming from Goldstone modes dominate the neutrino emissivity in the CFL phase. However, their contribution is much lower than that of the unsuppressed direct Urca

process. Therefore, if the star was made entirely out of CFL quark matter, its cooling would be very slow, too slow to be compatible with astrophysical observations. If the core of a hybrid star is made of CFL quark matter, with outer layers of nuclear matter where any kind of Urca process is possible, the cooling properties are utterly dominated by these outer layers.

We have mentioned that at lower densities, the CFL phase may not be the ground state anymore. Any other color-superconducting phase will have ungapped modes.[10] The simplest example is the so-called *2SC phase* where all blue and strange quarks are ungapped while the others are gapped. But there are more complicated candidate phase, where there are ungapped modes only in certain directions in momentum space. In any case, the neutrino emissivity of these phases will be dominated by these ungapped modes, and thus will only differ by the emissivity of unpaired quark matter by a numerical factor. We are thus interested in the neutrino emissivity of unpaired quark matter. To be a bit more ambitious, let us discuss the emissivity in the 2SC phase. From this calculation we will obtain the result for the unpaired phase "for free" because of the unpaired modes in the 2SC phase. Furthermore, we learn something about computing reaction rates in a superconductor which show some interesting features. And also we will see in an actual calculation why the emissivity of the gapped modes in exponentially suppressed. In other words, the goal of this section will be to understand

- the role of the Cooper pair condensate and the energy gap on the Urca process (we shall discuss this qualitatively)
- the result of the emissivity of unpaired quark matter (we shall compute this quantitatively)

All we shall need from the 2SC phase is the propagator. From Eq. (241) we know that the general form of the propagator is

$$G^{\pm} = \gamma^0 \Lambda_k^{\mp} \sum_r \mathcal{P}_r \frac{k_0 \mp (\mu - k)}{k_0^2 - \epsilon_{k,r}^2} \,. \tag{270}$$

where we also used Eq. (232) and where we dropped the antiparticle contribution. Note that this form of the propagator assumes that all flavor chemical potentials are the same. For the neutrino emissivity we need to drop this assumption, see below. The order parameter in the 2SC phase is characterized by $\phi_A^B = \delta_{A3}\delta^{B3}$ where ϕ is the matrix from Eq. (213). For simplicity, we drop the strange quarks and consider only a two-flavor system of up and down quarks.[11] Then, the color-flavor structure of the gap matrix is

$$\mathcal{M} = \tau_2 J_3 \,, \tag{271}$$

with the second Pauli matrix τ_2 in flavor space and J_3 in color space, as defined above Eq. (216). Technically, the color-flavor structure of the 2SC phase is much easier to deal with since color and flavor matrices factorize. Since $\tau_2^2 = \mathbf{1}$, we have $\mathcal{M}^2 = J_3^2$, whose eigenvalues are $\lambda_1 = 1$ (4-fold) and $\lambda_2 = 0$ (2-fold). The corresponding projectors are

$$\mathcal{P}_1 = J_3^2 \,, \qquad \mathcal{P}_2 = \mathbf{1} - J_3^2 \,. \tag{272}$$

They project onto red and green quarks (which are gapped) and blue quarks (which are ungapped), respectively.

Now we need to take into account that in a neutral two-flavor system, up and down chemical potentials are different, namely $\mu_u + \mu_e = \mu_d$, where μ_e turns out to be nonzero due to the neutrality constraint. We thus have to generalize the propagator (270) to this case.

Exercise 8: *Show that for the case of different flavor chemical potentials the fermion propagator of the 2SC phase has the flavor components*

$$G_u^{\pm} = \gamma^0 \Lambda_k^{\mp} \sum_r \frac{k_0 \mp (\mu_u - k)}{(k_0 \mp \delta\mu)^2 - \epsilon_{k,r}^2} \mathcal{P}_r \,, \qquad G_d^{\pm} = \gamma^0 \Lambda_k^{\mp} \sum_r \frac{k_0 \mp (\mu_d - k)}{(k_0 \pm \delta\mu)^2 - \epsilon_{k,r}^2} \mathcal{P}_r \,, \tag{273}$$

---

[10] A possible exception is the *color-spin locked phase* which has Cooper pairs with total angular momentum one and which we do not discuss here.

[11] The weak interaction between u and s quarks is suppressed compared to the one between u and d quarks due to the Cabibbo angle. However, the finite strange quark mass may partially compensate this effect because it leads to a larger phase space for the Urca process. Here in this lecture we do not want to deal with these complications and thus simply consider a system of massless up and down quarks, and thus only the processes (269a).

with

$$\epsilon_{k,r} \equiv \sqrt{(\bar{\mu}-k)^2+\lambda_r\Delta^2}\,, \qquad \delta\mu \equiv \frac{\mu_d-\mu_u}{2}\,, \qquad \bar{\mu} \equiv \frac{\mu_d+\mu_u}{2}\,, \tag{274}$$

and λ_r, $\mathcal{P}_r$ as above ($\mathcal{P}_r$ now being only matrices in color space since the flavor components are written separately).

This structure of the propagator and the resulting quasiparticle dispersion relations are interesting on their own, since they describe Cooper pairing with a mismatch in Fermi momenta, as discussed at the end of Sec. V C. However, in the current context of neutrino emissivity, we are only interested in the qualitative features of the gapped modes. Thus we shall ignore this complicated structure of the propagator and temporarily set $\mu_u = \mu_d$. Only when we compute the emissivity from the unpaired modes we shall reinstate the difference in up and down chemical potentials.

Next we need to set up the equation that determines the neutrino emissivity. One possible formalism is the finite temperature real-time formalism. We shall not explain this formalism but refer the reader for more details to the textbooks [8] and [9]. For our purpose it is enough to know that the real-time formalism can be used for nonequilibrium calculations. Therefore it is well suited for transport properties and neutrino emissivity. Since these properties are always close-to-equilibrium properties, one often simply uses an equilibrium formalism, such as the imaginary-time formalism, and adds whatever is needed as a small out-of-equilibrium feature by hand. In the real-time formalism we can start from the kinetic equation

$$i\frac{\partial}{\partial t}\mathrm{Tr}[\gamma_0 G_\nu^<(P_\nu)] = -\mathrm{Tr}[G_\nu^>(P_\nu)\Sigma_\nu^<(P_\nu) - \Sigma_\nu^>(P_\nu)G_\nu^<(P_\nu)]\,, \tag{275}$$

where $G_\nu^>$ and $G_\nu^<$ are the "greater" and "lesser" neutrino propagators, and P_ν is the neutrino four-momentum. The trace is taken over Dirac space. The two terms correspond to the two directions of both processes (269a). Because neutrinos leave the system, only one of the directions, the one given in Eq. (269a), contributes. The neutrino self-energies $\Sigma_\nu^{<,>}$ are given by the diagram in Fig. 13. Through the formalism, the diagram gets cut such that one recovers the Urca process. Part of the neutrino self-energy are the W-boson polarization tensors $\Pi^{<,>}$. They are defined through the imaginary part of the retarded polarization tensor $\mathrm{Im}\,\Pi_R$,

$$\Pi^>(Q) = -2i[1+f_B(q_0)]\mathrm{Im}\,\Pi_R(Q)\,, \tag{276a}$$
$$\Pi^<(Q) = -2i f_B(q_0)\mathrm{Im}\,\Pi_R(Q)\,, \tag{276b}$$

with the Bose distribution function f_B. We shall discuss the calculation of $\Pi^{<,>}$ in detail below. The kinetic equation (275) becomes

$$\frac{\partial}{\partial t}f_\nu(t,\mathbf{p}_\nu) = \frac{G_F^2}{8}\int\frac{d^3\mathbf{p}_e}{(2\pi)^3 p_\nu p_e}L_{\lambda\sigma}(\mathbf{p}_e,\mathbf{p}_\nu)f_F(p_e-\mu_e)f_B(p_\nu+\mu_e-p_e)\mathrm{Im}\,\Pi_R^{\lambda\sigma}(Q)\,, \tag{277}$$

where, due to four-momentum conservation,

$$Q = (p_e - p_\nu - \mu_e, \mathbf{p}_e - \mathbf{p}_\nu)\,, \tag{278}$$

and where

$$L^{\lambda\sigma}(\mathbf{p}_e,\mathbf{p}_\nu) \equiv \mathrm{Tr}\left[(\gamma_0 p_e - \boldsymbol{\gamma}\cdot\mathbf{p}_e)\,\gamma^\sigma(1-\gamma^5)(\gamma_0 p_\nu - \boldsymbol{\gamma}\cdot\mathbf{p}_\nu)\,\gamma^\lambda(1-\gamma^5)\right]. \tag{279}$$

For details of the derivation of Eq. (277) see Ref. [35], where the neutrino emissivity is computed in the same formalism (for anisotropic phases, which leads to more complicated calculations as we do here). Here we simply explain the features of this equation. The left-hand side is the change of the neutrino occupation number in time. It is related to the emissivity by

$$\epsilon_\nu \equiv -2\frac{\partial}{\partial t}\int\frac{d^3\mathbf{p}_\nu}{(2\pi)^3}\,p_\nu\,f_\nu(t,\mathbf{p}_\nu)\,, \tag{280}$$

where the factor 2 accounts for the contribution from antineutrinos. The neutrino emissivity is thus the change in energy per unit time and volume. Our task is to compute the right-hand side of Eq. (277) and integrate over the neutrino momentum according to Eq. (280) to obtain ϵ_ν. To understand the right-hand side of Eq. (277) first note that the vertex Γ^μ for the processes $d \leftrightarrow u + W^-$ and $e \leftrightarrow \nu + W^-$ is given by

$$\Gamma^\mu = -\frac{e}{2\sqrt{2}\sin\theta_W}\gamma^\mu(1-\gamma^5)\,, \tag{281}$$

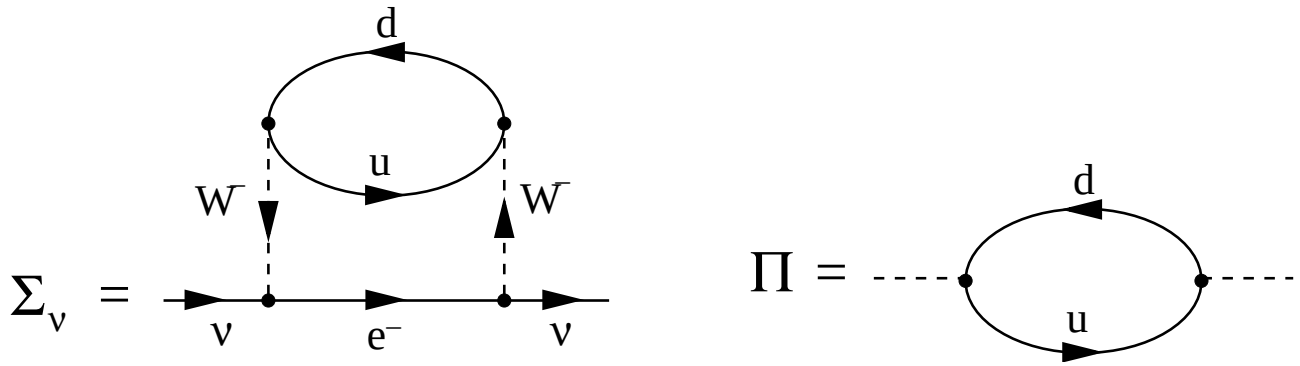

FIG. 13: Neutrino self-energy Σ_ν and W-boson polarization tensor Π needed for the neutrino emissivity from the quark Urca process.

with the Weinberg angle θ_W. (For the process $d \leftrightarrow u + W^-$ there is an additional factor V_{ud} from the CKM matrix; however, $V_{ud} \simeq 1$.) The W-boson propagators can be approximated by the inverse W-boson mass squared M_W^2 since all momenta we are interested in are much smaller than this mass $M_W \simeq 80\,\mathrm{GeV}$. Thus, pulling out the constant factors of the vertices in the W-boson polarization tensor, we obtain the overall factor G_F^2 with the Fermi coupling

$$G_F = \frac{\sqrt{2}e^2}{8M_W^2 \sin^2\theta_W} = 1.16637 \cdot 10^{-11}\mathrm{MeV}^{-2}\,. \tag{282}$$

The additional factors in the trace of Eq. (218) come from the electron and neutrino propagators. And finally, the distribution functions in Eq. (277) belong to the electron and the W-boson. Eventually, the Bose distribution of the W-boson will drop out since the W-boson does not appear in the initial or final state of the process we are interested in.

[End of 11th lecture, June 15, 2009]

1. *W-boson polarization tensor*

Next we need to compute $\mathrm{Im}\,\Pi_R^{\lambda\sigma}$ for which we first compute

$$\Pi^{\lambda\sigma}(Q) = \frac{T}{V}\sum_K \mathrm{Tr}[\Gamma_-^\lambda S(K)\Gamma_+^\sigma S(P)]\,, \tag{283}$$

where the trace is taken over Dirac, color, flavor, and Nambu-Gorkov space. We have defined $P \equiv K + Q$; K and P will play the role of the u and d quark momentum, respectively. The weak vertices in Nambu-Gorkov space are

$$\Gamma_\pm^\lambda = \begin{pmatrix} \gamma^\lambda(1-\gamma^5)\,\tau_\pm & 0 \\ 0 & -\gamma^\lambda(1+\gamma^5)\,\tau_\mp \end{pmatrix}, \tag{284}$$

where $\tau_\pm \equiv (\tau_1 \pm i\tau_2)/2$ are matrices in flavor space, constructed from the Pauli matrices τ_1, τ_2. Recall that, for notational convenience, we have pulled out the constants of the weak vertices already and absorbed them in the overall factor G_F^2. With the quark propagator (236), the trace over Nambu-Gorkov space yields

$$\begin{aligned}\Pi^{\lambda\sigma}(Q) \;=\; \frac{T}{V}\sum_K \Big\{ &\mathrm{Tr}\left[\gamma^\lambda(1-\gamma^5)\tau_- G^+(K)\gamma^\sigma(1-\gamma^5)\tau_+ G^+(P)\right] + \mathrm{Tr}\left[\gamma^\lambda(1+\gamma^5)\tau_+ G^-(K)\gamma^\sigma(1+\gamma^5)\tau_- G^-(P)\right] \\ &- \mathrm{Tr}\left[\gamma^\lambda(1-\gamma^5)\tau_- F^-(K)\gamma^\sigma(1+\gamma^5)\tau_- F^+(P)\right] - \mathrm{Tr}\left[\gamma^\lambda(1+\gamma^5)\tau_+ F^+(K)\gamma^\sigma(1-\gamma^5)\tau_+ F^-(P)\right] \Big\}\,. \end{aligned} \tag{285}$$

We see that there is a contribution from the anomalous propagators. This contribution is only present for the gapped modes. We shall ignore it here for simplicity (it is smaller than the contribution from the normal propagators, but not negligibly small). We shall rather focus on the contribution of the normal propagators (which of course also contain

the superconducting gap). The first two traces in Eq. (285) turn out to be identical which we shall use without explicit proof. We thus continue simply with twice the first term,

$$\Pi^{\lambda\sigma}(Q) \;\simeq\; 2\frac{T}{V}\sum_K\sum_{r,s}\mathrm{Tr}\left[\gamma^\lambda(1-\gamma^5)\tau_-\gamma_0\mathcal{P}_r\Lambda_k^-\gamma^\sigma(1-\gamma^5)\tau_+\gamma_0\mathcal{P}_s\Lambda_p^-\right]\frac{k_0-(\mu-k)}{k_0^2-\epsilon_{k,r}^2}\frac{p_0-(\mu-p)}{p_0^2-\epsilon_{p,s}^2}\,, \tag{286}$$

where we have inserted the propagator (270) (recall that we have set $\mu_u=\mu_d$ temporarily to avoid complications; this is sufficient to discuss the effects of superconductivity qualitatively, but eventually we shall reinstate the difference in μ_u and μ_d to compute the result for unpaired quark matter). The color-flavor traces are

$$\mathrm{Tr}[\tau_-\mathcal{P}_1\tau_+\mathcal{P}_1] \;=\; 2\,, \tag{287a}$$
$$\mathrm{Tr}[\tau_-\mathcal{P}_1\tau_+\mathcal{P}_2] \;=\; 0\,, \tag{287b}$$
$$\mathrm{Tr}[\tau_-\mathcal{P}_2\tau_+\mathcal{P}_1] \;=\; 0\,, \tag{287c}$$
$$\mathrm{Tr}[\tau_-\mathcal{P}_2\tau_+\mathcal{P}_2] \;=\; 1\,. \tag{287d}$$

Recalling that $\mathcal{P}_1$ projects onto the gapped red and green quarks and $\mathcal{P}_2$ onto the ungapped blue quarks, this is easy to interpret: the weak interaction cannot change colors. Therefore, the quark loop in the polarization tensor – see right-hand side of Fig. 13 – contains an up quark and a down quark of the same color. They are either both gapped (then they are red or green, hence the result 2 in Eq. (287a)), or they are both ungapped (then they are blue). There is no term involving one gapped and one ungapped quark. We thus get two contributions,

$$\Pi^{\lambda\sigma}(Q)\simeq 2\frac{T}{V}\sum_K\mathcal{T}^{\lambda\sigma}(\hat{\mathbf{k}},\hat{\mathbf{p}})\left[2\frac{k_0-(\mu-k)}{k_0^2-\epsilon_{k,1}^2}\frac{p_0-(\mu-p)}{p_0^2-\epsilon_{p,1}^2}+\frac{k_0-(\mu-k)}{k_0^2-\epsilon_{k,2}^2}\frac{p_0-(\mu-p)}{p_0^2-\epsilon_{p,2}^2}\right]\,, \tag{288}$$

where we abbreviated the Dirac trace

$$\mathcal{T}^{\lambda\sigma}(\hat{\mathbf{k}},\hat{\mathbf{p}})\equiv\mathrm{Tr}\left[\gamma^\lambda(1-\gamma^5)\gamma_0\Lambda_k^-\gamma^\sigma(1-\gamma^5)\gamma_0\Lambda_p^-\right]\,. \tag{289}$$

We notice that the second contribution in Eq. (288) is obtained from the first upon setting $\Delta=0$. Thus, for notational convenience, let us simply compute the first term and denote $\epsilon_k\equiv\epsilon_{k,1}$. In the end it is then straightforward to get the full result.

Next one has to perform the sum over the fermionic Matsubara frequencies. We have discussed this technique in detail in the previous semester. In fact we can use Exercise 4 from the lecture notes (see p. 20 of Ref. [10]) to obtain

$$T\sum_{k_0}\frac{k_0-(\mu-k)}{k_0^2-\epsilon_k^2}\frac{p_0-(\mu-p)}{p_0^2-\epsilon_p^2}=-\frac{1}{4\epsilon_k\epsilon_p}\sum_{e_1,e_2=\pm}\frac{[\epsilon_k+e_1(\mu-k)][\epsilon_p+e_2(\mu-p)]}{q_0-e_1\epsilon_k+e_2\epsilon_p}\frac{f_F(-e_1\epsilon_k)f_F(e_2\epsilon_p)}{f_B(-e_1\epsilon_k+e_2\epsilon_p)}\,. \tag{290}$$

(Remember $P=Q+K$.) Here the signs e_1, e_2 for now simply serve as a compact notation. They should not be confused with the sum over particles and antiparticles. To obtain the retarded polarization tensor, we need to replace $q_0\to q_0-i\eta$. Then, the imaginary part is obtained by using the identity (sometimes called *Dirac identity*)

$$\lim_{\eta\to0^+}\frac{1}{x\pm i\eta}=\mathcal{P}\frac{1}{x}\mp i\pi\delta(x)\,, \tag{291}$$

where $\mathcal{P}$ denotes the principal value. This yields

$$\mathrm{Im}\,\Pi_R^{\lambda\sigma}(Q)\simeq-2\pi\sum_{e_1e_2}\int\frac{d^3\mathbf{k}}{(2\pi)^3}\mathcal{T}^{\lambda\sigma}(\hat{\mathbf{k}},\hat{\mathbf{p}})B_k^{e_1}B_p^{e_2}\frac{f_F(-e_1\epsilon_k)f_F(e_2\epsilon_p)}{f_B(-e_1\epsilon_k+e_2\epsilon_p)}\,\delta(q_0-e_1\epsilon_k+e_2\epsilon_p)\,, \tag{292}$$

where we have defined the *Bogoliubov coefficients*

$$B_k^e\equiv\frac{1}{2}\left(1+e\frac{\mu-k}{\epsilon_k}\right)\,. \tag{293}$$

These coefficients appear in the theory of any kind of superconductor or superfluid, see for instance Ref. [30]. Inserting the result (292) back into Eq. (277) yields

$$\begin{aligned}\frac{\partial}{\partial t}f_\nu(t,\mathbf{p}_\nu) \;=\; -\frac{\pi G_F^2}{4}\sum_{e_1e_2}\int\frac{d^3\mathbf{p}_e d^3\mathbf{k}}{(2\pi)^3(2\pi)^3p_\nu p_e}L_{\lambda\sigma}(\mathbf{p}_e,\mathbf{p}_\nu)\mathcal{T}^{\lambda\sigma}(\hat{\mathbf{k}},\hat{\mathbf{p}})B_k^{e_1}B_p^{e_2}\\ \times f_F(p_e-\mu_e)f_F(-e_1\epsilon_k)f_F(e_2\epsilon_p)\delta(q_0-e_1\epsilon_k+e_2\epsilon_p)\,.\end{aligned} \tag{294}$$

Note that the Bose distribution from Eq. (277) cancels with the denominator from Eq. (292) since on the one hand $q_0 = p_e - p_\nu - \mu_e$ according to Eq. (278) and on the other hand $q_0 = e_1\epsilon_k - e_2\epsilon_p$ according to the δ-function.

In the rate of the process $u + e \to d + \nu_e$ one expects Fermi distributions of the form $f_e f_u(1 - f_d)$, the factors f_e and f_u standing for the incoming fermions, and the factor $1 - f_d$ standing for the outgoing fermion (for the neutrino $f_\nu \simeq 0$). So what is the meaning of the sum over e_1, e_2 in Eq. (294)? With $f(-x) = 1 - f(x)$ it seems that all combinations $f_e f_u f_d$, $f_e f_u(1 - f_d)$, $f_e(1 - f_u)f_d$, and $f_e(1 - f_u)(1 - f_d)$ appear. In other words also processes where both the up and down quark are created or annihilated give a contribution. This is indeed possible in a superconductor where particle number conservation is sponteneously broken and particles can be created from or deposited into the condensate. To see explicitly that in the unpaired phase only one of the four subprocesses survives, let us define the new Bogoliubov coefficients and the new dispersion relations

$$\tilde{B}^e_k \equiv \frac{1}{2}\left(1 + e\frac{k-\mu}{\tilde{\epsilon}_k}\right), \qquad \tilde{\epsilon}_k \equiv \mathrm{sgn}(k-\mu)\epsilon_k\,. \tag{295}$$

Then we use that for any function F we have

$$\sum_e \int_0^\infty dk\, B^e_k F(e\epsilon_k) = \sum_e \int_0^\infty dk\, \tilde{B}^e_k F(-e\tilde{\epsilon}_k)\,. \tag{296}$$

This reformulation is due to the mixing of particles and holes in a superconductor, which is manifest in the Bogoliubov coefficients. Had we taken the limit $\Delta \to 0$ with the original formulation in B^e_k, ϵ_k, we would have obtained the excitation energy $\epsilon_k = |k - \mu|$ which describes a hole for $k < \mu$ and a particle for $k > \mu$. The more conventional excitation $\epsilon_k = k - \mu$ which describes a particle for all k is only obtained as a limit using $\tilde{B}^e_k$, $\tilde{\epsilon}_k$ (both formulations are of course physically equivalent). Now, since in the unpaired phase $\tilde{B}^+_k = 1$, $\tilde{B}^-_k = 0$, we see that only the subprocess with $e_1 = e_2 = 1$ survives in the unpaired phase. The other three subprocesses are only possible in the superconducting phase.

The general result in the superconducting phase has to be computed numerically. The most important result is that at small temperatures, the emissivity is suppressed, $\epsilon_\nu \propto \exp(-\Delta/T)$. It is left as an exercise to confirm this behavior from the general expression. We shall continue now with the calculation for unpaired quark matter.

2. Result for unpaired quark matter

With the help of the new Bogoliubov coefficients it is now trivial to take the unpaired phase limit. We also need the following ingredients to proceed. First we need to perform the remaining traces in Dirac space and do the contraction over Lorentz indices. This is done in the following exercise.

Exercise 9: *Show that*

$$L_{\lambda\sigma}(\mathbf{p}_e, \mathbf{p}_\nu)\mathcal{T}^{\lambda\sigma}(\hat{\mathbf{k}}, \hat{\mathbf{p}}) = 64(p_e - \mathbf{p}_e\cdot\hat{\mathbf{k}})(p_\nu - \mathbf{p}_\nu\cdot\hat{\mathbf{p}})\,, \tag{297}$$

with $L_{\lambda\sigma}(\mathbf{p}_e, \mathbf{p}_\nu)$ and $\mathcal{T}^{\lambda\sigma}(\hat{\mathbf{k}}, \hat{\mathbf{p}})$ defined in Eqs. (218) and (289), respectively.

Next we observe that the result for the right-hand side of Eq. (294) would be zero without further corrections. We have to take into account so-called Fermi liquid corrections which are induced by the strong interaction. We have mentioned these corrections briefly in Sec. II C, see Eq. (80). To lowest order in the strong coupling constant α_s (which is related to the coupling g from Sec. V C by $\alpha_s = g^2/(4\pi)$) we have

$$p_{F,u/d} = \mu_{u/d}(1 - \kappa)\,, \qquad \kappa \equiv \frac{2\alpha_s}{3\pi}\,. \tag{298}$$

We illustrate in Fig. 14 how these corrections open up the phase space for the direct Urca process. As a consequence, there is a fixed angle θ_{ud} between the u and d quarks, and the δ-function in Eq. (294) can be approximated by

$$\delta(p_e - p_\nu + k - p) \simeq \frac{\mu_e}{\mu_u\mu_d}\delta(\cos\theta_{ud} - \cos\theta_0)\,, \qquad \cos\theta_0 \equiv 1 - \kappa\frac{\mu_e^2}{\mu_u\mu_d}\,. \tag{299}$$

(We have reinstated the different chemical potentials μ_u, μ_d.) Also we may approximate

$$(p_e - \mathbf{p}_e\cdot\hat{\mathbf{k}})(p_\nu - \mathbf{p}_\nu\cdot\hat{\mathbf{p}}) \simeq 2\mu_e p_\nu\kappa(1 - \cos\theta_{\nu d})\,, \tag{300}$$

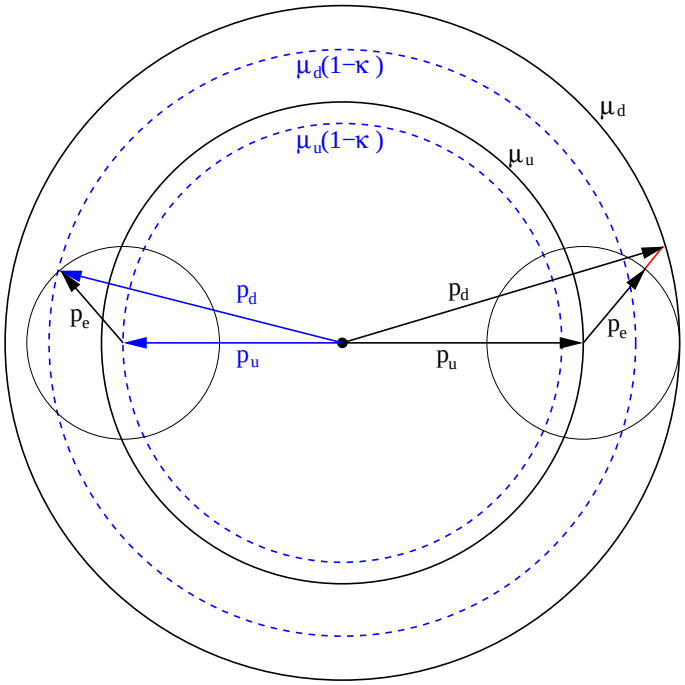

FIG. 14: Illustration of how Fermi liquid effects from the strong interaction open up the phase space for the direct Urca process in (unpaired) quark matter. Right-hand side (black): without Fermi liquid corrections, the Fermi momenta of the (massless) quarks are given by $p_{F,u} = \mu_u$, $p_{F,d} = \mu_d$. Start with the momentum of the up-quark, $\mathbf{p}_u$. The circle with center at its tip indicates possible endpoints of the electron momemtum $\mathbf{p}_e$. Since $p_{F,e} = \mu_e$ and $\mu_u + \mu_e = \mu_d$ (β-equilibrium), one cannot form a triangle with $\mathbf{p}_u$, $\mathbf{p}_e$ and the down-quark momentum $\mathbf{p}_d$, unless one chooses the three vectors to be collinear. In this case, the triangle collapses to a line and the phase space for the Urca process vanishes. Note that the neutrino momentum $p_\nu \sim T$ is negligibly small on the scale of the figure. Left-hand side (blue): the strong interaction changes the quark Fermi momenta to $p_{F,u} \simeq \mu_u(1-\kappa)$, $p_{F,d} \simeq \mu_d(1-\kappa)$ with $\kappa = 2\alpha_s/(3\pi)$. In other words, both Fermi momenta are reduced, but the down-quark Fermi momentum is reduced by a larger absolute amount. Since the electron Fermi momentum is not changed, a finite region in phase space opens up. The resulting triangle has a fixed angle between up- and down-quark momenta given by the values of the chemical potentials and κ.

with the angle $\theta_{\nu d}$ between the neutrino and the d quark. This factor vanishes for the case of collinear scattering. The α_s effect renders it nonzero, thus this factor and in consequence the total neutrino emissivity is proportional to α_s. Putting all this together and changing the integration variable from $\mathbf{p}_e$ to the d quark momentum $\mathbf{p}$ yields

$$\frac{\partial}{\partial t} f_\nu(t, \mathbf{p}_\nu) = -64 G_F^2 \alpha_s \mu_e \mu_d \mu_u \int \frac{dp\, d\Omega_p}{(2\pi)^3} \int \frac{dk\, d\Omega_k}{(2\pi)^3} (1 - \cos\theta_{\nu d}) \delta(\cos\theta_{ud} - \cos\theta_0) \times f_F(p_e - \mu_e) f_F(k - \mu_u)[1 - f_F(p - \mu_d)] \,. \tag{301}$$

Since we have taken only one color degree of freedom from Eq. (288), we have reinstated a factor $N_c = 3$. Next we introduce the variables

$$x = \frac{p - \mu_d}{T} \,, \qquad y = \frac{k - \mu_u}{T} \,, \qquad v = \frac{p_\nu}{T} \,. \tag{302}$$

Then, with the definition (280) of the total neutrino emissivity, we obtain

$$\epsilon_\nu = 128 \alpha_s G_F^2 \mu_e \mu_u \mu_d T^6 \int \frac{d\Omega_{p_\nu}}{(2\pi)^3} \int \frac{d\Omega_p}{(2\pi)^3} \int \frac{d\Omega_k}{(2\pi)^3} (1 - \cos\theta_{\nu d}) \delta(\cos\theta_{ud} - \cos\theta_0) \times \int_0^\infty dv\, v^3 \int_{-\infty}^\infty dx \int_{-\infty}^\infty dy\, f_F(v + x - y) f_F(y)[1 - f_F(x)] \,. \tag{303}$$

Here we have approximated the lower boundaries by $-\mu_{u/d}/T \simeq \infty$. With the integral

$$\int_0^\infty dv\, v^3 \int_{-\infty}^\infty dx \int_{-\infty}^\infty dy\, f_F(v + x - y) f_F(y)[1 - f_F(x)] = \frac{457}{5040} \pi^6 \,, \tag{304}$$

and the (trivial) angular integral

$$\int \frac{d\Omega_{p_\nu}}{(2\pi)^3} \int \frac{d\Omega_p}{(2\pi)^3} \int \frac{d\Omega_k}{(2\pi)^3} (1-\cos\theta_{\nu d})\delta(\cos\theta_{ud}-\cos\theta_0) = \frac{1}{16\pi^6}\,, \tag{305}$$

we obtain the final result

$$\epsilon_\nu \simeq \frac{457}{630}\alpha_s G_F^2 \mu_e \mu_u \mu_d T^6\,. \tag{306}$$

This result has first been computed by Iwamoto in 1980 [36].

C. Cooling with quark direct Urca process

We can now easily get a cooling curve for unpaired quark matter. Of course we are ignoring a lot of details of realistic stars. The result will simply show how a chunk of unpaired two-flavor quark matter cools via the direct Urca process. Nevertheless, the result is very illustrative and shows that the direct Urca process is indeed an efficient cooling mechanism. We use Eq. (209), which relates the temperature as a function of time to the emissivity and the specific heat. For the emissivity we use the result (306). For the specific heat, recall the result (200) which is valid for two fermionic degrees of freedom, taking into account spin; we thus have to multiply this result by the number of colors and add up the contributions of u and d quarks,

$$c_V = (\mu_u^2 + \mu_d^2)T\,. \tag{307}$$

Then, performing the integration in Eq. (209) yields

$$T(t) = \frac{T_0 \tau^{1/4}}{(t-t_0+\tau)^{1/4}}\,, \tag{308}$$

where we have defined

$$\tau = \frac{315}{914}\frac{\mu_u^2+\mu_d^2}{\alpha_s G_F^2 \mu_e \mu_u \mu_d}\frac{1}{T_0^4}\,. \tag{309}$$

To get an estimate for this characteristic time scale, we assume $\mu_d = 500\,\text{MeV}$, $\mu_u = 400\,\text{MeV}$, $\mu_e = 100\,\text{MeV}$, $\alpha_s = 1$, an initial temperature of $T_0 = 100\,\text{keV}$ at an initial time $t_0 = 100\,\text{yr}$, and use value of the Fermi coupling (282) to obtain

$$\tau \simeq 10^{-5}\,\text{yr} \simeq 5\,\text{min}\,. \tag{310}$$

This is a very short time for the time scales we are interested in. The function $T(t)$ is plotted in Fig. (15). We see the rapid drop in temperature on a time scale of minutes down to a few keV. We thus recover the shape of the direct Urca cooling from Fig. (12). For later times $t \gg t_0$, we have $T(t) \propto t^{-1/4}$.

[End of 12th lecture, June 22, 2009]

VII. DISCUSSION

At the end of the semester, let us summarize what we have learned about compact stars and about dense matter, having in mind the two questions we have formulated in the introduction. In addition, let us also list a few things which would have fitted into this lecture topic-wise, but didn't fit time-wise. I will give some selected easy-to-read references where you can find more information about the certain points.

A. What we have discussed

- *Astrophysical observables and their relation to microscopic physics.* The first thing you should have learned in this lecture is that compact stars are laboratories for the understanding of dense matter. The experiments we can do in this laboratory are less controlled as for example tabletop experiments in condensed matter. This

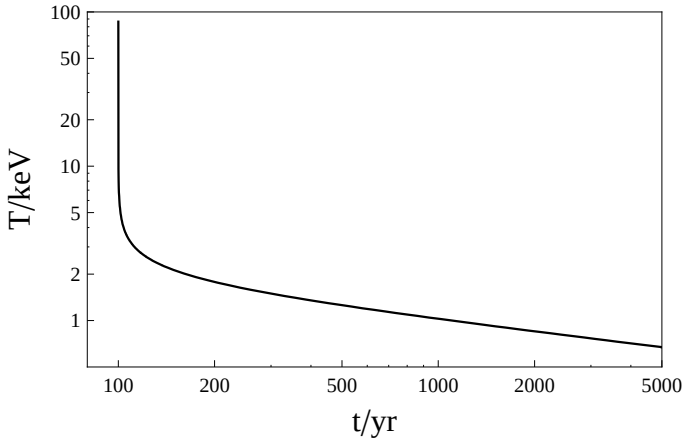

FIG. 15: Cooling scenario from the direct Urca process in unpaired quark matter, see Eq. (308).

means we cannot always measure the quantities we would like to know. And it means that it is often difficult to switch on or off certain effects which would be desirable to extract an exact value for a given observable. However, in spite of these restrictions (which can be expected to get looser through better technology in the future) we have seen that our observational data of compact stars can be closely linked to the properties of dense matter. Examples we have discussed in detail are the mass/radius relation which is related to the equation of state and the cooling curve which is related to the neutrino emissivity. Other examples which we have not discussed follow below.

- *Theoretical approaches to dense matter.* We have emphasized several times in this lecture that the density regime which is of interest for the physics of compact stars is very difficult to tackle. After all, this difficulty led us to consider compact stars not only as an application of QCD but also as an important means to understand QCD. The reason for the theoretical difficulty is of course the strong-coupling nature of QCD. We have discussed attempts to approach this density regime from two sides, coming from lower and higher density. First, we have discussed nuclear matter, for which we have solid knowledge at low densities. This knowledge is strongly built upon experimental data. In principle, even a single nucleon is theoretically a very complicated object if considered from first principles. Therefore, effective theories are used which we know describe nuclear matter well at low densities. One of the examples we have discussed is the Walecka model. However, finding the correct description of nuclear matter at high density is a challenge, and astrophysical data can be used to rule out or confirm certain models. Second, we have discussed QCD from first principles. This approach is rigorous at asymptotically high density and therefore is interesting on its own right. We have discussed that it predicts the CFL state. Whether CFL persists down to densities relevant for compact stars is unknown. We have discussed that, to get quantitative estimates for the low-density region, one may simply extrapolate the rigorous results. But this of course stretches the results beyond their range of validity. We have only mentioned a more powerful approach to deduce intermediate-density properties from the high-density calculations. This approach relies on the symmetries of CFL state. Building on these symmetries, one can write down an effective theory which can give us at least qualitative insight into the properties of CFL at lower densities (this approach cannot tell us whether CFL is indeed the ground state in a compact star). We have studied such an effective theory in a slightly different context, namely when we discussed kaon condensation in nuclear matter. For other theoretical approaches not discussed in this lecture, see below.

B. What we could have, but haven't, discussed

- *r-modes – bulk/shear viscosity.* We have said little about the rotation of a compact star except for stating that it can rotate very fast with periods in the ms range. For the purpose of our lecture, however, the rotation frequency is a very interesting observable because it is sensitive to the microscopic physics. The reason is

as follows. Certain non-radial oscillatory modes of a rotating star, in particular the so-called r-modes,[12] are generically unstable with respect to gravitational radiation. The reason can be understood in a rather simple argument. Consider the situation where the star rotates *counterclockwise*, seen from the polar view, and where an observer in the co-rotating frame sees non-radial oscillations which propagate *clockwise*. These modes lower the total angular momentum of the star, i.e., if the star's angular momentum is positive, the oscillations have negative angular momentum. Now assume that these propagating modes are seen from a distant observer to move counterclockwise, i.e., they are "dragged" by the star's rotation or, in other words, their angular velocity in the co-rotating frame is smaller in magnitude than the angular velocity of the star, seen from a distant observer. The pulsations now couple to gravitational radiation. The emitted radiation has positive angular momentum since a distant observer sees the pulsations move counterclockwise. Consequently, the total angular momentum of the star must be lowered. This, however, means that the angular momentum of the oscillations, which is already negative, is *increased* in magnitude (becomes more negative). Therefore, the emission of gravitational radiation tends to increase the amplitude of the pulsation which in turn leads to a stronger gravitational radiation etc. This is the r-mode instability. Note that the rotation of the star is crucial for this argument. Indeed, in a non-rotating star, the effect of gravitational radiation is dissipative, i.e., the non-radial oscillations would be damped. For a nice pedagogical introduction into this general relativistic effect see Ref. [37].

The energy loss from gravitational radiation due to the instability makes the star spin down drastically and quickly. Consequently, the observation of sufficiently high rotation frequencies implies that some mechanism must be at work to avoid the instability. The above argument for the instability is generic for all rotating perfect fluid stars. If there is dissipation, i.e., if the matter inside the star has a nonzero viscosity, the instability can be damped. Put differently, in order to rotate fast the star has to be viscous. This statement seems paradoxical at first sight but is clear from the above explanation.

It is thus very important to compute the viscosity of nuclear and quark matter. In hydrodynamics, there are two kinds of viscosity, shear and bulk viscosity.[13] Bulk viscosity describes dissipation for the case of volume expansion or compression while shear viscosity is relevant for shear forces. Both kinds of viscosities are relevant for the damping of the r-mode instability, typically they act in different temperature regimes. What is the microscopic physics behind the viscosity? Let us explain this for the case of the bulk viscosity. Imagine a chunk of nuclear or quark matter in thermal and chemical equilibrium in a volume V_0. Now we compress and expand this volume periodically, $V(t) = V_0 + \delta V_0 \cos \omega t$. In the astrophysical setting, these will be local volume oscillations where ω is typically of the order of the rotation frequency of the star. Through the volume change the matter gets out of thermal and, possibly, chemical equilibrium. The latter may happen if the matter is composed of different components whose chemical potentials react differently on a density change. An example is unpaired quark matter with massless up and down quarks and massive strange quarks. The system now seeks to reequilibrate. For instance, if the compression has increased the strange quark chemical potential compared to the down quark chemical potential, the system reacts by producing down quarks, for instance via the process $u + d \to u + s$. If it does so on the same time scale as the external oscillation, there can be sizable dissipation (think of compressing a spring and the spring changes its spring constant during the process; you will not get back the work you have put in). Consequently, the calculation of the bulk viscosity requires the calculation of the rate of processes such as $u + d \to u + s$ which indeed is the dominant process for the bulk viscosity in quark matter. Other processes which contribute are leptonic processes, such as the direct Urca process we have discussed in the context of neutrino emissivity in Sec. VI B. It is important to note that again the weak processes are the relevant ones. In principle, also strong processes contribute to the bulk viscosity since they reequilibrate the system thermally. However, they do so on time scales much smaller than the external oscillation. Therefore, the system reequilibrates basically instantaneously during the compression process and no energy is dissipated. These arguments also show that the bulk viscosity is a function of the (external) frequency. Maximal bulk viscosity is obtained when the rate of the respective process (which is a function of temperature) is closest to this frequency. Hence, it may well be that a superconducting state has *larger* bulk viscosity than a non-superconducting state. This may sound counterintuitive but note that the (partial) suppression of the rate of the microscopic process by $\exp(-\Delta/T)$ may actually help the viscosity if it brings the rate closer to the external frequency. See for instance Sec. VII in Ref. [7] for a brief review about viscosity in quark matter phases.

- *Magnetic fields.* We have mentioned in the introduction that compact stars can have huge magnetic fields, the highest magnetic fields measured for the surface of a star (then called *magnetar*) are about 10^{15} G. The first

---

[12] Oscillatory modes of compact stars are classified according to their restoring force. In the case of r-modes, this is the Coriolis force.
[13] In the case of a superfluid, there are in fact several bulk viscosities.

question one might ask is about the origin of these magnetic fields. The conventional explanation is that they are inherited from the star's progenitor, a giant star that has exploded in a supernova. While the magnetic flux is conserved in this process, the magnetic field is greatly enhanced because the magnetic field lines are confined in a much smaller region after the explosion. Other questions regarding the magnetic field concern their interplay with dense matter. We have learned that nuclear matter can contain superconducting protons. Protons form a type-II superconductor where the magnetic field is confined into flux tubes. Since at the same time the rotating neutron superfluid forms vortices, a complicated picture emerges, where arrays of flux tubes and vortices intertwine each other. Their dynamics is complicated and relevant for instance for the observed precession times of the star, see for instance Ref. [38]. This issue is also related to *glitches*, see below.

We only touched the interplay of color superconductors with magnetic fields. We have stated without calculation that the CFL phase is not an electromagnetic superconductor, i.e., a magnetic field can penetrate CFL matter. More precisely, Cooper pairs in CFL are neutral with respect to a certain mixture of the photon and one of the gluons. Because of the smallness of the electromagnetic coupling compared to the strong coupling, the gluon admixture is small and the new gauge boson is called "rotated photon". There are color superconductors which do expel magnetic fields, for instance the color-spin-locked (CSL) phase. In this case, Cooper pairs are formed of quarks with the same flavor, and a Cooper pair carries total spin one (instead of zero in the CFL phase). The CSL phase is an electromagnetic superconductor. It is of type I, i.e., expels magnetic fields completely. For a short review about spin-1 color superconductors in compact stars and their effect on magnetic fields see Ref. [39].

Magnetic fields also play a role in the cooling of the star since they have an effect on the heat transport, resulting in an anisotropic surface temperature, see Ref. [34] and references therein. An extensive review about magnetic fields in compact stars is Ref. [40].

- *Crust of the star.* The crust of the star is a very important ingredient for the understanding of the observations. After all, we get all our information from the surface of the star, and thus can only indirectly draw conclusions about the interior. In the conventional picture of a neutron star there is an outer crust with an ion lattice, and an inner crust with a neutron (super)fluid immersed in this lattice. This crust typically has a thickness of about 1 km. A lot about the crust can be found in Ref. [3]. In our discussion of neutron stars vs. quark stars vs. hybrid stars it is important that the crust provides a crucial distinction between an ordinary neutron star (or a hybrid star) and a quark star. How does the crust of a quark star look? Several scenarios have been suggested. First suppose that the surface of a quark star exhibits an abrupt transition from strange quark matter to the vacuum. This is possible under the assumption of the strange quark matter hypothesis we discussed in Sec. II B 1. "Abrupt" means that the density drops to zero on a length scale of about 1 fm, given by the typical length scale of the strong interaction. Now recall that (unpaired) 3-flavor quark matter contains electrons. They interact with quark matter through the electromagnetic interaction, therefore their surface will be smeared (several hundred fm) compared to the sharp surface of the quark matter. As a consequence, an outward-pointing electric field develops (i.e., at the surface positively charged test particles are accelerated away from the center of the star). This electric field can support a thin layer of positively charged ions, separated from the quark matter by a layer of electrons. Hence a "normal" crust for a quark star is conceivable, consisting of an ion lattice. In contrast to the crust of a neutron star, such a crust of a quark star would be very thin, at most of the order of 100 m. See Ref. [41] for more details about this picture of the surface of a quark star (and for other properties of quark stars). This picture may be challenged by the possibility of a mixed phase at the surface of the star. Here, mixed phase refers to a crystalline structure of strangelets immersed in a sea of electrons. In this case, there would be no electric field and thus no possibility for a "normal" crust. The quark matter would rather have its own crystalline crust. Estimates in Ref. [42] show that it is unlikely that such a mixed phase is formed once surface tension is taken into account. In any case, a rigid crust, if at all present, will be much thinner in a quark star than in a neutron star or a hybrid star.

  This qualitative difference is relevant in the context of "magnetar seismology". Quasi-periodic oscillations observed in the aftermath of X-ray bursts from magnetars can be related to typical oscillation frequencies of the crust. In other words, one looks at "star quakes" which have significanlty different properties depending on whether one assumes the star to be a neutron star or a quark star. In fact, the ordinary crust explains the data quite well while the crust of a quark star seems to be incompatible with the observed phenomenology [43].

- *Glitches.* Glitches are an interesting phenomenon related to the rotation frequency, the crust (more precisely the crystalline structure of the crust), and superfluidity. For spinning-down compact stars one observes sudden spin-ups, i.e., in the overall trend of a decreasing rotation frequency the frequency decreases in regular intervals dramatically on a very short time scale. This is conventionally explained through superfluid vortices in the neutron superfluid that pin at the lattice sites of the inner crust. To understand this statement and the

consequences for glitches, we recall the following property of superfluids. A superfluid, be it superfluid helium, superfluid neutron matter, or any other superfluid, is irrotational in the sense that the superfluid velocity has vanishing curl. Therefore, if the superfluid is rotated it develops regions where the order parameter vanishes, i.e., where it becomes a normal fluid.[14] The angular momentum is then "stored" in these regions which are called vortices. An array of vortices, which are "strings" in the direction of the angular momentum, is formed with the total angular momentum of the superfluid being proportional to the density of vortices (because each vortex carries one quantum of circulation). Consequently, if the rotation frequency decreases, the array of vortices becomes sparser, i.e., the vortices move apart. The next ingredient in the glitch mechanism is the pinning of the vortices at the lattice of nuclei in the inner crust. Generally speaking, there is an effective interaction between the vortices and the nuclei and a certain path through the lattice will minimize the free energy of the system. You may think of this preferred configuration as follows. Superfluidity, i.e., neutron Cooper pairing, lowers the free energy of the system. Therefore, the system may want to put the vortices, where there is no Cooper pairing, through the lattice sites because they are not superfluid anyway. Otherwise, i.e., by putting them in between the lattice sites, one loses pairing energy. Anyhow, the details of the pinning mechanism are more complicated and, depending on the density, the preferred path of the vortices may actually be in between the sites. Now we can put the ingredients for the mechanism together. In a rotating neutron star, the neutron vortices pin at the lattice of the inner crust. Now the star spins down. On the one hand, the vortices "want" to move apart. On the other hand there is an effective pinning force which keeps them at there sites. Hence, for a while they will not move which implies that the superfluid (the vortex array) is spinning faster than the rest of the star. At some point, when the "tension" is sufficiently large, the vortices will un-pin, move apart and thus release their angular momentum which spins up in particular the surface of the star whose rotation is observed. Then, they re-pin and the process starts again.

This scenario has become under discussion recently when it was pointed out that it is hard to reconcile with observed precession times. An alternative scenario with quark matter has been suggested. This scenario relies on one of the unconventional phases which are possible in the case of mismatched Fermi momenta, see brief discussion at the end of in Sec. V C. Some of these phases exhibit a crystalline structure, providing one of the ingredients for the explanation of glitches. Also the other ingredient, superfluidity, is present, as we have seen in our discussion of the CFL phase. It remains to be seen in the future which one these scenarios passes all observational constraints and can explain the glitches or if there is a yet unknown mechanism for these curious spin-ups.

- *Other theoretical approaches to dense matter.* What are the alternatives to understand QCD at large, but not asymptotically large densities? *Lattice QCD*, i.e., solving QCD by brute force on a computer, is by now a powerful tool for strong-coupling phenomena (at least for thermodynamic quantities) at zero chemical potential. However, at nonzero chemical potential, one encounters the so-called *sign problem* which renders lattice calculations unfeasible. Progress has been made to extend lattice calculations to small chemical potentials, more precisely to small values of μ/T. But calculations at large μ and small T, as needed for compact stars, are not within reach. See Ref. [44] for a non-technical recent overview article about lattice QCD, in particular its contributions to the QCD phase diagram and about the sign problem; you may also try Ref. [45]. Because of the problems of lattice calculations at finite chemical potential one has to rely on model calculations or on extrapolations similar to the ones discussed in this lecture. One model for quark matter we have not discussed is the Nambu-Jona-Lasinio (NJL) model. This model does not contain gluons and describes the interaction between quarks by an effective pointlike interaction. It has been used to compute the QCD phase diagram at intermediate densities. Since the result depends strongly on the parameters of the model, it should be taken as an indicator for how the phase diagram might look, not as an accurate prediction. Due to its simplicity it is widely used and can indeed give some interesting results which serve as a guideline for the understanding of QCD. For a long review about the NJL model in dense quark matter see [46].

  Let me conclude with another approach which is certainly beyond the scope of this lecture but which is worth to be mentioned. Namely, large-N_c arguments may be applied to gain some insight to $N_c = 3$ QCD. In particular, it has been argued that at $N_c = \infty$ an interesting novel phase, termed *quarkyonic*, populates the QCD phase diagram. The (yet unsolved) problem is to find out whether this phase survives for $N_c = 3$. More

[14] It is instructive to view this phenomenon in analogy to a type-II superconductor. There, a magnetic field (if sufficiently large but not too large) penetrates the superconductor through flux tubes. It partially destroys superconductivity, i.e., in the center of the flux tubes the order parameter is zero. Hence the analogy is superfluid – superconductor; angular momentum – magnetic field; vortices – flux tubes.

generally speaking, the large N_c approach is another approach where one performs calculations in a regime where everything is under rigorous control. From these rigorous results one then tries to get closer to the regime one is interested in. In this sense, this approach is not unlike the perturbative approach. In view of the possible (but not at all obvious) relevance of large-N_c physics to $N_c = 3$ physics, one can also apply the duality of certain string theories to field theories similar to QCD. This somewhat exotic but highly popular approach has recently been pursued especially for large-T, small-μ physics, but is also suited, in certain versions, for the physics at finite chemical potential.

[End of 13th lecture, June 29, 2009]

---

[1] F. Weber, *Pulsars as astrophysical laboratories for nuclear and particle physics*, CRC Press, 1999.
[2] N.K. Glendenning, *Compact Stars: Nuclear Physics, Particle Physics, and General Relativity*, Springer, 2000.
[3] P. Haensel, A.Y. Potekhin, D.G. Yakovlev, *Neutron Stars*, Springer, 2007.
[4] J. Madsen, Lect. Notes Phys. **516**, 162 (1999) [arXiv:astro-ph/9809032].
[5] F. Weber, Prog. Part. Nucl. Phys. **54**, 193 (2005) [arXiv:astro-ph/0407155].
[6] D. Page and S. Reddy, Ann. Rev. Nucl. Part. Sci. **56**, 327 (2006) [arXiv:astro-ph/0608360].
[7] M. G. Alford, A. Schmitt, K. Rajagopal and T. Schafer, Rev. Mod. Phys. **80**, 1455 (2008) [arXiv:0709.4635 [hep-ph]].
[8] J.I. Kapusta, C. Gale, *"Finite-temperature field theory: Principles and Applications"*, Cambridge Univ. Press, New York, 2006.
[9] M. Le Bellac, *"Thermal Field Theory"*, Cambridge Univ. Press, Cambridge, 2000.
[10] A. Schmitt, *Thermal Field Theory, WS 08/09*, *http://hep.itp.tuwien.ac.at/~aschmitt/thermal.pdf*.
[11] S.L. Shapiro and S.A. Teukolsky, *"Black Holes, White Dwarfs and Neutron Stars: The Physics of Compact Objects"*, Wiley-Interscience, New York, 1983.
[12] R. Balian and J. P. Blaizot, arXiv:cond-mat/9909291.
[13] R. R. Silbar and S. Reddy, Am. J. Phys. **72**, 892 (2004) [Erratum-ibid. **73**, 286 (2005)] [arXiv:nucl-th/0309041].
[14] I. Sagert, M. Hempel, C. Greiner and J. Schaffner-Bielich, Eur. J. Phys. **27**, 577 (2006) [arXiv:astro-ph/0506417].
[15] A. Chodos, R. L. Jaffe, K. Johnson, C. B. Thorn and V. F. Weisskopf, Phys. Rev. D **9**, 3471 (1974).
[16] A. Chodos, R. L. Jaffe, K. Johnson and C. B. Thorn, Phys. Rev. D **10**, 2599 (1974).
[17] A. R. Bodmer, Phys. Rev. D **4**, 1601 (1971).
[18] E. Witten, Phys. Rev. D **30**, 272 (1984).
[19] E. Farhi and R. L. Jaffe, Phys. Rev. D **30**, 2379 (1984).
[20] A. Bauswein *et al.*, arXiv:0812.4248 [astro-ph].
[21] M. Alford, M. Braby, M. W. Paris and S. Reddy, Astrophys. J. **629**, 969 (2005) [arXiv:nucl-th/0411016].
[22] M. Alford, D. Blaschke, A. Drago, T. Klahn, G. Pagliara and J. Schaffner-Bielich, Nature **445**, E7 (2007) [arXiv:astro-ph/0606524].
[23] A. B. Migdal, Phys. Rev. Lett. **31**, 257 (1973).
[24] D. B. Kaplan and A. E. Nelson, Phys. Lett. B **175**, 57 (1986).
[25] A. Ramos, J. Schaffner-Bielich and J. Wambach, Lect. Notes Phys. **578**, 175 (2001) [arXiv:nucl-th/0011003].
[26] V. Thorsson, M. Prakash and J. M. Lattimer, Nucl. Phys. A **572**, 693 (1994) [Erratum-ibid. A **574**, 851 (1994)] [arXiv:nucl-th/9305006].
[27] M. G. Alford, K. Rajagopal, S. Reddy and F. Wilczek, Phys. Rev. D **64**, 074017 (2001) [arXiv:hep-ph/0105009].
[28] U. Lombardo and H. J. Schulze, Lect. Notes Phys. **578**, 30 (2001) [arXiv:astro-ph/0012209].
[29] M. G. Alford, K. Rajagopal and F. Wilczek, Nucl. Phys. B **537**, 443 (1999) [arXiv:hep-ph/9804403].
[30] A. Fetter, J.D. Walecka, *"Quantum Theory of Many-Particle Systems"*, McGraw Hill, New York, 1971.
[31] R. D. Pisarski and D. H. Rischke, Phys. Rev. D **61**, 074017 (2000) [arXiv:nucl-th/9910056].
[32] A. Schmitt, *Color superconductivity in dense quark matter*, *http://www.physik.uni-bielefeld.de/igs/schools/Spring2009/schmitt.pdf*.
[33] D. G. Yakovlev, A. D. Kaminker, O. Y. Gnedin and P. Haensel, Phys. Rept. **354**, 1 (2001) [arXiv:astro-ph/0012122].
[34] D. Page, U. Geppert and F. Weber, Nucl. Phys. A **777**, 497 (2006) [arXiv:astro-ph/0508056].
[35] A. Schmitt, I. A. Shovkovy and Q. Wang, Phys. Rev. D **73**, 034012 (2006) [arXiv:hep-ph/0510347].
[36] N. Iwamoto, Phys. Rev. Lett. **44**, 1637 (1980).
[37] L. Lindblom, arXiv:astro-ph/0101136.
[38] B. Link, Phys. Rev. Lett. **91**, 101101 (2003) [arXiv:astro-ph/0302441].
[39] D. N. Aguilera, Astrophys. Space Sci. **308**, 443 (2007) [arXiv:hep-ph/0608041].
[40] A. K. Harding and D. Lai, Rept. Prog. Phys. **69**, 2631 (2006) [arXiv:astro-ph/0606674].
[41] C. Alcock, E. Farhi and A. Olinto, Astrophys. J. **310**, 261 (1986).
[42] M. G. Alford, K. Rajagopal, S. Reddy and A. W. Steiner, Phys. Rev. D **73**, 114016 (2006) [arXiv:hep-ph/0604134].
[43] A. L. Watts and S. Reddy, Mon. Not. Roy. Astron. Soc. **379**, L63 (2007) [arXiv:astro-ph/0609364].
[44] M. A. Stephanov, PoS **LAT2006**, 024 (2006) [arXiv:hep-lat/0701002].
[45] C. Schmidt, PoS C **POD2006**, 002 (2006) [arXiv:hep-lat/0701019].

[46] M. Buballa, Phys. Rept. **407**, 205 (2005) [arXiv:hep-ph/0402234].